Dissertation zur Erlangung des naturwissenschaftlichen Doktorgrades (Dr.rer.nat.) an der Fakultät für Biologie der Ludwig-Maximilians-Universität München

Identification of novel factors regulating human pancreatic endocrine lineage allocation

Noel Moya

München 2023

Dissertation zur Erlangung des naturwissenschaftlichen Doktorgrades (Dr.rer.nat.) an der Fakultät für Biologie der Ludwig-Maximilians-Universität München

Erstgutachter : Prof. Dr. Heinrich Leonhardt

Zweitgutachter : Prof. Dr. Heiko Lickert

Tag der Abgabe : Juli 26, 2023

Tag der mündlichen Prüfung : Dezember 19, 2023

0. Contents

1. List of Abbreviation

2D	Two dimensional
3D	Three dimensional
ARX	Aristaless related homeobox
Ca^{2+}	Calcium-ion
Cx36	Gap Junction Protein Delta 2
CCK	Cholecystokinin
CCKBR	Cholecystokinin β-Receptor
DAPI	4',6-Diamidine-2'-phenylindole dihydrochloride
DNA	Deoxyribonucleic acid
DM	Diabetes Mellitus
EGF	Epidermal growth factor
ER	Endoplasmatic reticulum
EP	Endocrine progenitors
ESC	Embryonic Stem Cell
FACS	Fluorescent activated cell sorting
FOXA2	Forkhead box transcription factors A2
FoxO1	Forkhead Box M1
GCG	Glucagon
GFP	Green fluorescent protein
GHRL	Ghrelin
GLP1	Glucagon Like Peptide 1
GPCR	G-Protein Coupled Receptor
GSIS	Glucose stimulated insulin secretion
GLUT1	Glucose Transporter 1
GLUT2	Glucose Transporter 2
H2B	Histone 2B
INS	Insulin
IPSC	Induced Pluripotent Stem Cell
JNK	c-Jun N-terminal kinase
Kir6.2 / Kcnj11	Potassium Voltage-gated Channel Subfamily J member 11
kDa	Kilo Dalton

KO	Knock out
MAFA	V-Maf Avian Musculoaponeurotic Fibroblast Oncogene Homo A
MAFB	V-Maf Avian Musculoaponeurotic Fibroblast Oncogene Homo B
MAPK	Mitrogen-activated Protein Kinase
mRNA	Messenger RNA
NeuroD1	Neuronal differentiation 1
Ngn3	Neurogenin 3
NKX6-1	NK6 Homeobox 1
NKX2-2	NK2 Homeobox 2
PAX4	Paired Box 4
PCP	Planar Cell Polarity
PCR	Polymerase Chain Reaction
PDX1	Pancreatic and duodenal Homeobox 1
PP	Pancreatic Progenitors
qPCR	Quantitative Polymerase Chain reaction
RNA	Ribonucleic acid
RT	Room Temperature
sd	Standard deviation
sem	Standard error of the mean
SOX9	Sry-Box 9
SSC	Side Scatter
SST	Somatostatin
SV40pA	Simian Virus 40 polyadenylation signal sequence
T1D	Type 1 Diabetes
T2D	Type 2 Diabetes
TF	Transcription Factor
TGFβ	Transforming Growth Factor β-Signaling pathway
UCN3	Urocortin 3
VEGF	Vascular Endothelial Growth Factor
Venus	Modified GFP (Constitutively yellow fluorescent protein YFP)

2. Abstract

Diabetes mellitus (DM) is a metabolic disorder characterized by the dysfunction or loss of insulin-producing β-cells, subsequently affecting blood glucose homeostasis. Restoring functional β-cells mass has become a critical unmet medical need to halt or reverse disease progression, stabilize blood glucose levels, and prevent secondary complications. Transplantation of cadaveric islets of Langerhans has proven to be a curative treatment; however, the scarcity of donor organs currently impedes β-cell-replacement therapies. Consequently, stem cell-derived α, β, and islet cells hold significant potential for cell replacement therapy, disease modeling, and drug screening. Nonetheless, differentiation cultures remain inefficient, the factors regulating endocrine induction and α- versus β-cell lineage allocation are unknown, and the produced cell types are immature. To overcome these hurdles, we: 1) established a protocol for scaled-up production of stem cell-derived islet-like aggregates, 2) generated an *ARX*$^{nCFP/nCFP}$ hiPSC reporter cell line to investigate α-cell differentiation, 3) conducted a screen for novel factors capable of enhancing endocrine induction and promoting α- versus β-cell fate allocation, and 4) examined the roles of gastrin (GAST) and cholecystokinin (CCK) hormones, as well as their corresponding CCKBR receptor, in the formation of endocrine hormone-producing cells.
Our work has resulted in the development of an improved and scaled-up *in vitro* differentiation protocol, which provides several advantages over commonly used methods. Specifically, this protocol facilitates drug screening and transplantation experiments, making it a valuable method for researchers. Moreover, our study generated an *ARX*$^{nCFP/nCFP}$ hiPSC reporter cell line that is karyotypically normal and multi-potent, capable of differentiating into islet-like aggregates and sorting for pre-α-cells. We utilized this reporter line alongside an existing C-peptide-mCherry-hiPSC line to investigate α- and β-cell lineage allocation. Our screen for novel differentiation factors identified gastrin as a factor in endocrine lineage allocation, with the GAST/CCK/CCKBR signaling system playing a role in endocrine induction and α- and β-cell differentiation. Early gastrin treatment primed the endocrine progenitor subpopulation and increased β-cell formation. These findings suggest the potential of gastrin in influencing endocrine lineage allocation for developing cell-replacement therapies. Targeting these pathways *in vivo* could potentially restore insulin secretion in patients with T2D.

3. Introduction

3.1 Diabetes mellitus

Diabetes mellitus (DM) is a global epidemic affecting more than 537 million people worldwide. This staggering prevalence continues to increase steadily, with DM rates predicted to increase to 783 million people worldwide by 2045 (IDF atlas version 10). DM affects the life expectancy of patients and the quality of life of patients and their family members. DM leads to a significant rise in the economic burden on healthcare systems in governments worldwide (IDF atlas version 9). DM is characterized by high glucose levels and is generally classified into three subgroups: type 1, type 2, and gestational diabetes. Type 1 Diabetes mellitus (T1DM) develops through the autoimmune destruction of pancreatic β-cells (Ahlqvist et al., 2018). Type 2 Diabetes mellitus (T2DM) is associated with insulin resistance and glucolipotoxicity, leading to the progressive dysfunction and loss of insulin-producing β-cells (Li et al., 2015). In T2DM, obesity is a significant risk factor, stemming from insulin demand surpassing production, leading to the exhaustion of β-cells (Ahlqvist et al., 2018). Another subgroup in type 2 diabetes includes lean diabetic subjects (Prasad et al., 2015). In lean diabetic patients, dysfunctional β-cells underperform in insulin production and secretion. Gestational diabetes can occur during pregnancy due to increased insulin demand by the fetus and weight gain of the pregnant mother, leading to insulin resistance and β-cell dysfunction (Schmidt et al., 2018).

DM complications affect every system in the body and are responsible for a high percentage of mortality. DM complications are classified as acute and chronic (Schlienger et al., 2013). Some of the acute complications include diabetes ketoacidosis, hyperosmolar hyperglycemia, and hypoglycemia. Importantly, all acute diabetes complications are medical emergencies that can lead to diabetic coma and death (Davidson et al., 2013). Chronic diabetes complications, which encompass both micro- and macrovascular complications, can lead to death and include cardiovascular diseases, nerve damage, kidney failure (Witte et al., 2018). These complications are extremely costly to healthcare systems around the world, with exogenous insulin currently serving as the only effective treatment.

Insulin is a peptide hormone secreted by the β-cells of the pancreas, playing a crucial role in regulating blood glucose levels. Insulin medical treatment is indicated for inadequate production of the hormone or increased insulin demand on the body (Sushmita et al.,

2020). Insulin treatments for type 1 and 2 diabetes mellitus have proven to be beneficial, although insulin treatment addresses only the symptom (high blood sugar levels) rather than the root cause of DM. Most patients manage their symptoms successfully using insulin injections (Heeransh et al., 2020). The use of insulin pumps offers flexible management of diabetes, enabling a more precise adjustment of basal insulin to daily requirements. Insulin pumps also allow for the downloading and transmission of data for analysis and treatment optimization. Insulin pump therapy also appears to be safe and effective (Revital et al., 2020). However, achieving normalized glycemic control with exogenous insulin treatment remains challenging.

Although insulin therapy has significantly improved the quality of life for diabetic patients, this treatment method is inefficient. Lifelong treatment can become very expensive for the patient without the possibility of a permanent cure (Noguchi et al., 2010). Bariatric surgery was initially designed for weight loss in morbidly obese patients. It is a surgery based on the principle of removing a section of the stomach. Following post-surgery studies, however, the procedure is now classified as metabolic surgery (Buchwald et al., 2019). The reclassification is based on post-surgical effects on intestinal physiology, bile acid metabolism, incretin hormone secretion, neuronal signaling, and microbiome changes. Bariatric surgery improves DM through both body weight-dependent and independent actions. Even without weight loss, insulin-dependent diabetes patients exhibit diabetes remission, providing strong evidence that endogenous β-cells can be restored even after years of damage. Results from bariatric surgery reveal remission of DM ranging from 33% to 90% one year after the surgery (Affinati et al., 2019).

Pancreatic islet transplantations offer another recognized DM cure. This treatment has become an established approach to β-cell replacement therapy. In diabetic patients, isolation and transplantation of islets from a deceased donor ameliorate hypoglycemia and help to maintain target glycemic control, consequently improving quality of life without the requirement for insulin therapy (Rickels et al., 2019; Shapiro et al., 2000). According to Vertex October 2021, a single-patient data show proof-of-concept. A type 1 diabetes patient restored islet cell function after being transplanted with stem cell-derived islets directly into the liver without encapsulation. The patient was able to reduce his insulin dose, and his body produced insulin independently (Vertex-diabetes-cell-therapy.com). Although this form of treatment works in principle, there are some remaining problems. Few patients are offered transplantation treatments, however, due to a lack of donor organs. Further, autoimmune rejection, which can be controlled only by treating patients

with immunosuppressive medications for an extended period, brings several unwanted side effects.

Achieving better treatment options and improving quality of life for the increasing population of diabetic patients, especially for the minority of patients who still suffer from life-threatening hypo- and hyperglycemia, makes it crucial to identify alternative sources of transplantable β-cells. Human embryonic stem cells (hESCs) or induced pluripotent stem cells (iPSC), collectively termed human pluripotent stem cells (hPSCs), offer, in theory, an unlimited source for β-cell differentiation in culture. Cell replacement therapy is a curative treatment, which may be achievable through the generation of an unlimited supply of monohormonal pancreatic β-cells (Siehler et al., 2021). Current approaches to generate functional pancreatic cell types from hPSCs are promising but have not yet reached the final goal of efficient production of functional, mature β-cells *in vitro* (Migliorini et al., 2021).

3.2 Pancreas structure, function and development

To understand how hPSC can be directed into the endoderm, pancreatic, endocrine and hormone-producing cell lineages, it is important to understand embryonic pancreas development. The pancreas is an organ divided into head, body and tail; and is comprised of two components: the exocrine and endocrine pancreas (see Figure 1) (Cerf et al., 2015). Acinar cells compose the exocrine part of the pancreas and produce lipases, proteases, and nucleases, which are released in the duodenum. Ductal cells, part of the exocrine pancreas, can secrete ions and develop into a branched system, which in conjunction with the acinar cells, secrete digestive enzymes and ions into the duodenum (Bjoern et al., 2015). The endocrine pancreas is comprised of the islet of Langerhans, whose primary function is to regulate blood glucose levels by secreting multiple hormones (see Figure 1). The insulin-secreting β-cells are the most abundant, followed by glucagon-secreting α-cells, and somatostatin-secreting δ-cells. The two additional cell types that compose the pancreatic islets are PP cells producing the pancreatic polypeptide and ε-cells producing ghrelin (Aamodt et al., 2017). These hormones perform their function based on islet architecture, innervation, and vascularization. The islet architecture concerning hormone functionality is well illustrated in adult rodent islets, where most β-cells are organized in rosette-like structures around the blood vessels. This organization helps the cells secrete insulin into the bloodstream (Migliorini et al., 2016). The pancreatic islet architecture plays

an essential role in the adequate secretion of hormones, responding to high glucose levels in the blood, however, additional studies exploring islet architecture are needed (Bjoern et al., 2015).

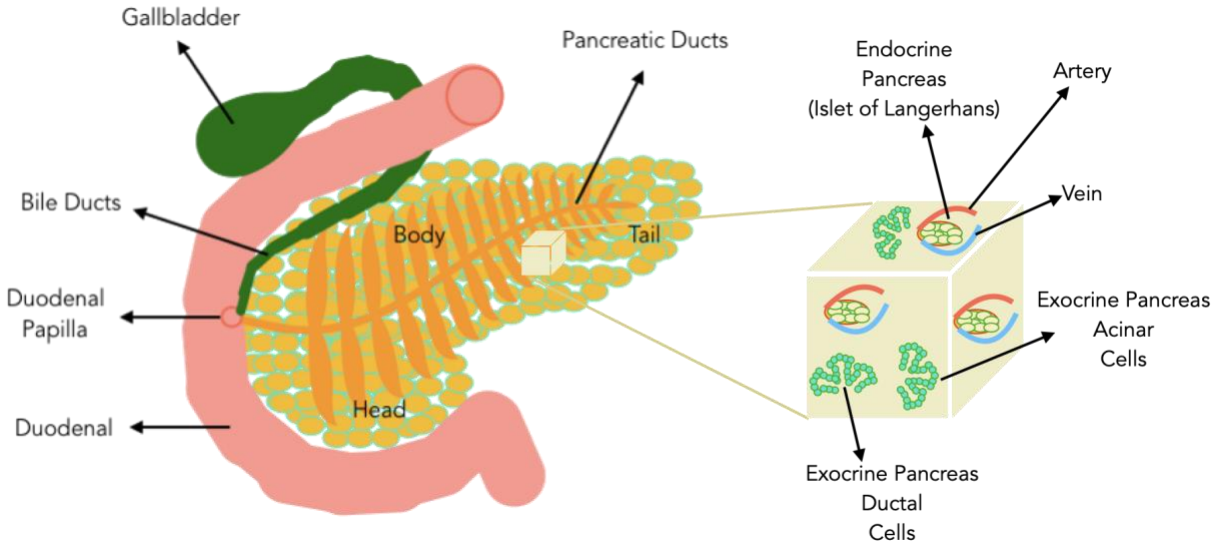

Figure 1. Anatomical Structure of the Pancreas, Gallbladder, and Duodenum.
The figure illustrates the different regions of the pancreas, including the head, body, and tail, as well as the pancreatic ducts. The exocrine pancreatic secretions, along with the gallbladder juice, are delivered to the duodenum through the duodenal papilla, facilitating the process of digestion. The endocrine pancreas is composed of the islets of Langerhans, which house specialized cells responsible for producing and secreting blood glucose regulatory hormones.

Pancreas development is relatively conserved among mammals. Pancreatic development is defined by two transitions. The primary transition during pancreatic organogenesis is mainly characterized by an increase in the pancreatic progenitor population and the first wave of expression of the transcription factor neurogenin 3 (Ngn3). In mouse, this first wave correlates with the formation of α-cells; these first-differentiated cells may not contribute to the islet of Langerhans (Herrera et al., 2000). The secondary transition, involves pancreas growth and is followed by branching morphogenesis and cell lineage allocation, encompassing the main wave of endocrinogenesis from E12.5 to15.5 (Pan et al., 2011). Some studies include a tertiary transition, or maturation, which occurs when cells undergo apoptosis and replication, creating a mature organ (Cerf et al., 2015). How a single progenitor pool of cells can develop from multipotent to bipotent and become different unipotent endocrine progenitors and cell types is still not well understood.

In contrast to mouse, in humans the first endocrine cells to appear in the pancreas are insulin-producing β-cells (Jennings et al., 2015). These cells arise as immature β-cells

followed by multiple molecular and metabolic changes during the embryonic and postnatal stages to become mature β-cells. We are considering mature β-cell as a cell characterized by an increase in glucose threshold for insulin secretion and the expression of the gene urocortin 3 (Blum et al., 2012). In response to plasma glucose levels, mature β-cells secrete the hormone insulin. To maintain optimal physiological function, β-cells preserve the acquired maturation machinery. Several studies have shown loss of β-cell maturation during DM (Russ et al., 2015). Therefore, it is essential to more thoroughly understand the maturation process of β-cells in order to develop mechanisms that reduce the loss of cell maturity or restore the maturation machinery in the necessary cases (Salinno et al., 2019). Individual β-cells do not acquire the maturation identity simultaneously, leading to heterogeneity in the β-cell population. β-cell heterogeneity is based on the phenotype and functionality of the different cells (Migliorini et al., 2016; Bader et al., 2016; Roscioni et al., 2016).

The loss of β-cell identity can lead to different cellular identities and phenotypes that have been observed upon T1DM and T2DM stress, such as dedifferentiated, senescent, and transdifferentiated β-cells (Salinno et al., 2019). The terminology β-cell dedifferentiation has been assigned to dysfunctional β-cells that return in developmental history to a progenitor-like state. Studies of human samples have found stress factors, such as autoimmunity, glucotoxicity and lipotoxicity to be responsible for forcing β-cells to lose their identity by downregulation of critical transcription factors (TFs) and their mature function in terms of glucose-sensing and insulin secretion. β-cell transdifferentiation occurs when non-β-cell hormones and TFs are ectopically expressed. A classic example was revealed in studies using mice where β-cell expression of insulin-glucagon and insulin-somatostatin was found (Herrera et al., 2000). β-cell senescence is related to the physiological or pathological aging of the β-cells (Helmann/Yuval Dor 2016 Nature Medicine; Thompson et al., 2019). Premature stress-induced senescence of β-cells has been associated with hyperglycemia and hyperinsulinemia (Thompson et al., 2019).

3.3 Transcription factor and hormone expression during pancreas and islet development

TFs are proteins that control the transcription initiation rate of a genes by binding to cis-regulatory elements, such as promoters, enhancer and repressors (Yaxi et al., 2017). During pancreatic development, a plethora of TFs play critical role for exo- and endocrine

lineage specification. Forkhead Box A2 (Foxa2), known as a pioneer factor in human endoderm and pancreas formation, helps to start and maintain a definitive endoderm program (Ye et al., 2009). There are three *Foxa* genes encoded in the mammalian genome: *Foxa1, Foxa2* and *Foxa3. Foxa2* is the earliest expressed and knock-out leads to lack of endoderm formation (Ang et al., 1994). As one of the critical regulators of endocrine genes, the expression level of Foxa2 varies during the different stages of islet-like differentiation. Moreover, knockout of Foxa2 in hiPSCs generates a reduced number of pancreatic progenitors (Kihyun et al., 2019). Another important endoderm specific TF at this early developmental stage is SRY-box transcription factor 17 (Sox17) (see Figure 2). This TF directs the specification of the definitive endoderm and is subsequently involved in endoderm-derived organ formation, such as the pancreas (Kanai-Azuma et al., 2002). In contrast to Foxa2, Sox17 expression decreases once the cells move past the endoderm stage (Anik et al., 2015; Bjoern et al., 2019). The misexpression of Sox17 suppresses pancreas development by promoting ectopic biliary-like tissue within the posterior foregut region that expresses the posterior foregut and pancreas master regulatory gene, Pancreatic and Duodenal Homeobox 1 (*Pdx1)* (Pan et al., 2011).

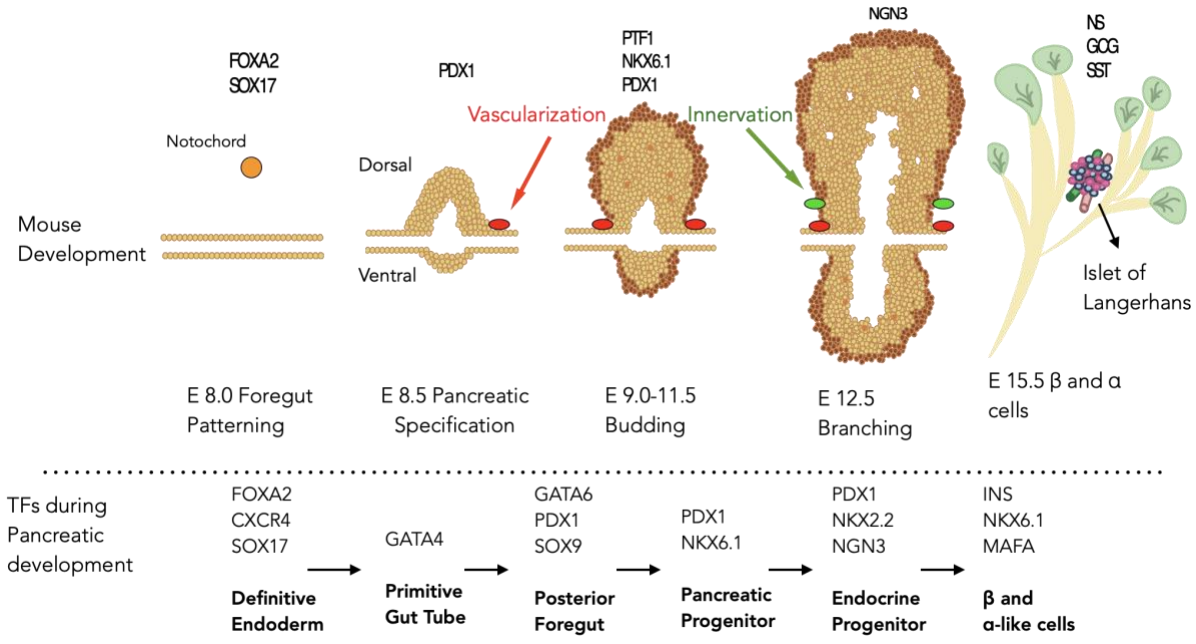

Figure 2. Physiological Development of Pancreatic Islets in the Mouse.
This figure presents a chronological depiction of the physiological development of pancreatic islets in mice. In the top panel, key developmental events are illustrated at specific embryonic stages. The foregut patterning

process is shown at E 8.0, followed by the formation of ventral and dorsal buds at E 8.5. Vascularization and innervation within the forming islets, as well as the branching process and the formation of α- and β-cells, are depicted from E 9.0 to E 15.5. The bottom panel provides further insights into the transcription factors (TFs) involved in pancreatic development. It highlights the most prominent TFs at distinct stages of development, these TFs play crucial roles in regulating gene expression and cell fate determination during pancreatic development.

Multipotent pancreatic progenitor cells of the early pancreatic epithelium express several TFs associated with the initiation of the pancreatic program. Some of these regulate allocation of pancreas fate within the primitive gut tube, while others promote proliferation and suppress differentiation (Pan et al., 2011). These factors are also expressed in several regions of the endoderm. For example, during E8.0, Mnx1 appears in the dorsal and ventral endoderm, while Hnf1B appears in the foregut-midgut region.

During development of the pancreatic buds in mice, expression of the Pdx1 appears in the newly formed pancreatic progenitor population. Pdx1 is first TF expressed in the dorsal and ventral pre-pancreatic endoderm at E8.5, and its expression is maintained throughout pancreas development (Pan et al., 2011). In mouse, the fibroblast growth factor 4 (Fgf4) from the mesoderm influences the anterior/posterior character of the definitive endoderm. Studies suggested that Fgf4 acts directly suppressing the anterior endodermal NK2 Homeobox 1 (*Nkx2-1)*, which is required for foregut endoderm formation, and to promote the expression of the posterior TF gene *Pdx1*. Loss-of-function studies show that *Pdx1* mutants show an almost complete agenesis of the pancreas and also have defects throughout the posterior foregut region (Pan et al., 2011). The TF SRY-Box Transcription Factor 9 (Sox9) also plays a critical role in governing embryonic development of the pancreas. The expression of Sox9 is first detected in the primordium at E10.5. Lineage tracing revealed that $Sox9^{+}$ progenitors, produce cells of all three pancreatic lineages (see Figure 2). The proper expression of Pdx1 determines the cells progression towards a pancreatic fate. The expression of the TF NK6 Homeobox 1 (Nkx6-1) marks pancreatic progenitor cells. Sox9 is also present in the pancreatic progenitor population maintaining Notch signaling.

Continued maintenance of Pdx1 is essential for the development of the exocrine and endocrine pancreas (Yaxi et al., 2017). The expression of Sox9 also persists in the endocrine progenitor pool (Pan et al., 2011). This TF is specific later in cells expressing markers of exocrine compartment, maintaining the pancreatic ductal identity (Seymour et al., 2017). The co-expression of Pdx1 and Nkx6-1 (double Pdx1/Nkx6-1 cells) in pancreatic progenitors propels the first transition, the differentiation towards the endocrine

lineage. After the endocrine induction stage, the TF Nkx6-1 is restricted to β-cells. Importantly, the master regulatory TF Ngn3 is transiently expressed at the endocrine progenitor stage and is absolutely necessary for endocrine cell formation in mice and man (Pan et al., 2011; Nair et al., 2020; Mellitzer et al., 2006;). In mice as well as in humans, the endocrine progenitor has low Ngn3 expression, followed by a shift to high Ngn3 expression, resulting in the acquisition of secretory machinery and hormone-producing cells. The endocrinogenesis events are tightly controlled by dynamic gene regulatory networks (Nair et al., 2015). The expression of Ngn3 in this population allows the formation of the first hormones in the islet. The TF NK2 Homeobox 2 (Nkx2-2), expressed in the endocrine progenitor population, is considered a pan-endocrine factor (Cerf et al., 2015). During endocrinogenesis, expression of Gata4 and Gata6 becomes uncoupled to different pancreatic endo- and exocrine domains. The expression of Gata4 between E13.5 to E18.5 is restricted to acini in the case of Gata6 the expression is detected in the central epithelial duct (Decker et al., 2006). Any alteration to the expression levels of these factors leads to abnormal ductal, exocrine and endocrine differentiation as well as ´agenesis of the endocrine pancreas.

The second transition commences in the mouse with a period of epithelial expansion and the differentiation of endocrine, acinar and duct cells at E13.0. Where endocrine cells appear from the trunk epithelium showing high levels of proendocrine Ngn3, endocrine progenitors differentiate towards endocrine precursors which delaminate from epithelium to form pancreatic islets (Jensen et al., 2000; Schwitzgebel et al., 2000). Hormone-producing cells, specifically β-cells, start appearing and continuing expanding during this period. A large number of endocrine cells that form the mature islets present at the end of gestation are generated during this secondary transition period (Pan et al., 2011).

3.4 Expression of transcription factors Arx and Pax4 during islet formation

During endocrine induction, while Ngn3 and Nkx2-2 are expressed, two other TFs gain importance due to their role in α- and β-cell differentiation: Aristaless Related Homeobox (Arx) and Paired Box 4 (Pax4). Previously, (Collombat et al., 2005) reported that Arx mutation leads to a lack of mature α-cells concomitant with an increase in β- and δ-cells. In contrast, Pax4 mutations result in the absence of β-cells and in an increase in the number of α- and δ-cells, showing that these two TFs are essential for α- and β-cell differentiation (Beucher et al., 2005) (see Figure 3).

Furthermore, when both Arx and Pax4 are mutated, mice exhibit a dramatically enlarged δ-cell population, while lacking α- and β-cells. These studies collectively suggested that Arx and Pax4 play a significant role in the allocation of α- and β-cells to their respective endocrine fate. Moreover, the results hint that islets possess an unknown mechanism to maintain a constant number of α- and β-cells and that mechanism can be regulated by the expression of Arx and Pax4. There are at least two school of thought defining α- and β-cell allocation. The first points out that during the endocrine induction stage, pancreatic progenitors are already fate-specified towards α- and β-cell fate, a view that is reinforced by the fact that α-cells form first and β-cells appear later. An alternative hypothetical model states that endocrine progenitors are not yet unipotent and still can allocate towards α- and β-cell fate. Pax4 and Arx become expressed after Ngn3-mediated endocrine induction and might be the reason for the mutually exclusive α- and β-cell fate (Gage et al., 2004; Collombat et al., 2005). The TF Ngn3 is a master regulator of endocrine induction, as studies conducted have shown the Ngn3 knock-out leads to the complete absence of endocrine cells in mice and humans (Gradwohl et al., 2000; Mellitzer et al., 2006; Rukstalis et al., 2009). Ngn3 is likely responsible as it is a master regulator during this stage. Currently, it is unknown how pancreatic progenitor lineage allocation between α- and β-cells occurs. It is also undetermined how the feedback mechanisms, which regulate the number of cells produced in the islet occur. Moreover, the upstream factors regulating the activation and inhibition of main TFs that drive endocrine induction and maturation like Arx/Pax4 remain unknown (Collombat et al. 2005).

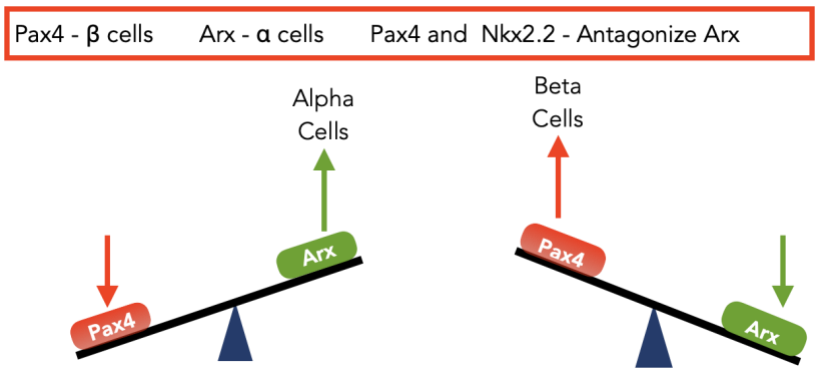

Figure 3. Balance of Arx and Pax4 Transcription Factors in Promoting α- and β-Cell Fate Allocation in Pancreatic Islets. This figure illustrates the dynamic interplay between the transcription factors Arx and Pax4 and their role in determining the allocation of α- and β-cell fates within pancreatic islets. Arx and Pax4 play crucial roles in regulating the differentiation and maturation of pancreatic endocrine cells. Arx promotes α-cell fate, while Pax4 favors β-cell fate allocation. The balance between the expression and action of these

transcription factors is critical for maintaining the appropriate ratio of α- and β-cells in pancreatic islets, thereby ensuring proper functioning of the endocrine system.

3.5 Gastrin

In adults, the hormone gastrin plays a critical role in stimulating gastric acid secretion in the stomach (Engevik et al., 2020). Gastrin is commonly synthesized in the pyloric G cells in the form of a 101 amino acid precursor, which eventually becomes the biologically active forms gastrin-17 and gastrin-34. The C-terminal site of gastrin binds to the cholecystokinin β-receptor on histamine containing enterochromaffin-like cells (ECL). Histamine triggers the nearby parietal cells by binding to H2-receptors and activating hydrochloric acid secretion. Gastrin also helps maintain the gastric mucosa integrity by activating proliferation of ECL cells (Rehfeld et al., 2019).

During embryonic development, Ngn3 is the central regulator generating enteroendocrine cells in the intestine. Enteroendocrine cells produce and secrete the hormones gastrin, CCK, GLP-1, GIP, and somatostatin. However, it is not well understood how $Ngn3^{+}$ cells give rise to different hormone-producing cells in the pancreas and intestine. In the case of gastrin-expressing cell generation, Ngn3, Nkx2-2, and Arx are required (Glaser et al., 2013). It is noteworthy that Ngn3-expressing cells that are present in the stomach during embryonic formation cannot trigger the formation of gastrin-secreting G cells, leaving the expression of gastrin in the stomach to appear at postnatal stage (Glaser et al., 2013).

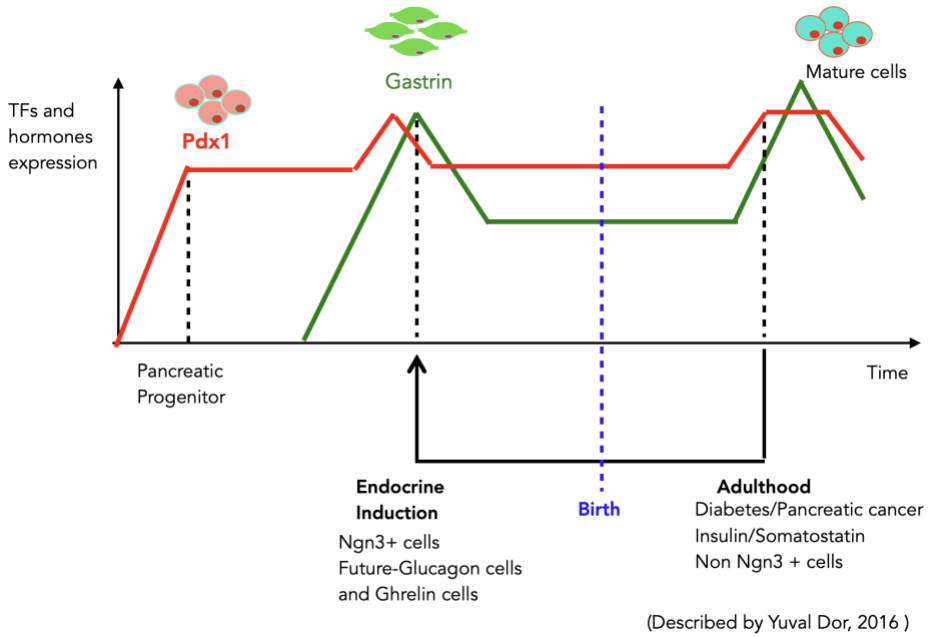

Figure 4. Expression Pattern of the Hormone Gastrin during Islet Development and in Adult Islets in Relation to Pdx1. This figure depicts the expression pattern of the hormone gastrin in relation to Pdx1, as reported by Yuval Dor and colleagues in 2016 (Yuval Dor et al., 2016). According to their observations in prenatal mice and postnatal humans, the expression of Pdx1 shows an increase during the pancreatic progenitor stage. Subsequently, during the endocrine induction stage and the transient expression of Ngn3, the hormone gastrin becomes detectable.

Gastrin is one of the earliest hormones expressed during islet formation in Ngn3 positive cells. As islet development continues, these first gastrin-expressing cells give rise to cells producing glucagon and ghrelin. Gastrin expression continues until the end of the islet's maturation process. However, the expression of Pdx1 decreases as cells progress from endocrine progenitors, where Pdx1 is widely expressed, to islet formation where Pdx1 is only found in β- and δ-cells. During the prenatal period, gastrin is found in the embryonic pancreas and not in the embryonic stomach. In the pancreas of healthy individuals, gastrin expression disappears after birth. Gastrin appears in the adult pancreas in association with neuroendocrine tumors, in other forms of maligned tumors, and during diabetes progression and β-cell dedifferentiation (Yuval Dor et al., 2016).

In the case of pancreatic tumors or diabetes, an increase in Pdx1 expression is observed, coinciding with an increase in gastrin. Insulin- and somatostatin-producing cells produce gastrin, and no connection was found between adult expression of gastrin and Ngn3. Yuval Dor et al. (2016) pointed out that many diabetic islets have a reduced number of β-cells, but cell apoptosis was not increased. They concluded that the islet cells do not die but instead lose their β-cell identity and dedifferentiate, very similar to what was described upon sustained hyperglycemia in a toxin-mediated β-cell ablation model (Sachs et al., 2020). It is likely that the increase in the expression of gastrin in the adult islets protects the cells from apoptosis by reverting the damaged cells back to a more progenitor-like stage (Yuval Dor et al., 2016).

3.6 Cholecystokinin

Cholecystokinin (CCK) is a neuropeptide commonly present in the gastrointestinal system and in the nervous system. It is mainly produced by I cells, part of the intestinal enteroendocrine cells located in the duodenum and jejunum. To facilitate the digestion of fats and proteins, CCK stimulates organs like the gallbladder, stomach, and pancreas. The most common CCK isoforms circulating in the blood are O-sulphated CCK-33 and the less common CCK-58. In the central nervous system, CCK is highly expressed in the

limbic system and the pituitary gland. It is also present in the peripheral nervous system, including neurons responsible for islet innervation and intra-pancreatic ganglia. On the one hand, in the case of CCK as a neurotransmitter, the most common form is O-sulphated CCK-8. CCK acting on the central and peripheral nervous system is considered a neurotransmitter. On the other hand, CCK in non-neuroendocrine cells acts as a paracrine peptide messenger (Rehfeld et al., 2019).

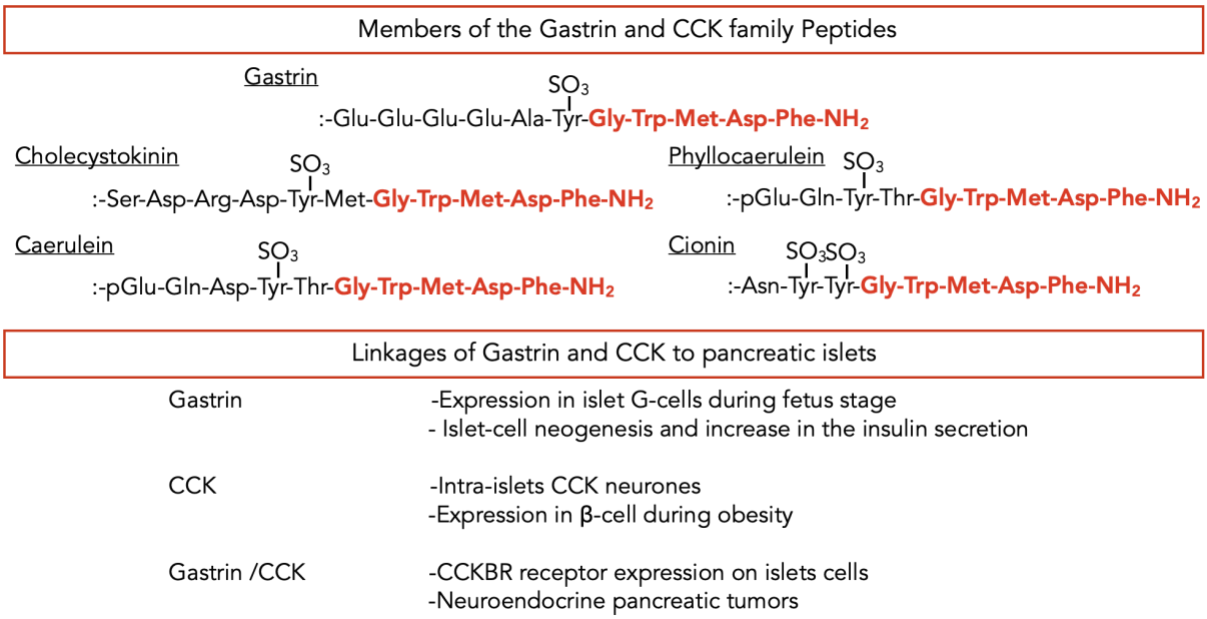

Figure 5. Members of the Gastrin and Cholecystokinin (CCK) Family Peptides and their Linkage with Pancreatic Islets. This figure illustrates the C-terminal bioactive amino acid sequences of diverse members belonging to the gastrin/cholecystokinin (CCK) family of peptides. The gastrin and CCK family of peptides encompasses multiple biologically active molecules that have crucial roles in gastrointestinal functions and signaling. These peptides display structural resemblances and possess conserved regions in their C-terminal amino acid sequences, which are responsible for their bioactivity. Furthermore, the figure highlights the association of these peptides with pancreatic islets, emphasizing their potential involvement in pancreatic physiology and regulation.

3.7 Cholecystokinin B Receptor

Gastrin and CCK target the same G-protein-coupled receptors, the Cholecystokinin Receptors. There are two subtypes of these receptors, CCKAR and CCKBR. CCKAR participates in gallbladder contraction, pancreatic growth, enzyme secretion and the inhibition of gastric acid secretion by a feedback loop with the hormone somatostatin. This receptor is highly expressed in the central nervous system, specifically in the midbrain and the pituitary gland. CCKAR binds with a high affinity to carboxyamidated and tyrosyl O-sulfated CCK peptides. At the same time, the affinity to non-sulfated CCK peptides and

gastrin is negligible. The subtype receptor CCKBR binds to sulfated and non-sulfated gastrin and CCK peptides. Also, CCKBR binds with a high affinity to the C-terminal fragments of CCK-5 and CCK-4. CCKBR is highly expressed in enterochromaffin cells in the stomach as well as islet cells and ganglionic neurons in the pancreas. Gastrin and CCK generated and released by islet cells stimulate the islet cells and their receptors. Also, islet cells and their CCKBR are stimulated by endocrine gastrin and CCK coming from the circulation (Rehfeld et al., 2019).

Studies conducted in mice have shown Ngn3 positive pancreatic progenitor cells can secrete fetal gastrin (Dahan et al., 2016). Similar studies showed gastrin binding to CCKBR in the early pancreatic foregut leads to an increase of Pdx1 expression (Moore et al., 2013). So far, neither the mechanisms involving gastrin acting on $Pdx1^{+}$ pancreatic progenitors nor the role that gastrin could play regarding Arx^{-} and Pax4-mediated α- and β-cell lineage allocation has been studied.

3.8 Human embryonic stem cells

Human embryonic stem cells (hESCs), derived initially from the inner-cell mass of the blastocyst, are self-renewing and pluripotent. These cells have the potential to generate all three embryonic germ layers and differentiate into every cell type of the human body. The mesoderm is capable of generating bone and muscle, and the ectoderm is capable of creating neural epithelium. The endoderm, which is the focus of this study, gives rise to internal organs, including the gastrointestinal and respiratory tracts, as well as organs, such as the thymus, thyroid, pancreas, liver, prostate and bladder (Nowotschin et al., 2019).

hESCs are defined by elevated telomerase activity compared to somatic cells which directly correlates with the immortality of these cell lines. hESCs also express cell surface markers that are common in the undifferentiated cell including embryonic antigens SSEA-3, SSEA-4, TRA-I-60, TRA-1-81, and alkaline phosphatase (Thomson et al., 1998).

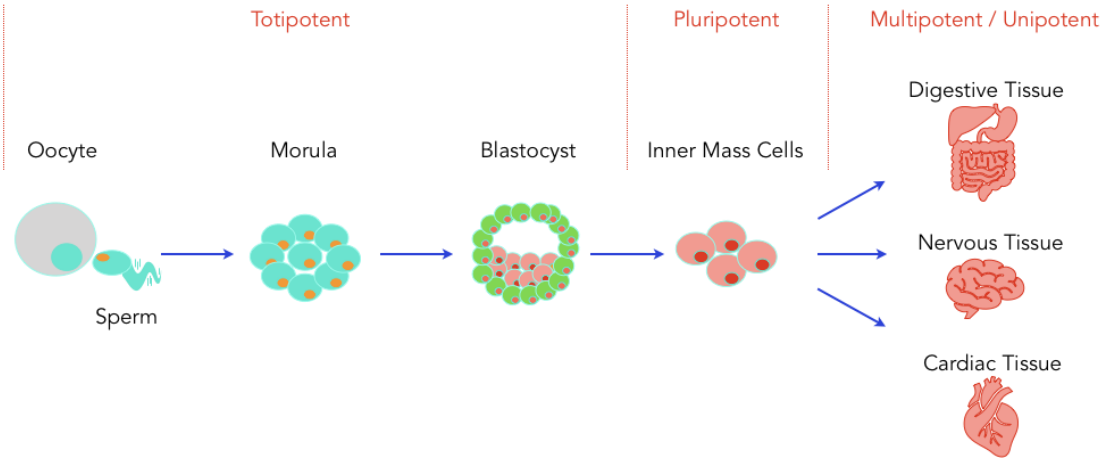

Figure 6. Schematic representation of the stages composing the four types of potency levels in human embryonic stem cells. The totipotent stage, with the formation of the morula, followed by the generation of the blastocyst. The pluripotent stage, with the ability of the inner mass cells to generate any cell in the human body. The multipotent stage, with the capacity to form a different type of cell from the same organ. For example, pancreatic progenitors are multipotent cells, capable of generating endocrine and exocrine cells. Finally, the unipotent stage allows the creation of a unique type of cell. For example, endocrine progenitors are unipotent, only capable of generating endocrine cells.

The abilities of hESCs make these cells appealing for use in cell replacement therapy and drug/toxin screening studies as well as to help researchers better understand human developmental biology in a controlled system, which is otherwise not accessible (see Figure 6). These advantages have elicited both public attention and ethical issues; many connect the study of hESCs with the acquisition of these cells from live human embryos, which would destroy life. Limitations in acquiring the cells have therefore forced researchers to find other ways to create human pluripotent stem cells, opening the way for establishing human-induced pluripotent stem cells (Takahashi et al., 2006; Yong Moon et al., 2005).

3.9 Human-induced pluripotent stem cells

Human-induced pluripotent stem cells (hiPSC) are a type of stem cell generated directly from somatic cells. They hold great promise in regenerative medicine as they offer the same advantages as hESCs. For instance, skin epithelial cells or any other somatic cell type can be obtained from any individual by a simple biopsy, blood draw or urine filtration, allowing for further reprogramming of the human somatic cells into induced pluripotent stem cells. The introduction of hiPSC offers tremendous advantages, particularly for the

use of cell replacement therapy, disease modelling and drug screening. For cell replacement, cells taken from a patient reprogrammed into hiPSCs, differentiated, and transplanted into the same individual significantly reduced the immune response towards the transplanted cells compared to cells extracted from one patient and transplanted to a different individual. However, human iPSCs application could be restricted by mutations as the result of the reprogramming, culture and expansion process. These possible mutations could increase the risk of tumor formation after transplantation of iPSCs-derived cells (Yamanaka et al., 2020). Moreover, the generation and maintenance of multiple iPSC lines and the differentiation protocols suitable for the lines is time consuming and cost intensive, as described for stem cell-derived islets as an example (Sieher et al., 2021).

In 2006, Yamanaka and colleagues showed that adult somatic cells reprogramed with four specific TFs converted into induced pluripotent stem cells (Takahashi et al., 2006) (see Figure 7). The initial TFs for reprogramming were SOX2, C-MYC, KLF4, and OCT4. These factors are capable of reprogramming mouse somatic cells into induced pluripotent stem cells successfully. One year later, using the same factors, Yamanaka and colleagues reprogramed hiPSCs (Takahashi et al., 2006). The generated hiPSCs shared similar characteristics with hESCs, including morphology, demethylation of OCT4, NANOG promoter regions, and the capability to differentiate into all three germ layers (Takahashi and Yamanaka et al., 2016).

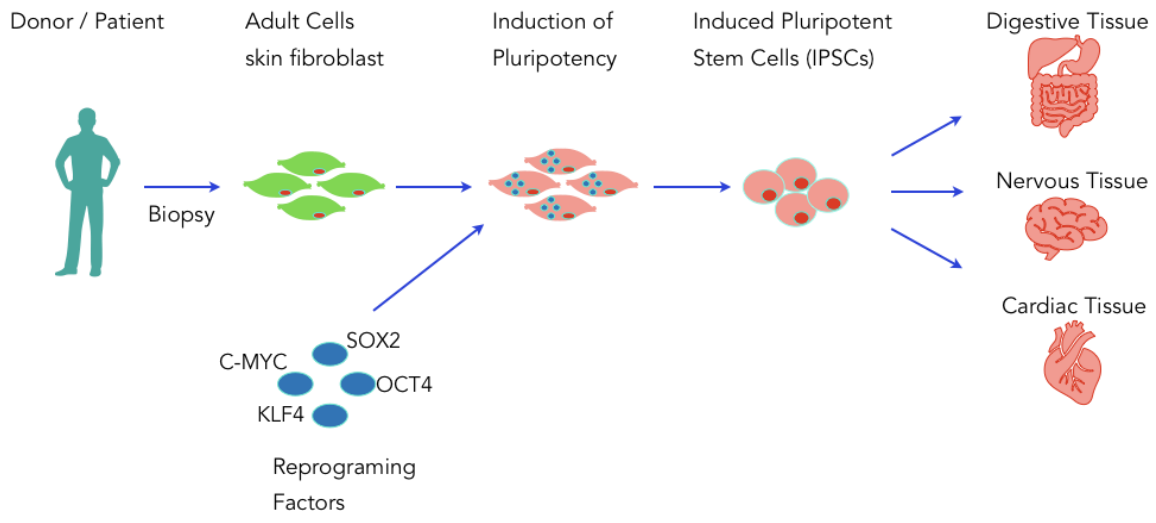

Figure 7. Steps to Generate Human Induced Pluripotent Stem Cells (hiPSCs) from Skin Fibroblasts Using Reprogramming Yamanaka Factors and the Potential of hiPSCs to Differentiate into Cells from Multiple Organs. This figure illustrates the sequential steps involved in the generation of hiPSCs from skin

fibroblasts using reprogramming factors. The process includes the introduction of specific transcription factors, such as Oct4, Sox2, Klf4, and c-Myc, leading to the reprogramming of somatic cells into pluripotent stem cells. Furthermore, the figure highlights the potential of hiPSCs to differentiate into cells from multiple organs.

The ability to reprogram skin fibroblasts into hiPSCs opens the way for unexplored research areas. Consequently, following a detailed study, it is possible to perform disease modeling *in vitro* by generating hiPSCs from patients for specific diseases. This alone advances the understanding of formation and progression of many diseases including diabetes, Parkinson's, and Alzheimer's (Kim et al., 2008).

The generation of hiPSCs from fibroblasts brings advantages in the pharmacological field as well, which could considerably improve the design and production of new drugs. Testing newly designed drugs using hiPSCs ensures efficacy at a molecular level and can help reduce drug toxicity. This extra step added to the drug design protocol ensures a more effective drug with less adverse side effects. Moreover, the generation of hiPSCs provides a significant advantage in the field of gene therapy. The ability to generate hiPSCs from a patient exhibiting a congenital anomaly allows for gene editing *in vitro*, followed by a detailed understanding of the genetic abnormality. As a result of these studies, gene therapy promises a future medical treatment with gene editing (Takahashi et al., 2006).

3.10 CRISPR-Cas9 gene editing in stem cells

Genetic engineering marks a significant accomplishment in the field of biology. Gene editing technologies, particularly the clustered, regularly interspaced short palindromic repeats/CRISPR-associated protein 9 (CRISPR/Cas9) system, allow for unique editing of the genome sequence (see Figure 8). There are two parts that form the CRISPR/Cas9 system. One part is the programmable single strand guide RNA (sgRNA) molecule. The other part is the Cas9 endonuclease system. The role of the sgRNA is to direct the Cas9 to a pre-selected site of the genome so that the Cas9 can cleave both DNA strands in a sequence-specific manner. The specific DNA cleavage occurs at three base pairs upstream of the protospacer adjacent motif (PAM). The genome is typically repaired after the double-strand break by one of two DNA repair pathways, either the non-homologous end-joining (NHEJ) or the high-fidelity homology-directed repair (HDR) pathway. Using CRISPR/Cas9, the gene of interest can be targeted by introducing small insertions or

deletion sequences. The DNA repair pathways identify the segment of DNA damage and replace it with the introduced segment of modified DNA (Xueli et al., 2019).

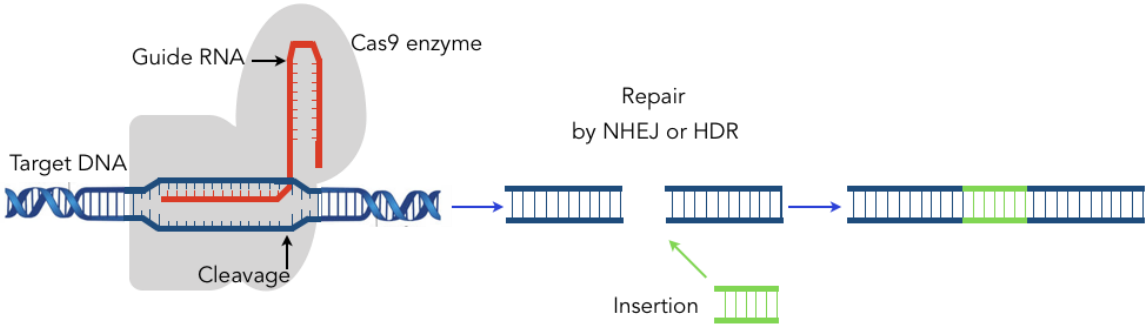

Figure 8. Schematic Representation of the CRISPR/Cas9 Genome Editing Site. This figure depicts the essential components of the CRISPR/Cas9 system for genome editing. The system comprises a plasmid containing the necessary genetic elements and the Cas9 protein complexed with a specific guide RNA (sgRNA). In the schematic representation, the Cas9 protein binds to the target site on the genome, inducing a precise double-strand break (DSB) in the DNA molecule. The repair of the DSB can occur through two primary pathways: non-homologous end joining (NHEJ) and homology-directed repair (HDR). The NHEJ pathway often results in small insertions or deletions (indels), leading to gene disruption. Alternatively, the HDR pathway allows for precise modification of the genome using an exogenous DNA template.

3.11 β-cell differentiation protocols

To better understand and ultimately discover a cure for diabetes, the scientific community tries to decipher how the pancreatic islets, TFs and hormones, behave in different conditions, especially during embryogenesis. Elucidation of the mechanisms behind pancreatic islet formation, hormone production, and secretion will provide researchers with tools to overcome DM. The *in vitro* generation of islet-like aggregates from hiPSCs shows similar differentiation stages as the pancreatic islets during *in vivo* embryogenesis. They allow for the generation of islet-like aggregates, which serves as an excellent model for understanding the root causes of DM. By contrast, cell replacement in the pancreas can be achieved through stem cell differentiation (Kopp et al., 2016).

Several β-cell differentiation protocols have been developed over the last decade. Two of these protocols have generated much attraction based on the quantity of β-cells generated as well as their ability to respond to high glucose concentrations. One of these protocols is from the Melton laboratory (Pagliuca et al., 2014). Here, the authors were able to generate cells capable of producing and secreting insulin. At the same time, these cells were able to respond in a limited way to glucose stimulation. Transplantation of the

generated cells into mice reduced hyperglycemia. Another β-cell protocol was developed around the same time by the Kieffer group (Rezania et al., 2014). This protocol very well describes the seven stages of differentiation towards β-like cells.

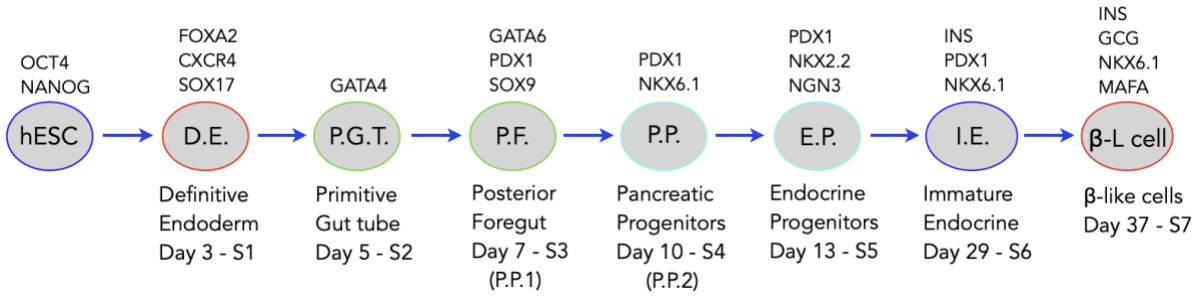

Figure 9. Seven Stages of the β-Cell Differentiation Protocol for Generating Immature Islet-Like Aggregates and Key Marker Expression of Pancreatic Endocrine Cells. This figure illustrates the seven stages involved in the differentiation protocol for β-cell generation, leading to the formation of immature islet-like aggregates. The stages include definitive endoderm, primitive gut tube, posterior foregut, pancreatic progenitor, endocrine progenitor, immature endocrine, and β-cell stages. Throughout the differentiation process, key markers specific to each stage are expressed by the differentiating pancreatic endocrine cells. These markers serve as indicators of the progression and maturation of the cells during the differentiation protocol.

Current protocols can generate the α- and β-cells present in the pancreatic islets (see Figure 9). However, *in vitro* generated β-cell are functionally immature, as shown by impaired glucose-stimulated insulin secretion (GSIS) compared to human pancreatic islets. Consequently, their therapeutic application for β-cell replacement, diabetes disease modeling, and drug screening is currently limited (Kroon et al., 2008; Rezania et al., 2012; Pagliuca et al., 2014). However, IPSC-derived β-cells can mature when transplanted into mice and exposed to an *in vivo* environment, although the maturation *in vivo* could take several weeks and delay the functionality of these cells. It is imperative to produce IPSCs-derived β-cells that mimic as well as possible the *in vivo* counterpart. Therefore, the protocols must keep improving (Rezania et al., 2013; Kelly et al., 2011; Vegas et al., 2016). The formation of functional human islets is determined by the proper ratio of different endocrine cell types (Borden et al., 2013). The islets go through several crucial TF activations and inhibitions at various development stages to achieve the ideal endocrine cell composition (Augsornworawat et al., 2020). The proportion of β-cells and other cell types in the aggregates generated *in vitro* is critical for functionality after transplantation.

3.12 Aims of the thesis

Pancreatic islet cell transplantation has been a clinical viable approach for over two decades, owing to the establishment of the Edmonton protocol (Shapiro et al., 2020; NEJM). Despite the safety and minimally invasive nature of isle transplantation therapy, a scarcity of available organ donors remains a major hurdle. Consequently, generating β-cells and islet cells from pluripotent stem cells could overcome the organ shortage and provide an unlimited source of donor cells for islet cell replacement therapy.

The aims of this Ph.D. thesis were multifaceted and can be summarized as follows. Firstly, the primary objective was to establish an iPSC/hESC differentiation protocol that is highly efficient in generating large quantities of β-like cells. Secondly, the focus was on optimizing the *in vitro* differentiation process, closely monitoring the induction of endocrine cells, and accurately tracking the allocation of α- and β-cells. To achieve this, a novel $ARX^{nCFP/nCFP}$ hiPSC reporter cell line was generated, enabling the precise study of α- and β-cell fate allocation. Moreover, the aim was to further enhance the existing β-cell differentiation protocol to ensure its efficiency and scalability for the production of SC-islets. Concurrently, an extensive screening process was conducted to identify and characterize novel molecules involved in the regulation of endocrinogenesis and α-, β-cell lineage allocation from pancreatic progenitors.

Through these combined efforts, the thesis aimed to make contributions to the successful generation of substantial quantities of β-cells from human embryonic stem cells (hESCs), which would significantly contribute to the treatment of DM. The central focus of this thesis was to develop an effective approach for the *in vitro* generation of β-cells in culture.

4. Results

4.1 Establishment of a modified differentiation protocol for enhanced aggregate production

The conventional monolayer differentiation protocol presents limitations in terms of generating a large number of pancreatic progenitors, endocrine progenitors and hormone-producing islet cells from hPSCs, hindering high-throughput screening and transplantation experiments for *in vivo* testing. This study aimed to develop a modified 3D suspension differentiation protocol to generate a substantial quantity of homogenous aggregates with consistent size and shape. The existing differentiation protocol, as described by (Rezania et al., 2014), begins in a monolayer format until day 10, after which the protocol transfers the differentiation to a suspension format. Due to the cells' initial growth as a monolayer, only about 20 to 40 aggregates can be formed from one 10 cm plate. Moreover, these aggregates exhibit varying sizes and are grown in air-liquid interface culture on filters, complicating subsequent analysis and transplantations.

To address the limitations of the conventional protocol, we developed a modified 3D suspension differentiation protocol. We cultured aggregates in suspension starting from the pluripotent stage and throughout the differentiation process towards definitive endoderm, pancreatic progenitors, and islet-like cells (Fig. 10). Our modified protocol employed the same small molecules and factors as the original Rezania protocol. However, to generate a large number of aggregates, we incorporated a partial modification of the original protocol: On the first day of the differentiation, we utilized StemMACS iPS-Brew XF medium instead of the MCDB 131 medium supplemented with sodium bicarbonate, Glutamax, and glucose. This medium modification facilitated the formation of robust aggregates. Additionally, we differentiated our aggregates using an orbital shaker operating at 75 revolutions per minute (RPM) and six-well-low attachment plates to prevent cell-matrix adhesion, which enabled the formation and maintenance of 3D aggregates. These modifications allowed for the generation of more than 400 homogeneous 3D aggregates per well in a 6-well plate. These 3D aggregates measured 150 to 200 µm in size and could be sustained in a healthy state for over 40 days during the step-wise differentiation protocol.

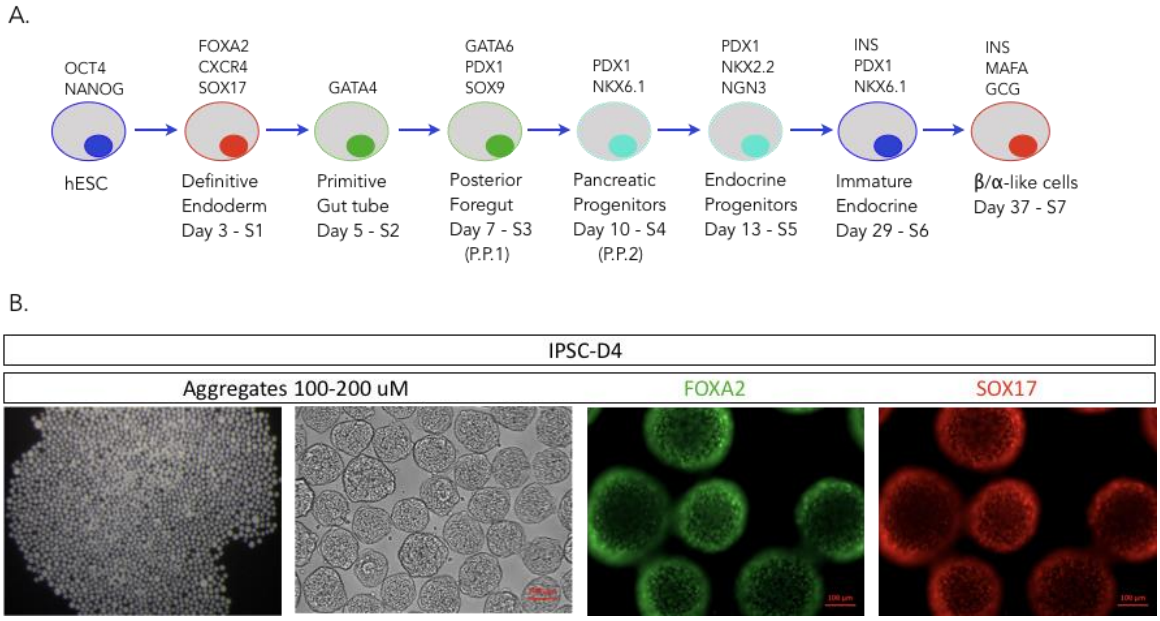

Figure 10. Differentiation protocol for generating islet-like aggregates. (A) Schematic representation of the 3D suspension differentiation protocol, adapted from (Rezania et al., 2014) protocol. (B) Substantial production of aggregates generated in low-binding 6-well plates. Representative immunofluorescence images of aggregates at day 4 of the differentiation process, exhibiting positive expression for definitive endoderm TFs FOXA2 and SOX17. Scale bar 100 µm.

Our modified protocol generated more than 400 homogeneous aggregates per well in a 6-well plate, measuring 150 to 200 µm in diameter, with roughly 1,000 cells per 100 µm aggregate. In contrast, the original protocol produced only 20 to 40 aggregates from 20 million cells (1 x 10 cm plate), with varying sizes larger than 150 to 200 µm. The 150 to 200 µm size of the 3D aggregate turned out to be optimal for perfect nutrient and growth factor supply and to avoid a diffusion barrier. During the definitive endoderm stage, our protocol produced a high percentage of $FOXA2^{+}/SOX17^{+}$ endoderm cells, with aggregates exhibiting consistent shape and size. The induction factors and concentrations employed in our modified protocol were identical to those reported in the previously published *in vitro* differentiation protocol by (Rezania et al., 2014) (refer to Figure 10 and Materials & Methods). The modified 3D suspension differentiation protocol offers numerous advantages, primarily in terms of quantity and homogeneity of material generated. It facilitates the formation of a substantial number of similarly sized aggregates that are easily collected, thus overcoming the limitations of the conventional protocol. This enhanced aggregate production enables more efficient execution of high-throughput screening, glucose-stimulated insulin secretion (GSIS) analysis, fluorescence-activated

cell sorting (FACS), and transplantations experiments, paving the way for advanced research and therapeutic applications in diabetes.

Parameters	(Rezania, 2014) Mono-Layer	(Modified Protocol) Suspension
Format	10 cm plate	1 well of 6 well plate
Starting number of cells	~20 Million of cells	1.5 million cells
Medium volume/day	10 ml	4 ml
Number of aggregates generated	20 to 40	400 plus (2400/6 well plate)
Application	Experimental work	Experimental work Screening Transplantation

Table 1. Comparison of the Rezania 2014 Protocol and Our Modified Suspension Differentiation Protocol. This table provides a detailed comparison between the Rezania 2014 protocol and our modified suspension differentiation protocol. It highlights key parameters, including the plate format of the protocols, the starting number of cells, the daily volume of medium used, the number of aggregates generated, and the applications of the protocols. The table allows for a side-by-side evaluation of these parameters, enabling researchers to assess the differences and potential advantages of our modified protocol compared to the original Rezania 2014 protocol.

In this study, we compared the conventional differentiation protocol outlined by (Rezania et al., 2014) with our modified suspension differentiation protocol, considering several key factors including the plate format, the number of cells used to initiate differentiation, the medium quantity, the number of aggregates generated, and the application of these aggregates (see Table 1). Our findings demonstrate that the 3D differentiation protocol, which employs fewer starting cells and a smaller volume of medium compared to the original 2D/3D protocol, significantly simplifies the method and reduces the culture and differentiation cost while improving the quality of the resulting aggregates and the overall efficiency and applicability of the process.

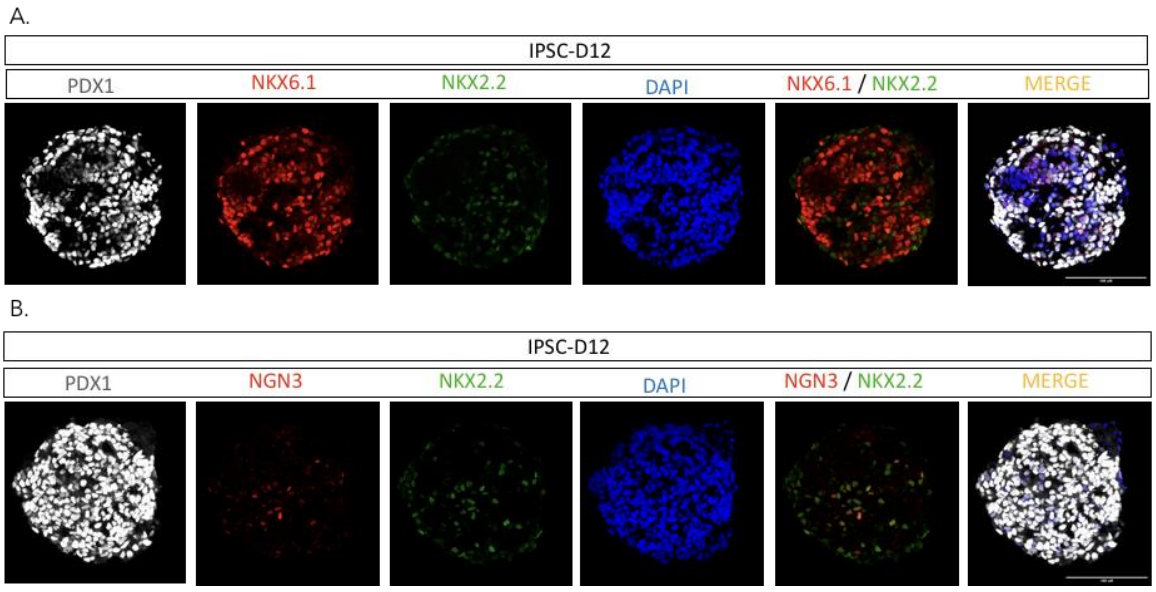

Figure 11. Immunofluorescence Analysis of 3D Aggregates at Pancreatic Progenitor Stage. Representative immunofluorescence images of 3D aggregates at day 12 of differentiation, specifically at the pancreatic progenitor stage (PP2) - (S4). (A) The images demonstrate the high expression of transcription factors PDX1 and NKX6-1 in the 3D aggregates (n=30 aggregates). (B) The images reveal a limited number of NGN3-positive cells present in the 3D aggregates at the pancreatic progenitor stage (n=30). Scale bar: 100 µm.

The pancreatic progenitor stage is crucial for β-cell formation due to the appropriate expression of the TFs PDX1^{+}/NKX6-1^{+} (Pan et al., 2011). We investigated the expression of the TFs and other relevant markers during the pancreatic progenitor stage in aggregates differentiated using our modified suspension differentiation protocol (Fig. 11). Aggregates were differentiated and harvested on day 12, during the pancreatic progenitor stage. The 3D aggregates were cryosectioned and immunostained using markers anticipated to be present at this stage. As expected, 3D aggregates exhibited a high number of PDX1^{+}/NKX6-1^{+}cells. We observed few positive cells of the pan-endocrine TF NKX2-2, which was not anticipated at this early differentiation stage. Additionally, we detected several positive cells for the TF Neurogenin 3 (NEUROG3 or NGN3), a master regulator of endocrine cell induction (Gradwohl et al., 2000; Villasenor et al., 2008). Our findings suggests that endocrine induction does not synchronously initiate suddenly on day 15 of the differentiation, but rather occurs asynchronized throughout the stage 5 differentiation process. At stage 5, some cells began to express TFs NGN3 and NKX2-2 as early as day 12 of the differentiation. The high expression of PDX1^{+}/NKX6-1^{+}cells is indicative of a high number of ductal/endocrine progenitors, previously shown to generate numerous polyhormonal cells, thought to be wrong specified cell types (Nostro et al.,

2015). However, it is now well known that these cells represent α-cell progenitors that resolve over time into monohormonal Gcg-expressing α-cells (Veres et al., 2019) (see Figure 11). These results provide valuable insights into the dynamics of endocrine induction and lineage allocation dynamics during the differentiation process.

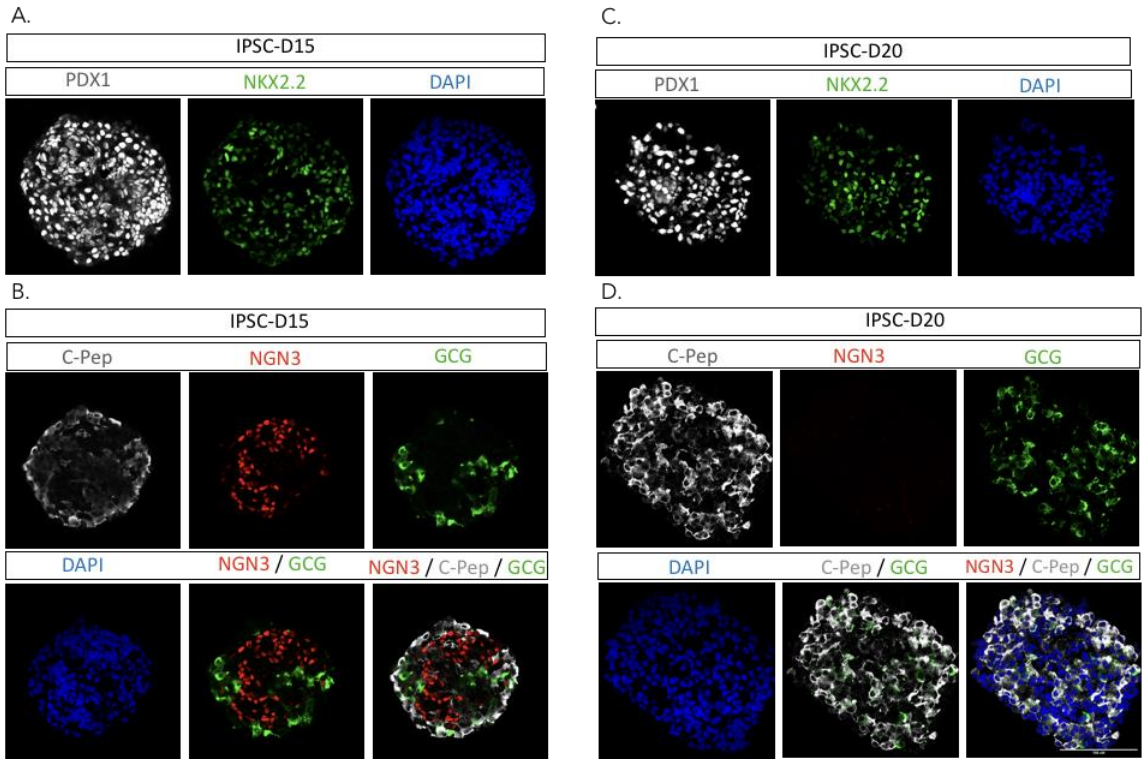

Figure 12. Representative immunofluorescence images of aggregates at endocrine progenitor stage (EP) – (S5) day 15 of differentiation and hormone positive stage – (S6), day 20 of differentiation. (A) 3D aggregates were expressing high levels of TF NKX2-2 in comparison to day 15 (n=30 aggregates). (B) Transient expression of NGN3 noticeably increases at d15, when we believe it is selected for endocrine induction (n=30). Aggregates also began to express insulin and glucagon. Scale bar 100 µm. (C) Expression of the TF PDX1 and the pan-endocrine TF NKX2-2 on day 20. (D) 3D aggregates at day 20 shown no expression of endocrine regulator NGN3 (n=30). High expression of the C-peptide (C-pep) and glucagon (GCG). Scale bar 100 µm.

The endocrine progenitor stage, characterized by the transient expression of the TF NGN3, and the immature hormone positive α- and β-cell stage, known for the high expression of immature insulin-and glucagon-producing cells, are essential steps in α- and β-cell formation (Pagliuca et al., 2014; Russ et al., 2015). We evaluated the expression of relevant TFs and hormones during these stages in aggregates differentiated using our modified suspension differentiation protocol (Fig. 12). We differentiated and harvested the aggregates on day 15 and day 20. Following our modified protocol, aggregates were cryosectioned and immunostained. We analyzed the expression of TFs

PDX1, NKX2-2, and NGN3 as well as insulin and glucagon. On day 15, endocrine progenitors exhibited high expression levels of NKX2-2 and NGN3 (Fig. 12A, B). Interestingly, cells expressing the endocrine master regulator NGN3 appeared at the center of many of the aggregates (see Figures 12B). we observed more NGN3-positive cells than at any other time and we detected the early expression of the hormones INS (C-Pep) and GCG on day 15 of the differentiation (see Figure 12A and 12B). Thus, we considered day 15 in our differentiation the peak of endocrine induction in our differentiation process.

3D aggregates harvested, cryosectioned, and immunostained on day 20 of the differentiation displayed the highest expression of NKX2-2 and the lowest expression of NGN3. It is; worth pointing out that NGN3 is transiently expressed during endocrinogenesis. The reduction of NGN3 expression indicated that the endocrine induction process had ceased, and the hormone-positive stage had commenced. We identified many more INS (C-Pep) and GCG positive cells on day 20 compared to day 15. Additionally, we observed more polyhormonal cells on day 20 than on day 15 of the differentiation (see Figures 12C and 12D).

Our suspension differentiation protocol follows a similar stage-wise differentiation and TF expression dynamics to β-cell formation via endoderm, pancreas, and endocrine progenitors as observed *in vivo* during pancreas organogenesis (Pan et al., 2011) and *in vitro* during hESC differentiation (Rezania et al., 2014; Nair et al., 2020; Russ et al., 2015). We also concluded that the expression of NGN3 is transient, consistent with previous descriptions in mice.

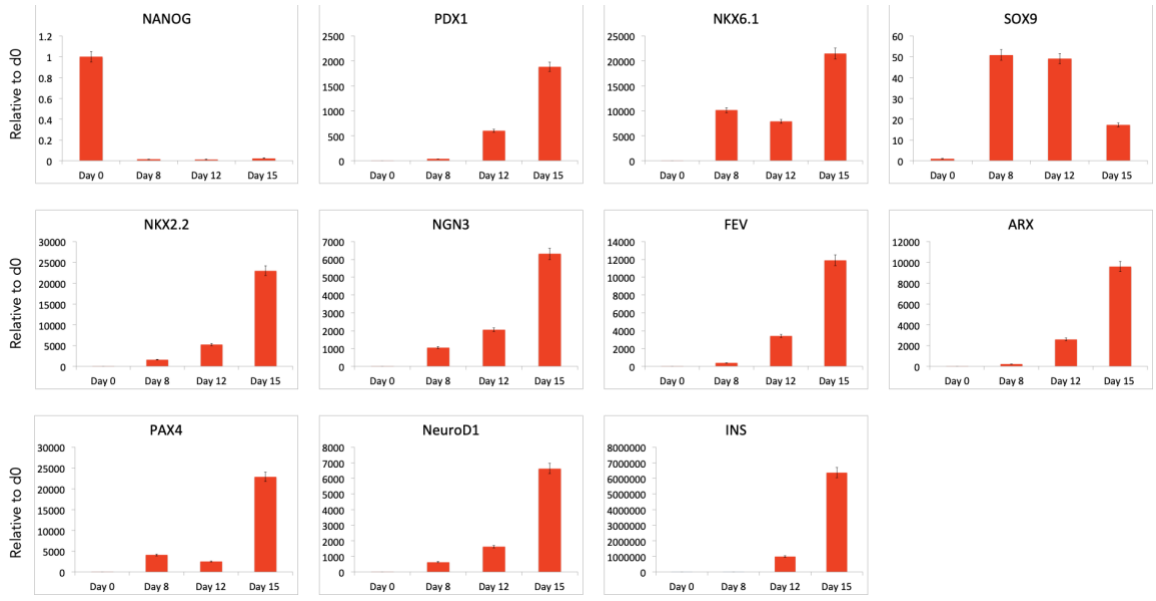

Figure 13. Analysis of gene expression profiles during the modified suspension differentiation protocol at different stages: pluripotent (day 0), posterior gut tube (day 8), pancreatic progenitor (day 12), and endocrine progenitor (day 15). The gene expression levels were assessed using qPCR analysis, with three biological replicates and four technical replicates for each time point in the modified differentiation protocol.

Understanding the gene expression profile during the implementation of our modified suspension differentiation protocol is essential for evaluating its effectiveness in directing cellular differentiation. To test this, we examined the quantitative mRNA expression of critical markers throughout the differentiation process (Fig. 13). We differentiated aggregates and harvested them at the pluripotency stage (day 0), gut tube stage (day 8), pancreatic progenitor stage (day 12), and endocrine progenitor stage (day 15) for quantitative mRNA expression analysis. We performed qPCR analysis to evaluate the temporal induction of genes coding for crucial TFs and hormones, comparing these results to TF and hormone protein production (see Figures 11,12). Our qPCR analysis demonstrated the appropriate temporal induction of the genes coding for critical TFs and hormones. 3D aggregates at day 8, 12, and 15 differentiated adequately and did not contain pluripotent stem cells, as the expression of the pluripotency marker *NANOG* was absent at day 8 onwards (see Figure 13). Although the expression levels of *PDX1*, *NKX6-1*, *NKX2-2*, and *NGN3* increased as differentiation progressed towards the pancreatic and endocrine fate, the expression levels of TF *SOX9* (a marker for the ductal progenitors) decreased. The downregulation of *SOX9* and the upregulation of *NKX6-1* from bipotent to endocrine primed pancreatic progenitors are consistent with previous findings in mouse pancreas development (Nair et al., 2015; Cerf et al., 2015). We also observed the early

appearance of insulin-expressing β-cell progenitors (see Figure 13). We concluded that our suspension differentiation follows a step-wise differentiation process from pancreatic to endocrine to hormone-producing cells, as has been shown previously (Rezania et al., 2014). This gene expression analysis confirms the efficacy of our modified protocol in guiding cellular differentiation and supports its potential for further development and application in the generation of functional pancreatic and endocrine cells.

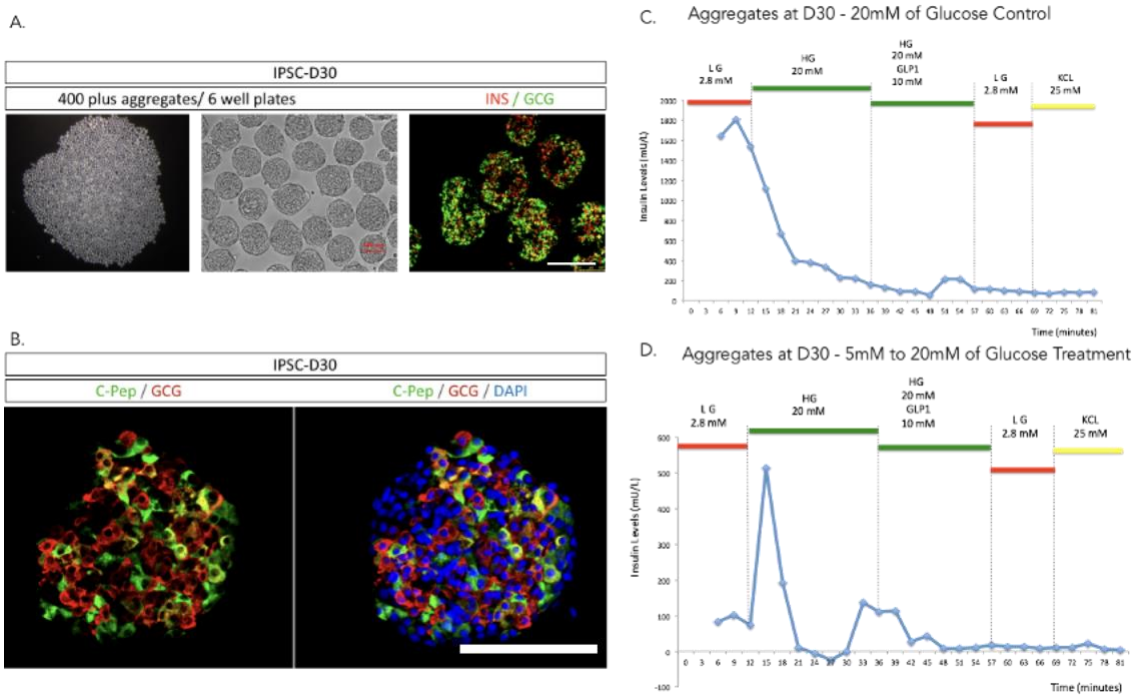

Figure 14. Aggregates at the α/β-like cell stage – (S7) stage, day 30 of differentiation. Glucose stimulation insulin secretion (GSIS) test. (A) Representative immunofluorescence images of aggregates after 30 days of differentiation, our modified protocol showed high aggregates survival rate, generating around 400 aggregates per well of a 6 well format. (B) Representative immunofluorescence images of aggregates expressing C-peptide and glucagon at day 30 of differentiation (n=30 aggregates). Scale bar 100 µm. (C) Aggregates were cultured and harvested to perform the dynamic GSIS (n=2). Control sample were culture at 20 mM of glucose (n=20 aggregates). (D) Aggregates were treated with cycles of high and low glucose concentrations, ranging from 20 mM to 5 mM of glucose (n=20 aggregates).

The generation of functional pancreatic β-cells from stem cells has been a promising approach for diabetes treatment. Our modified suspension protocol generated around 400 evenly sized 200-250 µm smooth round aggregates per well in a six-well plate (see Figure 14A). These aggregates consisted of approximately in equally amount of INS-expressing cells and glucagon-positive cells, other cells like polyhormonal and progenitor cells would be present in lower percentage (Da Silva Xavier et al., 2018; Rorsman et al., 2018) (see Figures 14A and 14B). To evaluate the functionality of the β-cells within these aggregates,

we conducted glucose-stimulated insulin secretion (GSIS) test. GSIS is a test based on the ability of the glucose to elicit rapid insulin release through glucose-coupling. The test measures the ability of the β-cells to sense the presence of high glucose levels and release insulin adequately. SC-derived islet aggregates or pancreatic mouse or human islets are exposed to low glucose (2.8 mM), where no insulin should be released, followed by a high glucose challenge (20 mM), where the β-cells should secrete insulin. Further secretagogues can also be included in a GSIS to test the response of β-cells to the incretin hormone glucagon-like peptide 1 (GLP-1) that amplifies insulin secretion. Whereas KCl will lead to rapid membrane depolarization and release of the insulin stores. During the normal course of differentiation process, we used 10 mM of glucose from day 1 of the differentiation to day 10. After day 10, we used 20 mM until the end of the differentiation. The regular glucose exposure in human islets is around 3 mM and in mouse 5 mM before food intake. In both human and mouse, insulin secretion is half-maximal at 10 mM to 12 mM glucose and saturates at glucose concentrations above 20 mM (Rorsman et al., 2018). However, our differentiation protocol exposed aggregates to supraphysiological levels of glucose of 20 mM.

As a high glucose level is critical in forming insulin-producing cells (Plecita-Hlavata et al., 2020), there was the question on whether or not to use high glucose levels in the differentiation process. To resolve this, we performed an experiment in which we exposed aggregates to cycles of high and low glucose concentration to adopt the cells to fasting and feeding cycles. We based our system on the observation that during fetus formation, the mother goes through pre- and postprandial periods that alter glucose levels from 3 mM to 7.5 mM (Kautzky et al., 2019). After day 20 of the differentiation, approximately 30% to 40% of INS-positive cells had been produced. We started treatment cycles by reducing the glucose concentration to 5 mM for four hours each day, and we treated the cells with 20 mM glucose before returning to 5 mM of glucose. We repeated this cycle for 10 days until day 30 of the differentiation. At that stage, we collected 20 aggregates of control samples and 20 aggregates treated with different glucose concentrations (5 mM and 20 mM). We performed dynamic GSIS in both samples, revealing that samples treated with glucose cycles yielded better results than the control (see Figures 14C and D). The control sample showed the aggregates secreted insulin when exposed to 2.5 mM glucose but were depleted and unable to secrete insulin when the glucose concentration was increased to 20 mM and GLP1 was added. In contrast, sample treated with cycles of high and low glucose concentration maintained insulin secretion during the low glucose

concentration (2.8 mM) and successfully secreted insulin when the glucose concentration was increased to 20 mM and GLP1 was added. Our modified suspension protocol generated β-cells with improved GSIS performance. The application of glucose cycles after day 20 of the differentiation, when most insulin-producing cells were formed, led to better GSIS test results. These findings suggest that our modified suspension protocol is an effective approach for generating β-cells.

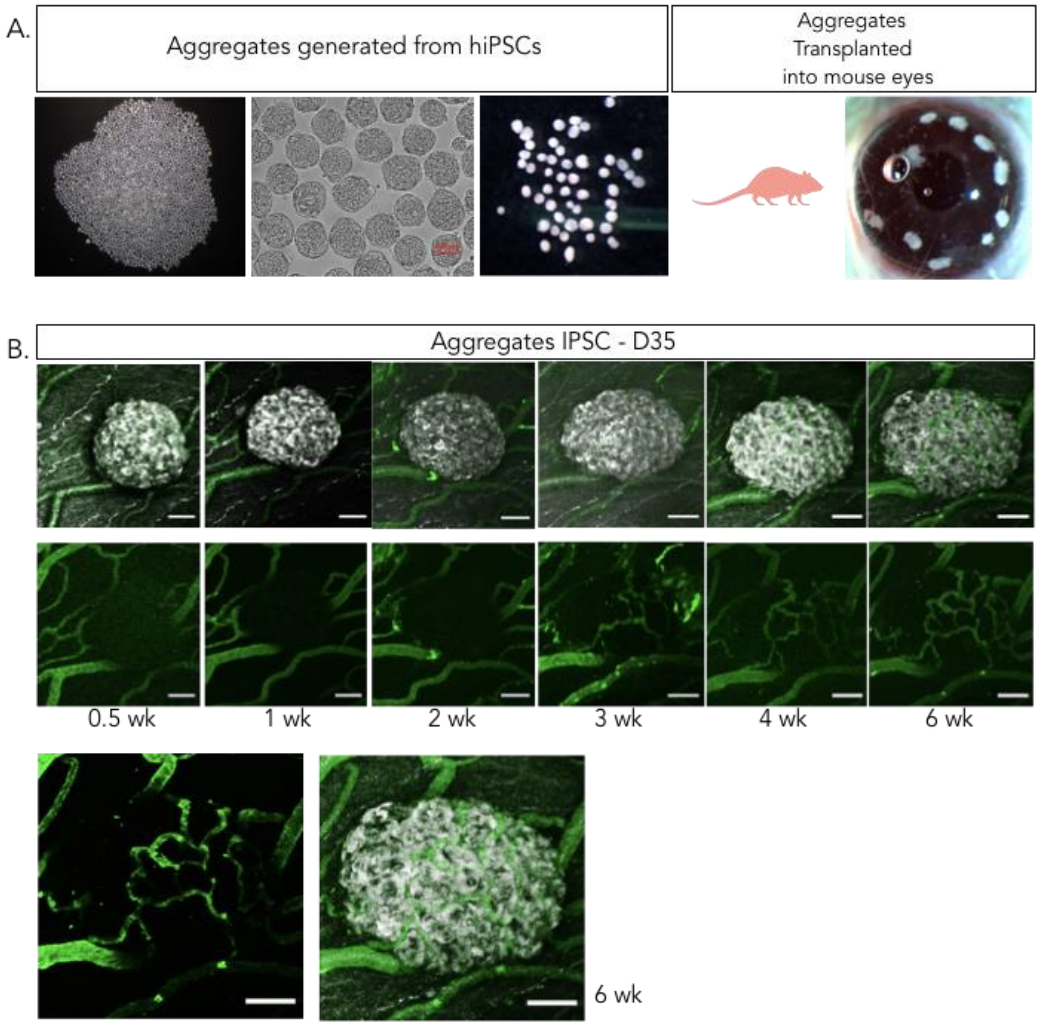

Figure 15. Non-invasive longitudinal live cell imaging of transplanted stem cell-derived islet aggregates in the anterior chamber of the mouse eye. (A) Islet-like aggregates transplanted in the anterior chamber of the mouse eye, shown in a photograph depicting the engrafted aggregates on the iris. (B) Non-invasive live imaging of the transplanted aggregates at different time points after transplantation, with a total of 10 samples analyzed for each time point. Over time, the images capture the process of vascularization and the development of blood vessels around and inside the transplanted aggregates. The green color in the image represents the fluorescent (FITC) labeling of the vascularization. The scale bar represents 25 µm, indicating the size of the imaged area.

We aimed to elucidate the temporal dynamics of vascularization in islet-like aggregates engrafted within the interior chamber of the mouse eye. Furthermore, we recognized that islets are highly vascularized, capable of sensing glucose and secreting insulin into the bloodstream. In addition, an endothelial-endocrine cell interaction is also essential for proper α- and β-cell function. Consequently, we investigated pancreatic progenitor proliferation following transplantation. Simultaneously, we assessed the formation of cysts or acinar differentiation in transplanted aggregates, which could constitute a safety risk for future transplantations.

Our protocol, capable of generating large quantities of the material, enables us to perform transplantations. We know that the transplantation of non-differentiated pancreatic progenitor cells results in the differentiation of the cells into ductal cells, forming lumen and cavities. In the case of transplantation aggregates at an early stage, like endocrine progenitor, we can see proliferation when the graft expands over the weeks. We performed this experiment to assess the aggregates' engraftment and understand the aggregate's survival rate and stability. In collaboration with the Stephan Speier's group at the Paul Langerhans Institute in Dresden, we transplanted stem cell-derived islet aggregates into the anterior chamber of the eyes to test safety and vascularization (Speier et al., 2008). Anterior chamber transplantation offers a unique opportunity to monitor how aggregates adapt to new environments after transplantation, how the cells survive and react the new niche and how long it takes until the islet aggregates are connected to the hosts blood stream (Gotthardt et al., 2020). We previously performed transplantations with differentiated aggregates until day 25, leading to an increase in the aggregates' size; as the relative high number of pancreatic progenitors showed proliferation and likely differentiated into ductal cells forming lumens and cavities. These preliminary results suggested that our islet clusters should be more terminally differentiated to avoid high numbers of pancreatic progenitors. By day 35, aggregates demonstrated minimal or negligible proliferation, and exhibited a substantially higher backscatter, which serves as an indirect indicator of insulin granules and, therefore, insulin content. Backscatter is a physical property in light microscopy, where insulin secretory granules reflect light as a result of their increased density. Consequently, the light undergoes backscattered and does not easily pass through the imaged object. Although this provides an approximation of hormone-positive cells, definitive evidence can only be obtained through insulin staining. Although staining for ductal or acinar markers was not conducted, we noted that these aggregates exhibited limited growth and did not form lumens. Furthermore, we did

not observe significant pancreatic progenitor proliferation or ductal differentiation. Lastly, the aggregates underwent vascularization, a process involving the recruitment of blood vessels, likely mediated by VEGF, which is analogous to the vascularization observed in mouse and human islet transplants within the anterior chamber of the mouse eye (Speier et al., 2008). These transplantation experiments showed the dynamics of the vascularization process and suggested that stem cell-derived islet clusters secrete attraction factors and are likely to be vascularize at any transplantation site (see Figure 15).

4.2 INS-H2B-mCherry/hiPSC reporter cell line re-aggregation and transplantation

To enhance β-cell differentiation and facilitate the detailed investigation of stem cell-derived β-cells, our lab developed a heterozygous fluorescent hiPSC reporter line. This reporter line was generated by targeting the *INS* locus using homologous recombination and CRISPR/Cas9 technology to knock in a T2A-H2B-mCherry cassette, replacing the translational stop codon. This modification allowed for the co-transcription of the cassette and the *INS* gene, as well as T2A-peptide-mediated co-translational cleavage of INS-T2A and H2B-Cherry (Blochinger et al., 2020).

The INS-H2B-mCherry reporter line demonstrated efficient differentiation using our modified suspension protocol (see Figure 38). We observed a remarkably intense nuclear Cherry signal in live imaging, co-expressed in insulin hormone-positive β-cells. On day 18 of differentiation, 15.2% of the aggregates were INS positive (see Figure 40). Re-aggregation of sorted cells on day 20 of the differentiation generated aggregates highly enriched for insulin-positive β-cells (see Figure 16A/B). Preliminary experiments on re-aggregation after day 30 of the differentiation showed the aggregates' tendency to disaggregate.

The novel INS-H2B-mCherry reporter line provides an effective tool for enhancing β-cell differentiation and facilitating detailed investigation of stem cell-derived β-cells. Re-aggregation of sorted cells at day 20 of the differentiation resulted in highly enriched insulin-positive β-cells aggregates, offering valuable insights into β-cell development and potential applications in diabetes research and treatment.

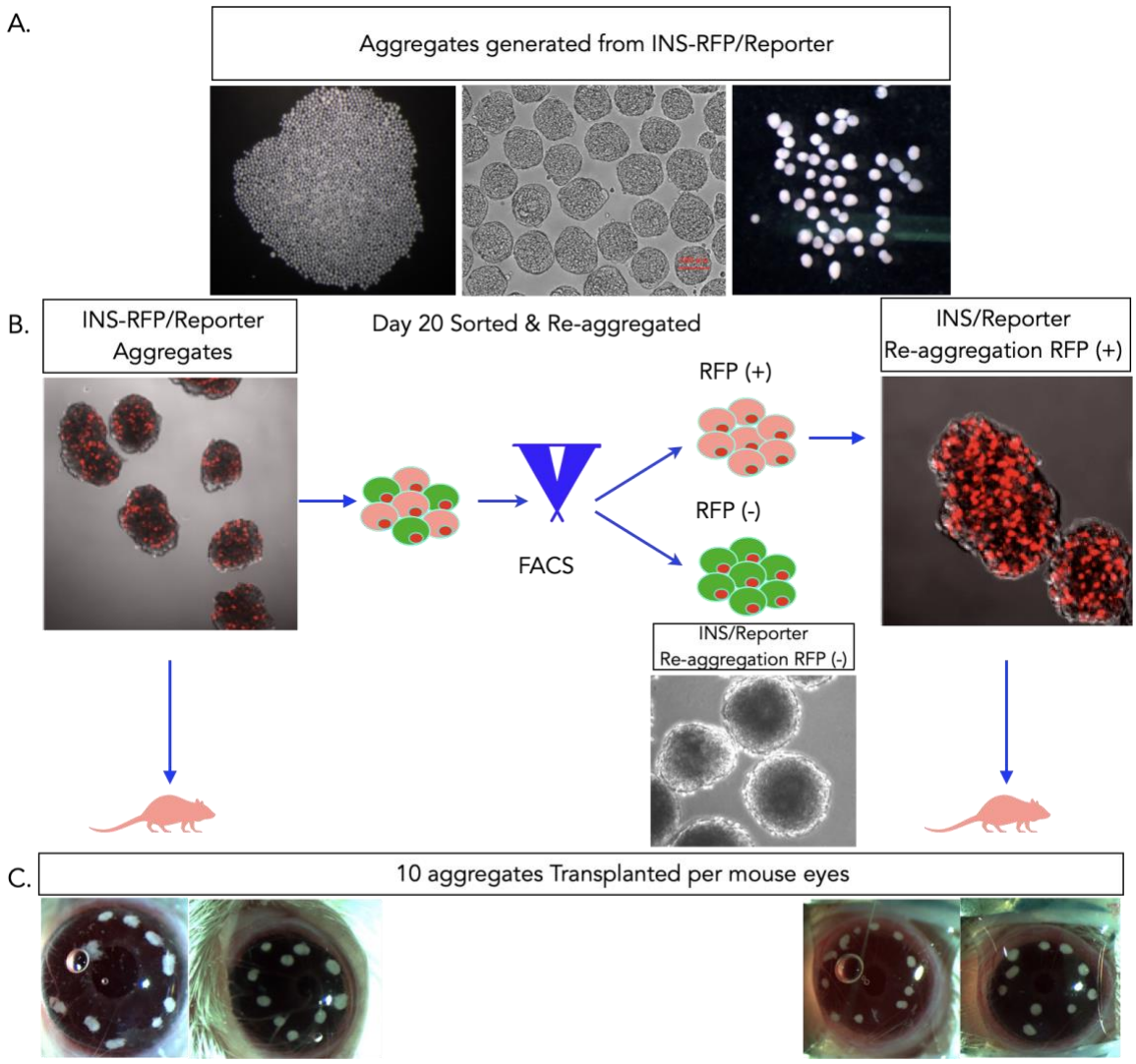

Figure 16. Transplantation of aggregates generated from the INS-mCherry/hiPSC cell line in mouse eyes. (A) The INS-mCherry/hiPSC line successfully generated large quantities of aggregates. Scale bar represents 100 µm. (B) At day 20 of differentiation, aggregates were FACS-sorted into two populations: mCherry-positive INS cells and mCherry-negative non-INS cells. (C) Two batches of aggregates were generated for transplantation: control non-sorted aggregates and aggregates with all INS cells expressing mCherry. The schematic scheme illustrates the experimental setup, and the pictures are not shown to scale.

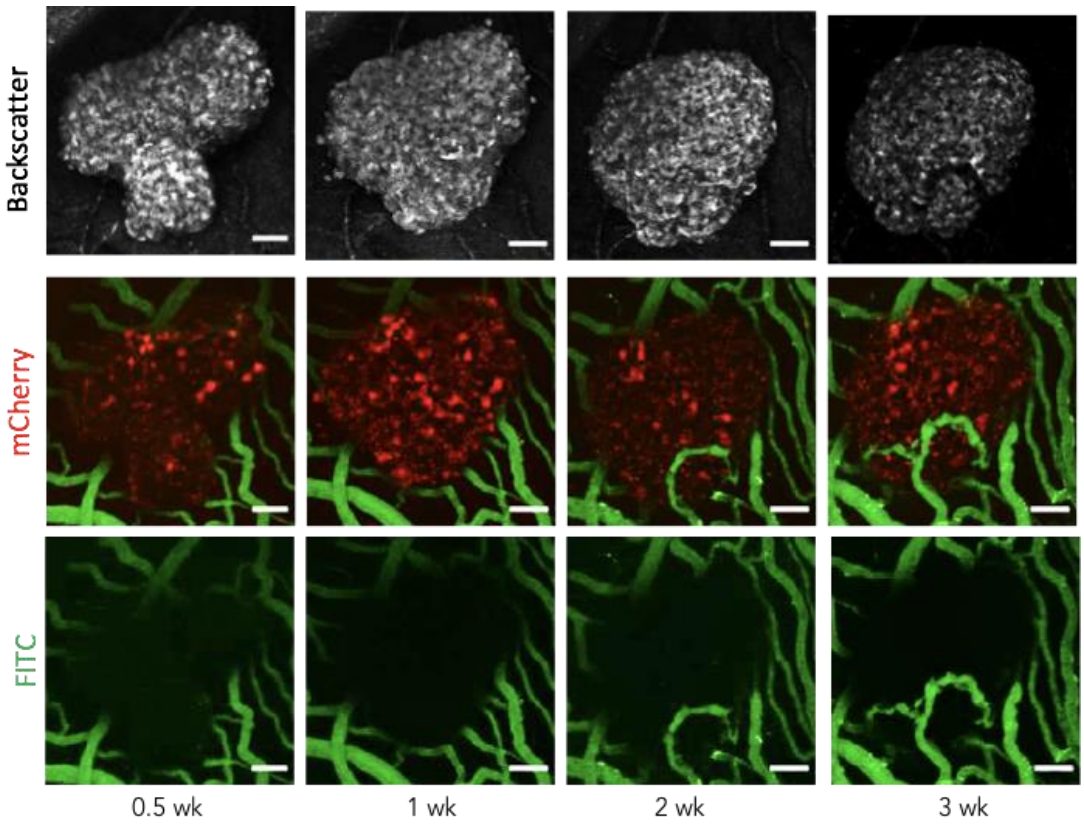

Figure 17. *In vivo* longitudinal live cell imaging of SC-islet engraftment to investigate survival, stability and vascularization of transplanted INS-H2B-Cherry positive β-cells. This figure showcases the weekly monitoring of aggregates transplanted into mouse eyes, observing the time when vascularization occurred. The mCherry expression showed insulin-positive cells, while the intravenous (IV) injection of dextran-fluorescein-isothiocyanate isomer (FITC) enable the staining of blood vessels. The backscatter channel demonstrated light is backscattered, which does not easily pass through the imaged sample, serving as a proxy for insulin granules. Scale bar 25 µm.

The primary objective of this study was to investigate the survival and stability of INS-H2B-Cherry positive β-cells following transplantation, as well as to assess the persistence of reporter activity. Furthermore, we aimed to determine whether there were any differences in vascularization between enriched β-cells clusters and non-enriched β-cell clusters. By exploiting the fact that Zn^{2+} insulin hexamers undergo a phase transition and form insoluble crystals that reflect light, we employed the backscatter of light as a proxy for insulin secretory granules. In addition, we sought to ascertain whether islet-like aggregates and β-cells survived the engraftment process, as hypoxia, endoplasmic reticulum (ER) stress, and inflammatory stress have been reported to cause a loss of up to 50% of an islet graft following transplantation (Rickels et al., 2005). We then differentiated the INS-H2B-Cherry reporter line until day 20 of the differentiation, followed by the disintegration of the aggregates into single cells and FACS sorting into RFP^{+} (INS

cells) and RFP$^-$ (non-INS cells) (see Figure 16 B). We used non-sorted aggregates derived from INS-H2B-Cherry as control and transplanted them along with INS-H2B-Cherry positive β-cells re-aggregated in the anterior chamber of mice eye in collaboration with the Speier group (see Figure 16C). We performed this experiment at three independent time points using different batch of stem cell-derived islets/clusters, transplanting 10 SC-islets per eye and we followed a total of 100 SC-islets in 10 eyes experiment. We conclude that 1) the reporter works well to enrich for the differentiated β-cell population, 2) the β-cells are stable upon transplantation and remain reporter positive over time, 3) no unwanted proliferation and differentiation was observed, and 4) the vascularization happened around 2 to 3 weeks after the transplantation (see Figure 17).

4.3 Generation of *ARX$^{nCFP/nCFP}$* hiPSC reporter cell line for studying α-cells differentiation

Human islets are a mixture of approximate 60% β-cells and 30% of α-cells, with the remainder of 10% δ-cells (somatostatin-producing), γ- or PP cells (pancreatic polypeptide-producing), and ε-cells (ghrelin-producing). These are endocrine cells randomly distributed throughout the islet (Da Silva Xavier et al., 2018). The primary objective was to generate an *ARX$^{nCFP/nCFP}$* hiPSC reporter line to enhance our understanding of α-cell differentiation and elucidate the interactions between α-and β-cells crosstalk during development and physiological processes. The Aristaless-related homeobox (*ARX*) gene, a TF specific to α-cells, is expressed in α-cell progenitors and remains present in mature adult α-cells (Collombat et al. 2005). Given that *ARX* is a X-linked gene, we generated a homozygous reporter line from a female parental iPSC line in order to circumvent mosaic reporter gene expression due to X-linked inactivation. That prompt us to design a targeting strategy to generate a transcriptional and translational reporter for *ARX*, as it uses a 2A-peptide approach for co-translational cleavage. The generation of the *ARX$^{nCFP/nCFP}$* hiPSC reporter cell line was performed by targeting the Arx locus, using homologous recombination and CRISPR/Cas9 technology. We then, created the *ARX*-2A-H2B-CFP-Flag targeting vector by cloning the *ARX* genomic sequence. We introduced a 2A sequence followed by a Histone 2B (H2B), which was fused to the cyan fluorescent protein (CFP) and flowed by a FLAG tag. In this way, the reporter line would translate equal amounts of *ARX* and H2B-CFP-Flag protein, separated by an autonomous intra-ribosomal self-processing of the 2A-peptide from *thosea asigna virus*. Only homozygous

ARX$^{nCFP/nCFP}$ hiPSC clones were selected to avoid mosaic reporter expression due to X chromosome inactivation (see Figure 18A).

The *ARX*$^{nCFP/nCFP}$ hiPSC reporter line expressed the nuclear H2B-CFP (nCFP)-reporter, as illustrated in (see Figure 20B). The populations of α-cells and β-cells exhibit a close interrelationship and mutually regulate each other. Research has demonstrated that neurotransmitters produced by these cells function as paracrine signals, facilitating cross-communication between the cells and modulating pancreatic islet functionality (Rodriguez-Diaz et al., 2014). Our aim was to determine whether stem cell-derived β-cell transplants require only β-cells for proper physiological function or if the presence of stem cell-derived-islets containing both α- and β-cells is necessary. Consequently, we generate stem cell-derived β-cells and stem cell-derived-islets through a tissue engineering approach. This process necessitated the implementation of α- and β-cell differentiation, as well as the sorting of stem cell-derived-α and β-cells. To optimize differentiation and facilitate the sorting of α-cells for analysis, reaggregation, and transplantation, we required an α-cell reporter. We concluded that the *ARX*$^{nCFP/nCFP}$ hiPSC reporter cell line provides a powerful tool for studying α-cell differentiation and the interactions between α and β-cells during development and physiological processes.

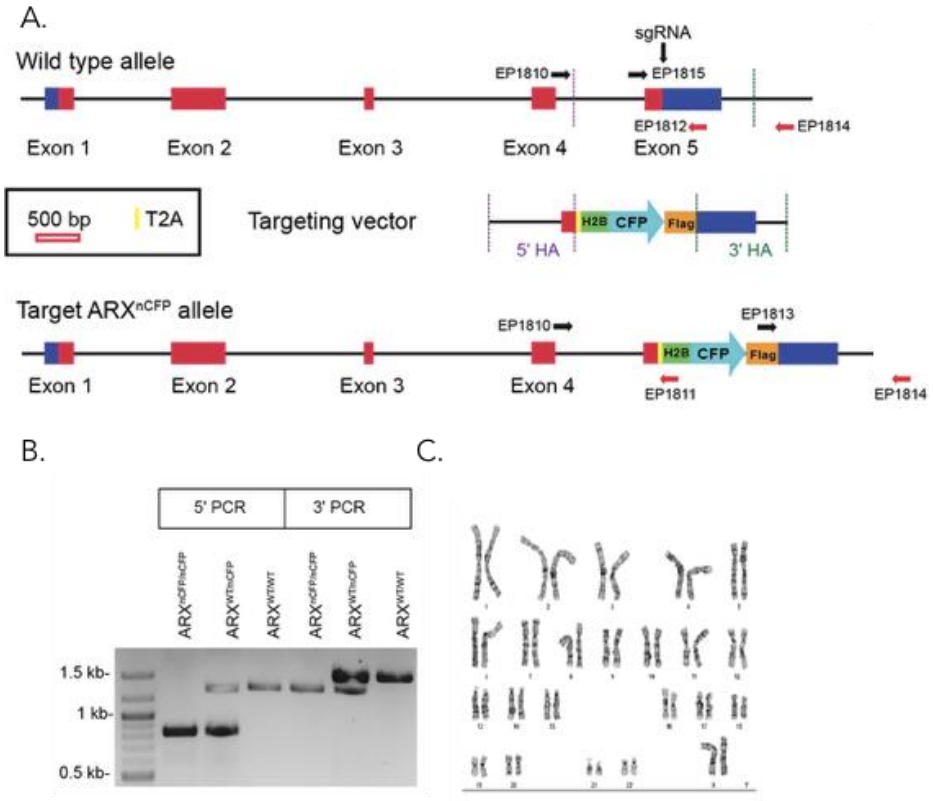

Figure 18. Targeting strategy for the generation and karyotyping of *ARX*$^{nCFP/nCFP}$ hiPSC reporter cell line. (A) Cloning strategy to generate *ARX*$^{nCFP/nCFP}$ hiPSC reporter cells. (B) PCR was confirming 5' and 3' recombination borders after homologous recombination of homozygous clones compared to wild type and heterozygous clones. (C) Normal karyotype (46, XX) of the *ARX*$^{nCFP/nCFP}$ hiPSC reporter clone.

The objective was to confirm accurate integration at the *ARX* locus through homologous recombination and to ensure that *ARX*$^{nCFP/nCFP}$ hiPSC reporter cell line is karyotypically normal. Homologous recombination and accurate integration at the *ARX* locus were confirmed through 5′ and 3′ genomic PCR analyses. The PCR characterization was followed by karyotyping. Chromosomes from *ARX-nCFP* iPSCs' metaphases were classified using the standard G banding technique. We counted approximately 20 metaphases and determined the final karyotype based on the average of 85% of metaphases (see Figure 18C). The 5' PCR demonstrated proper integration of the H2B-CFP and the 5' homology arm, while the ARX $^{wt/wt}$ sample displayed only the ARX 5' arm. In the case of 3' PCR, the integration of the CFP-Flag tag and the homologous 3' arm was observed, whereas the ARX $^{wt/wt}$ sample revealed only the 3' arm (see Figure 18B). Karyotyping analysis showed that the *ARX*$^{nCFP/nCFP}$ hiPSC reporter cell line is karyotypically normal (see Figure 18C). We concluded that the *ARX*$^{nCFP/nCFP}$ hiPSC reporter cell line demonstrated precise and locus-specific integration of the *T2A-H2B-CFP-polyA* reporter cassette and is karyotypically normal. This supports the use of this reporter line for studying α-cell differentiation and the interactions between α- and β-cells during development and physiological processes.

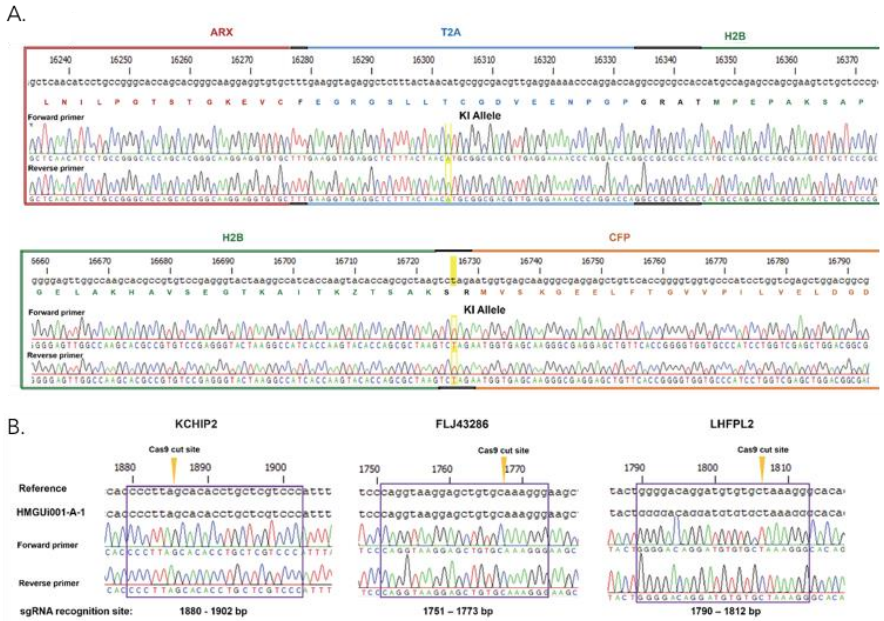

Figure 19. Genomic sequencing to confirm accurate knock-in (KI) of reporter and to avoid off-target effects. Homozygous insertion of T2A-H2B cassette, confirmed by Sanger sequencing. (A) Confirmation of T2A-H2B-CFP downstream of the *ARX* gene. (B) Bioinformatic predicted sgRNA putative off-target sites of *KCHIP2, FLJ43286, LHFPL2.*

The objective was to ensure that the *ARX*$^{nCFP/nCFP}$ hiPSC reporter cell line has no off-target mutations, particularly at the sites with the highest predicted probability. We confirmed the reporter cassette's insertion in the desired location (see Figure 19A). We then analyzed three putative off-target sites for the sgRNA by performing Sanger sequencing to check for any point mutations, deletions, or insertions (see Figure 19B). Sanger sequencing revealed no random mutations at the three putative off-target site analyzed (see Figure 19B). We concluded that the *ARX*$^{nCFP/nCFP}$ hiPSC reporter cell line has likely no off-target mutations, at least at the sites with highest predicted probability. This finding supports the use of this reporter cell line.

Mycoplasma Results

Cell line : ARX $^{nCFP/nCFP}$ hiPSC reporter line Passage number: P23

Test method : Biochemical Luminescence MycoAlertTM Plus Mycoplasma Dectection Kit, Lonza

Reading A : 5232 Reading B : 4127 Ratio (A/B) : 0.78

Comments : Ratios < 0.9 are negative for Mycoplasma
Ratios 0.9 - 1.2 are borderline
Ratios > 1.2 are positive for Mycoplasma

Results : Mycoplasma negative

Table 2. Mycoplasma test performed on *ARX*$^{nCFP/nCFP}$ hiPSC reporter cells at passage 23. Confirming absence of mycoplasma contamination.

The objective was to confirm that the *ARX*$^{nCFP/nCFP}$ hiPSC reporter cell line was mycoplasma-free. Mycoplasma testing was performed using the Lonza MycoAlert Mycoplasma Detection kit (Lonza, Cat. No. LT07-418). The results indicated that the *ARX*$^{nCFP/nCFP}$ hiPSC reporters were mycoplasma free (see Table 2).

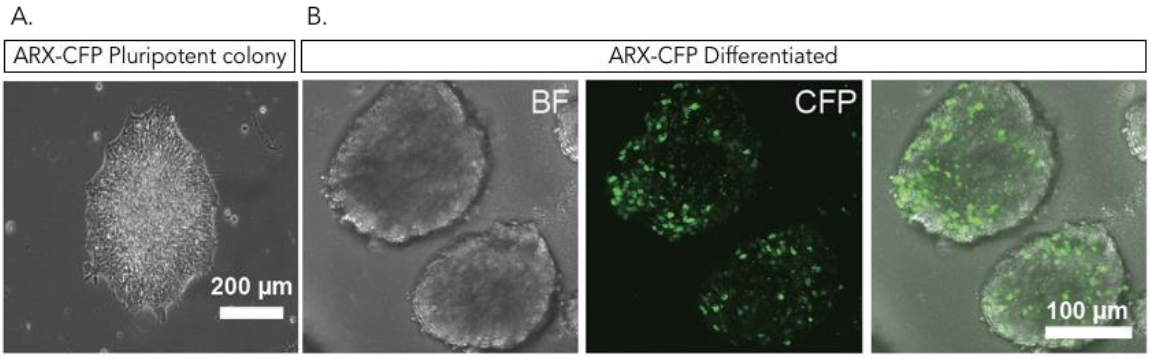

Figure 20. Morphological analysis and utility of the *ARX*$^{nCFP/nCFP}$ hiPSC reporter cell line in studying α-cell differentiation . (A) Phase contrast of *ARX*$^{nCFP/nCFP}$ hiPSC reporter colony at the pluripotent stage. (B) Live image of *ARX*$^{nCFP/nCFP}$ hiPSC reporter at day 21 of the differentiation. Bright-field (BF) channel showing aggregates morphology, cyan fluorescent protein (CFP) channel showing the ARX expression, and merge channel. Scale bar, 100 µm.

We next used the reporter line to facilitate our understanding of the timing and intensity of the ARX TF expression and α-cell lineage formation. We demostrated that the *ARX*$^{nCFP/nCFP}$ hiPSC reporter line enabled the successful isolation of live, positively expressing cells (see Figure 23C). This approach also helped elucidate the upregulation of the ARX TF during differentiation and lineage allocation, as well as the specific cell type in which it is expressed. This reporter line allowed us to accurately determine the time points and cell types associated with ARX expression. By sorting ARX-expressing cells during onset of expression in α-cell progenitors, which are known to be α-cell specific (Collombat et al., 2005), we could observe when ARX progenitors upregulate the hormone glucagon. Profiling the changes at the transcriptional and protein levels enables us to better understand the initiation and determination of α-cell fate.

The morphology of hiPSCs colonies serves as an informative indicator of the cell's pluripotency capabilities, suggesting their potential for self-renewal and multi-lineage differentiation. However, cell morphology alone is insufficient as evidence and requires validation through the analysis of pluripotency TF expression. Selecting a clone that exhibits appropriate morphological characteristics contributes to the successful differentiation of hiPSCs. We showed that the *ARX*$^{nCFP/nCFP}$ hiPSC reporter cell line exhibited proper morphological characteristics and no visual signs of differentiated cells at the pluripotent stage (see Figure 20A). We concluded that the *ARX*$^{nCFP/nCFP}$ hiPSC reporter cell line is morphologically normal at pluripotency stage.

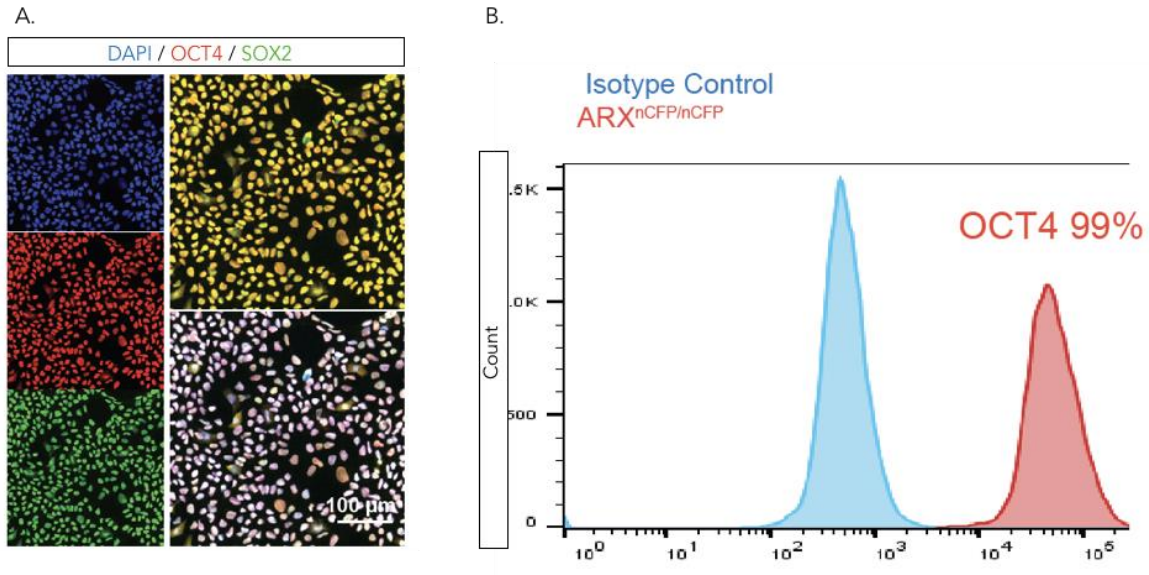

Figure 21. Pluripotency marker analysis of *ARX*$^{nCFP/nCFP}$ hiPSC reporter cell line. (A) Immunostaining showing SOX2 and OCT4 as pluripotent markers in the *ARX*$^{nCFP/nCFP}$ hiPSC at the pluripotency stage. Scale bar, 100 μm. (B) Representative FACS plot of OCT4^{+} cells in the *ARX*$^{nCFP/nCFP}$ hiPSC reporter cells.

To confirm the pluripotency of the newly generated *ARX*$^{nCFP/nCFP}$ hiPSC reporter cell line by analyzing the expression of pluripotency markers, SOX2 and OCT4. Immunostaining was performed to assess the expression of pluripotent TFs SOX2 and OCT4 in *ARX*$^{nCFP/nCFP}$ hiPSC reporter cell line. FACS analysis was conducted to determine the percentage of OCT4^{+} cells in the reporter cell line. Immunostaining exhibited uniform and high expression of both pluripotent TFs SOX2 and OCT4 in almost all cells (Fig. 21A). In addition, FACS analysis showed that 99% of the *ARX*$^{nCFP/nCFP}$ hiPSC reporter cells were positive for OCT4 (see Figure 21B). We concluded that the *ARX*$^{nCFP/nCFP}$ hiPSC reporter cell line expressed pluripotency markers, confirming its pluripotent nature. This validates its potential for self-renewal and multi-lineage differentiation.

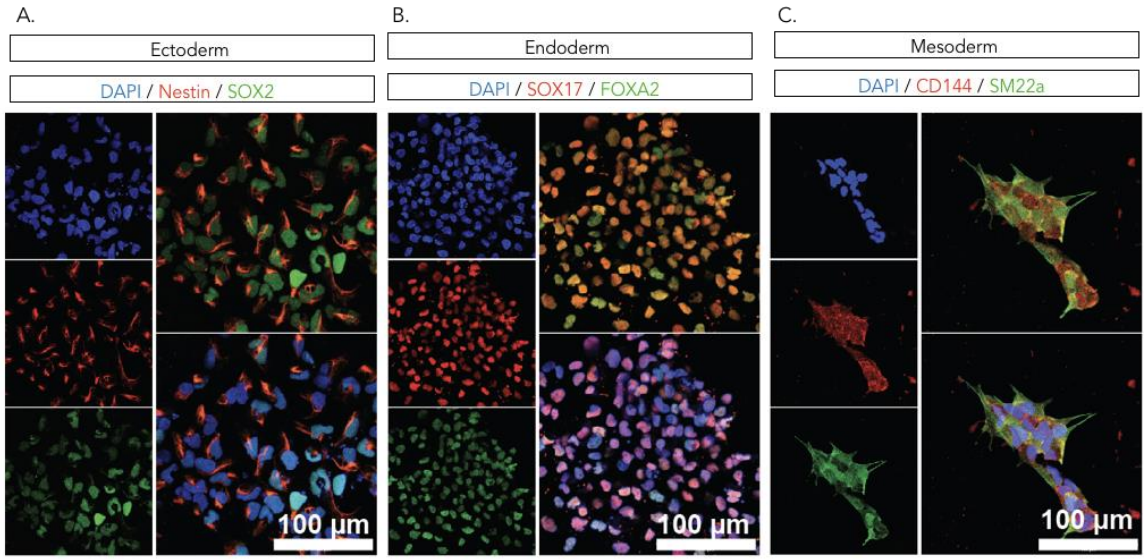

Figure 22. Representative immunofluorescence images of multi-lineage potency assay of *ARX*$^{nCFP/nCFP}$ hiPSC line. (A) *ARX*$^{nCFP/nCFP}$ hiPSC line differentiated towards ectoderm, expressing Nestin and SOX2 positive cells. Scale bars, 100 µm. (B) Reporter line differentiated towards endoderm positive for SOX17 and FOXA2. (C) Differentiation towards mesoderm, CD144 and SM22a positive cells.

The next objective was to validate the pluripotency of the *ARX*$^{nCFP/nCFP}$ hiPSC clone by demostrating its ability to differentiate into all three germ layers: ectoderm, mesoderm, and endoderm. The *ARX*$^{nCFP/nCFP}$ hiPSC line was differentiated into the three germ layers (Fig. 22). After seven days of differentiation, the expression of specific marker proteins for each germ layer was analyzed. Ectoderm differentiation was confirmed by the expression of marker protein Nestin and SRY- homeobox transcription factor 2 (SOX2). Our *ARX*$^{nCFP/nCFP}$ hiPSC line also successfully differentiated towards endoderm, as indicated by high levels of the endodermal TFs *SOX17* and *FOXA2* protein expression. Likewise, we achieved and confirmed mesoderm differentiation by the expression of the marker proteins, CD144 and smooth muscle 22 a (SM22a) (Fig. 22). Showing the *ARX*$^{nCFP/nCFP}$ hiPSC reporter cells conserved the pluripotent capability, as evidenced by successful differentiation into all three germ layers. This further confirms the cell line's potential for self-renewal and multi-lineage differentiation, making it suitable for studying α-cell differentiation.

4.4 Endocrine lineage differentiation of the *ARX*$^{nCFP/nCFP}$ hiPSC reporter cell line

Having established a suitable reporter iPSC, we next wanted to study the temporal ARX reporter expression pattern during α- and β-cell differentiation in generated *ARX*$^{nCFP/nCFP}$ hiPSC line report cell line. Using our modified β-cells differentiation protocol, we differentiated *ARX*$^{nCFP/nCFP}$ hiPSC towards islet-like aggregates. We generated approximately 400 plus aggregates per one well of a six-well plate. Samples were collected on day 8, day 14, and day 21 and performed FACS and qPCR analysis to correlate *ARX* mRNA and H2B-CFP reporter activity. Immunostaining was performed to further investigate α- and β-cell fate specification. At day 21 of differentiation, the aggregates displayed a substantial number of ARX-CFP positive cells, which were visible using phase-contrast and fluorescent live imaging (see Figure 23A). We also demonstrated co-localization of ARX with nCFP reporter at day 21. This co-localization proved that our newly generated *ARX*$^{nCFP/nCFP}$ hiPSC line reports on ARX positive cells and detects both ARX and 2A-H2B-CFP reporter in equal amounts (see Figure 23B). Moreover, homozygous targeting of ARX using T2A-H2B-CFP strategy likely does not influence ARX function by the addition of the C-terminal 22 aminoacid T2A-peptide sequence, as α-cells differentiate at comparable ratios to untargeted iPSC clones. Arx has been shown to be necessary for α-cell differentiation in mice (Collombat et al., 2005).

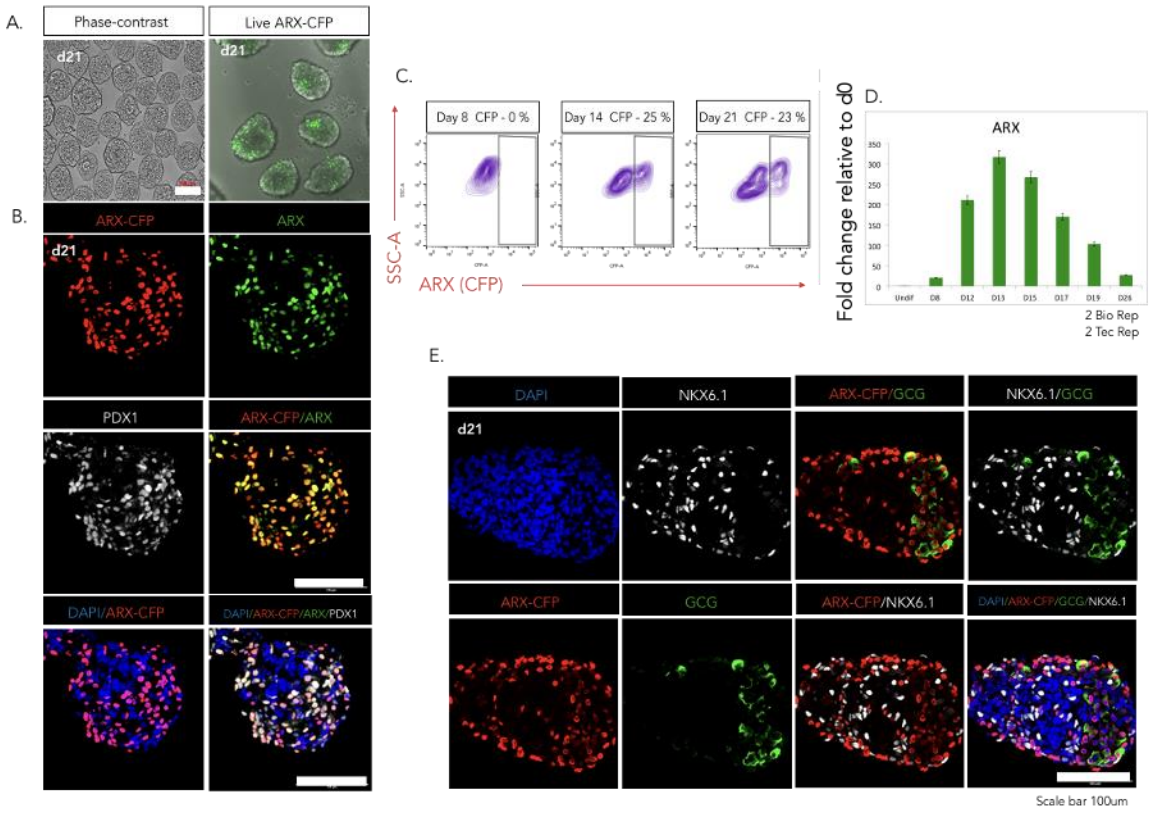

Figure 23. Representative immunofluorescence images of aggregates on day 21, illustrating co-localization of *ARX*$^{nCFP/nCFP}$ hiPSC reporter protein. (A) Aggregates at d21 of the differentiation, phase contrast, and live expression of ARX-CFP. (B) Co-localization of ARX-CFP reporter with endogenous ARX (n=30 aggregates). (C) FACS analysis of the *ARX*$^{nCFP/nCFP}$ hiPSC reporter line at days 8, 14, and 21 shows the nCFP+ cells' appearance as differentiation progresses. N=2 technical replicates from two biological replicates. (D) qPCR analysis revealing the *ARX* expression progression during the differentiation. N=2 technical replicates from two biological replicates. (E) Immunostaining demonstrating the ARX reporter cells to be distinct to the NKX6-1 population at d21 of the differentiation (n=30). ARX cells stained using GFP against CFP. All GCG positive cells are ARX expressing cells, but not all ARX cells are GCG cells. Scale bars, 100 µm.

Samples were collected on day 8, 14, and 21, followed by FACS and qPCR analyses. Day 8 of the differentiation exhibited no reporter activity, whereas day 14 exhibited 25% of H2B-CFP induction. The sample on day 21 revealed 23% reporter-positive cells. Considering that there is peak in mRNA expression during α-cell and β-cell specification. The ARX reporter activity and ARX protein shown more stability after ARX^{+} and the α-cell lineage is specified. The ARX expression may have begun to decline to attain greater co-localization with α-cells. Using a qPCR to verify the FACS results, we found a high mRNA expression on day 13 of the differentiation which decreased towards day 21 (see Figure 23C/D). Immunostaining analysis helped elucidate α-cell progenitor induction (ARX^{+}/GCG^{-}) and α-cell differentiation (ARX^{+}/GCG^{+}). According to literature, during this stage of the differentiation, NKX6-1 is expressed in both β-cells and pancreatic progenitor (PP) cells,

although the latter only shows a small percentage of expression (Nostro et al., 2015). Furthermore, PDX1^{+}/NKX6-1^{+} pancreatic progenitors are primed for endocrine differentiation. Following NGN3-dependent endocrine induction, it is unclear whether the β-cell-specific NKX6-1 TF is rapidly allocated to the β-cell fate. The TF ARX is expressed in α-cell progenitors and their progeny. ARX marks α-cell progenitors (ARX^{+}/GCG^{-}) and remains expressed in mature α-cells (ARX^{+}/GCG^{+}) (Collombat et al., 2005). The literature also describes INS^{+}/GCG^{+} polyhormonal cells, which are thought to resolve into α-cells (GCG^{+}) with extended culture. Interestingly, ARX^{nCFP} , when stained using GFP against CFP, and NKX6-1 were expressed in mutually exclusive manner (Figure 23E). Additionally, all GCG cells were ARX^{nCFP}-positive, although not all ARX^{nCFP}-positive cells were GCG-positive (see Figure 23E). The immunostaining data suggest that a significant number of ARX^{+}/GCG^{-} α-cell progenitors can be detected at this stage of the differentiation. The *ARX$^{nCFP/nCFP}$* hiPSC line reporter cell line provides a valuable tool to study endocrine lineage differentiation, including the specification of α-and β-cells.

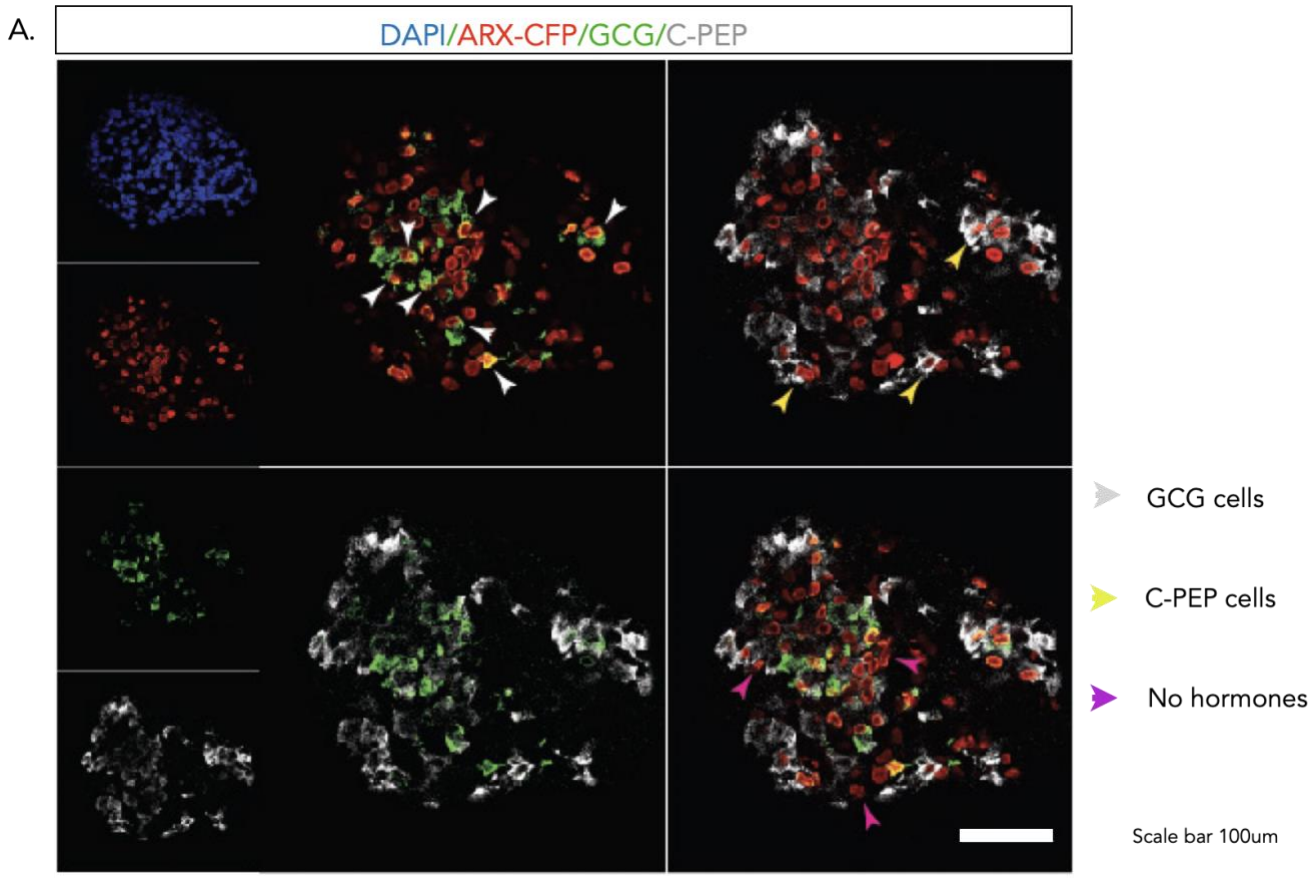

Figure 24. Representative immunofluorescence images of aggregates at day 21, displaying the expression of nCFP in relation to C-Peptide and GCG-positive cells. (A) Immunostaining demonstrating ARX reporter cells stained using GFP against CFP (n=30 aggregates). Scale bars, 100 µm.

Understanding the differentiation of α- and β-cells is crucial for advancing our knowledge of endocrine lineage development. In particular, the role of ARX in cell fate determination and its relationship with other TFs during endocrine lineage differentiation remains unclear. The co-expression of ARX with hormone-producing cells, particularly those displaying a polyhormonal phenotype, raises questions about the role of ARX in cell fate determination during endocrine lineage differentiation. To investigate the role of ARX in α- and β-cell differentiation, we differentiated the *ARX*$^{nCFP/nCFP}$ hiPSC reporter cell line and conducted immunostaining for ARX^{nCFP}, C-peptide, and GCG. We then analyzed the expression patterns of these markers, particularly in cells exhibiting a polyhormonal phenotype, on day 21 of the differentiation. We identified immunostaining on ARX^{nCFP}, C-peptide (yellow arrow), and GCG (grey arrow). Most importantly, some of the cells producing hormones exhibited a polyhormonal phenotype and expressed INS/C-peptide and GCG on day 21 (Figure 24). The immunostaining showed that all GCG-producing cells expressed the ARX^{nCFP} reporter. We also observed that C-peptide-producing cells were positive for ARX^{nCFP}, assuming that the ARX^{nCFP}/C-peptide-positive cells were still plastic and not fate determined, whereas the C-peptide-positive cells with no ARX^{nCFP} expression had committed to the β-cell fate. This data also revealed that α-cell progenitors positive for ARX^{nCFP} exhibit no hormone expression yet (see Figure 24). We concluded that NKX6-1 and ARX have mutually exclusive expression patterns (Figure 23E), suggesting that ARX can only be induced in cells expressing PDX1, but not co-expressing PDX1 and NKX6-1 during the pancreatic progenitor stage. This further suggests that NKX6-1 and ARX may mutually repress each other, similar to what was proposed for ARX and PAX4 by the Collombat group (Collombat et al., 2005).

4.5 *ARX*$^{nCFP/nCFP}$ hiPSC reporter cell line re-aggregation

Dissociation and FACS sorting cells offer significant advantages in distinguishing different cell types. These benefits are further enhanced when using a live reporter line, which enables better understanding of cell behavior during the differentiation process. To determine whether ARX^{+} cells are specified or committed to the α-cell fate, we sorted ARX^{-} and ARX^{+} cells and assessed their fate potential. This was accomplished by using the

ARX$^{nCFP/nCFP}$ hiPSC reporter line, we FACS sorted the ARX^{-} and ARX^{+} cells into two populations on day 18 of the differentiation (Figure. 25A).

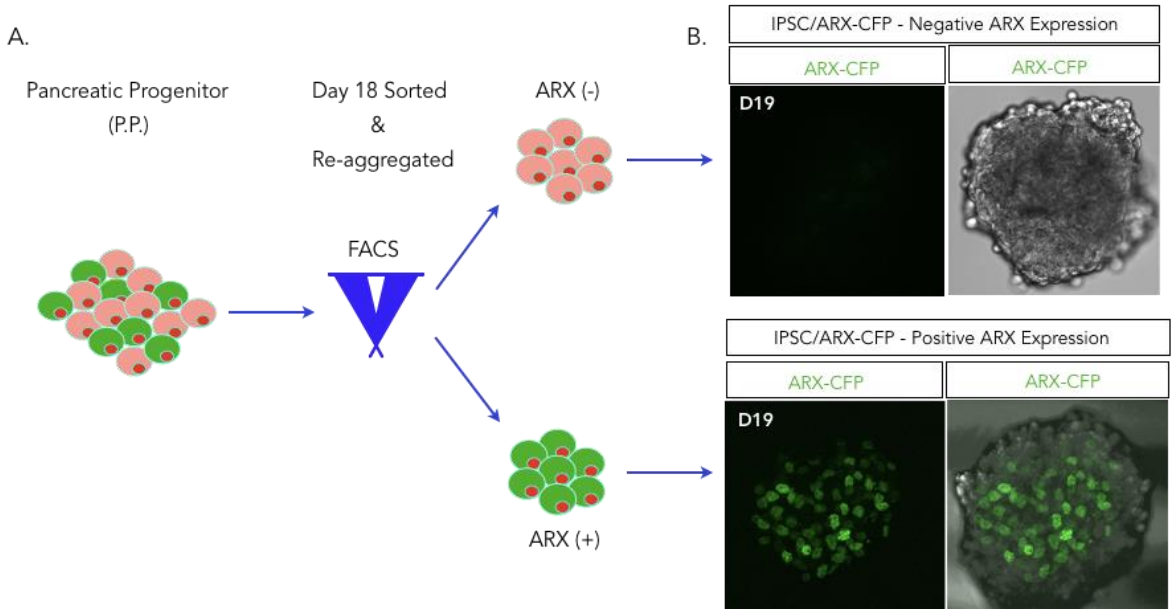

Figure 25. *ARX*$^{nCFP/nCFP}$ hiPSC reporter line sorting and re-aggregation. (A) Schematic representation of *ARX*$^{nCFP/nCFP}$ hiPSC reporter line differentiated to day 18, sorted into ARX-CFP positive and ARX-CFP negative. (B) Live imaging of the re-aggregation of ARX positive and negative sorted cells.

After sorting, we re-aggregated the populations into ARX^{-} and ARX^{+} aggregates. We confirmed that the ARX^{-} population was not expressing the H2B-CFP reporter (see Figure 25B). Our results demonstrate that we successfully generated aggregates where the majority of the cells were ARX^{+} as well as aggregates were the majority of the cells were ARX^{-}. We concluded that, although FACS sorting and re-aggregation at this later stage were technically challenging, they were possible. This approach enabled the generation of aggregates with no predicted α-cell progenitors and aggregates with the majority of the cells predicted to be α-cell progenitors.

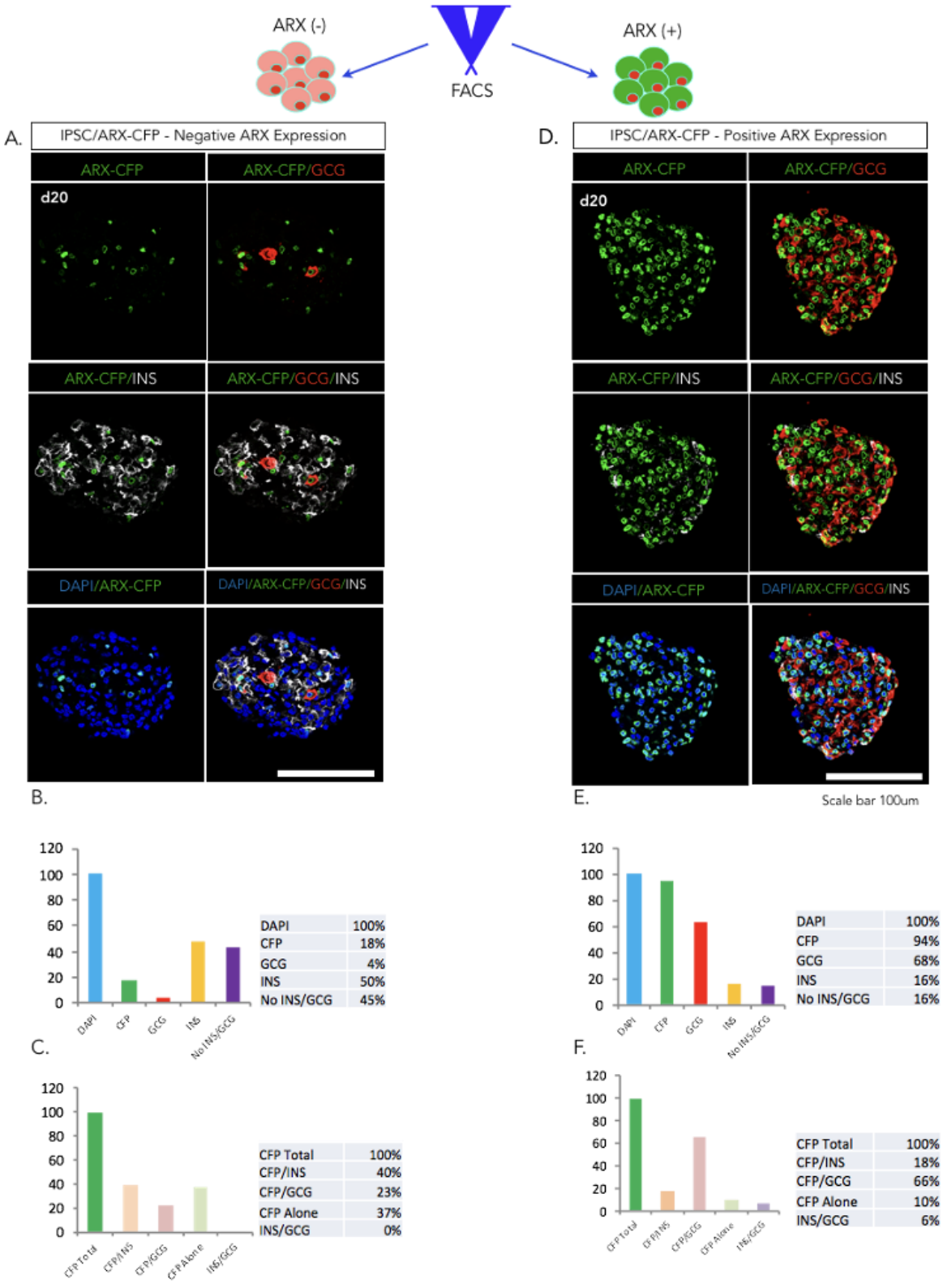
ARX (-)
FACS
ARX (+)
A.
IPSC/ARX-CFP - Negative ARX Expression
ARX-CFP
ARX-CFP/GCG
d20
ARX-CFP/INS
ARX-CFP/GCG/INS
DAPI/ARX-CFP
DAPI/ARX-CFP/GCG/INS
D.
IPSC/ARX-CFP - Positive ARX Expression
ARX-CFP
ARX-CFP/GCG
d20
ARX-CFP/INS
ARX-CFP/GCG/INS
DAPI/ARX-CFP
DAPI/ARX-CFP/GCG/INS
B.
120
100
80
60
40
20
0
DAPI
CFP
GCG
INS
No INS/GCG
DAPI 100%
CFP 18%
GCG 4%
INS 50%
No INS/GCG 45%
E.
Scale bar 100um
120
100
80
60
40
20
0
DAPI
CFP
GCG
INS
No INS/GCG
DAPI 100%
CFP 94%
GCG 68%
INS 16%
No INS/GCG 16%
C.
120
100
80
60
40
20
0
CFP Total
CFP/INS
CFP/GCG
CFP Alone
INS/GCG
CFP Total 100%
CFP/INS 40%
CFP/GCG 23%
CFP Alone 37%
INS/GCG 0%
F.
120
100
80
60
40
20
0
CFP Total
CFP/INS
CFP/GCG
CFP Alone
INS/GCG
CFP Total 100%
CFP/INS 18%
CFP/GCG 66%
CFP Alone 10%
INS/GCG 6%

Figure 26. Representative immunofluorescence images of aggregates expressing C-peptide and glucagon cells in *ARX$^{nCFP/nCFP}$* hiPSC reporter line following sorting and re-aggregation. (A) Immunostaining of ARX-CFP negative cells revealed few ARX positive cells and more C-peptide cells (n=30 aggregates). (B, C) Quantification of re-aggregated ARX negative population, including ARX-CFP α-cells progenitors (ARX= GCG$^-$), α-cells (ARX$^+$/GCG$^+$), polyhormonal (ARX$^+$/INS$^+$). (D) Immunostaining of ARX-CFP positive cells demonstrated enrichment for ARX positive cells, with the majority being glucagon positive cells (n=30). (E, F) Quantification of re-aggregated ARX positive population, encompassing ARX-CFP α-cells progenitors (ARX=GCG$^-$), α-cells (ARX$^+$/GCG$^+$), polyhormonal (ARX$^+$/INS$^+$). Scale bars, 100 μm.

To test whether ARX-CFP reporter negative and positive cells differentiate into non-α- and α-cells, respectively, we FACS sorted on day 18, and we re-aggregated the culture of the aggregates until day 20. At this time, we performed immunostainings of the ARX-CFP positive and negative clusters. The ARX-CFP (-)/re-aggregated population showed few ARX$^+$ cells, which had emerged between days 18 and 20 of the differentiation. Around 23% of these newly formed ARX$^+$ cells showed glucagon expression. The majority of the cells in the aggregates were C-peptide positive (see Figure 26A/B/C). However, 94% of ARX-CFP positive re-aggregated population were ARX-CFP-positive cells and 68% glucagon-expressing cells. These aggregates included 16% of insulin-positive cells, although these insulin-positive cells were also positive for glucagon, thus polyhormonal (see Figure 26 B/E/F). In summary, the *ARX$^{nCFP/nCFP}$* hiPSC line provided the opportunity to sort cells into ARX$^-$ and ARX$^+$ and further assess the differentiation potential of these populations. Taken together, the behavior of ARX$^+$ cells and ARX$^-$ cells suggests that ARX suppresses a β-cell program and promotes α-cell differentiation.

4.6 Screen for factors that regulate endocrine induction and lineage segregation

Islets of Langerhans are innervated for neuronal control of glucose metabolism and are highly vascularized to sense glucose (Brissova et al., 2006). Innervation and vascularization occur early during islet formation and is essential for islet cell differentiation (Reinert et al., 2013). During pancreatic and islet development, epithelial pancreatic progenitors, vascular endothelial cells, neurons and mesenchymal cells condense to form a niche. Niche factors likely influence the growth, proliferation, and differentiation of pancreatic and endocrine progenitors. Surprisingly, β-like cell differentiation protocols exclude niche-derived factors and only incorporate one hormone, Triiodothyronine (T3), despite evidence of hormones and neurotransmitters in the literature as early as E12.5 and E15.5 in mice (Borden et al., 2013). *In vivo*, neurotransmitters reach the islet via innervation after α- and β-cell formation or are being produced and used by the islet's cells

for intra-islet communication after endocrine induction (Molina et al., 2014). The heavy presence of hormones and neurotransmitters during islet development suggests a potential role in endocrinogenesis. However, current differentiation protocols generate hormone-positive cells with limited functionality, indicating the possible omission of factors related to the developing human pancreatic islet cell niche, such as neurotransmitters, hormones, and other extrinsic factors (see Table 3).

Factors	Endogenous Sources	Effects	Molecules	Reference
Acetylcholine	Nervous System and Alpha Cells	Agonist	Acetyl-β-Methylcholine Chloride (1 mM)	(Phillips et al., 2010)
		Antagonist No Selective	Atropine (1 μM)	
		Ach-M3 Antagonist	Darifenacin (1 μM)	
		Ach-M1 Antagonist	Pirenzepine (1 μM)	
Somatostatin	Nervous System, Delta Cells & Intestine	Agonist	SST (100 μM)	(Ballian et al., 2006)
		Antagonist	CYN154806 (10 nM)	
GABA	Nervous System and Beta Cells	Agonist	γ-Aminobutyric Acid (100 μM)	(Feng et al., 2017)
		GABA-R, A Antagonist	Bicuculline (3 μM)	
		GABA-R, B Antagonist	CGP35348 (100 μM)	
GLP1	Alpha Cells and Intestine	Agonist	Exendin 4 (10 nM)	(Pinto et al., 2019)
Glucagon	Alpha Cells	Agonist	Glucagon Recombinant Human (2.8 mM)	(Gage et al., 2014)
Insulin	Beta Cells	Agonist	Insulin Recombinant Human (500 pM)	
Adrenergic System	Nervous System	Agonist	Phenylepine (0.1 nM)	(Kotaka et al., 2017)
Gastrin	Embryonic Pancreas and Stomach	Agonist	Gastrin 1-7 Human (100 nM)	(Banerjee et al., 2018)
Wnt Pathway	Intra-Islet and Vascular System	Agonist	Wnt4 (100 ng/ml)	(Petersen et al., 2018)
Estradiol	Vascular System	Agonist	17-β-Estradiol (10 nM)	(Wu et al., 2017)
Ca 2+	Intra-Islet	Agonist	Calcium Chloride Dihydrate (1 mM)	(Wang et al., 2005)
ATP	Intra-Islet	Agonist	Adenosine 5'-Triphosphate (1 μM) Disodium Salt Hydrate	(Mitchell et al., 2017)
Yap Inhibitor	Intra-Islet	Antagonist	Verteporfin (5 μM)	(Petersen et al., 2018)
DOPA	Intra-Islet and Nervous System	Agonist	Levodopa (200 μM)	(Yorifuji et al., 2014)

Table 3. Screening of Factors with Potential to Enhance Endocrine Lineage Induction.
This table lists factors to be screened for their ability to increase the induction of the endocrine lineage. The factors included are those known to be present during human islet formation but are not commonly utilized in β-cell differentiation protocols, as reported in the existing literature.

To identify novel hormonal and neuronal factors regulating endocrinogenesis, we used our modified suspension protocol and tested 20 factors present during human pancreatic development. We used several publications to generate a list of the 20 extrinsic factors with known functions and potential roles during early human pancreatic islet formation (Banerjee et al., 2018; Phillips et al., 2010; Pinto et al., 2019). They are mainly agonist and antagonist of neurotransmitters, hormones, and extrinsic factors present in direct contact with endocrine induction and/or the islet cell niche. To perform the screen, we differentiated around 400 aggregates from one well of a six-well low binding plate. On the initial day of treatment, we redistributed 20 aggregates per well into a 24-well low-binding

plate, administering the various triggering molecules during four distinct time intervals: day 5 to day 8, day 8 to day 11, day 11 to day 14, and day 14 to day 17. The decision to utilize a smaller plate format, specifically a 24-well low-binding plate, was driven by the need to substantially reduce experimental costs (see Table 4).

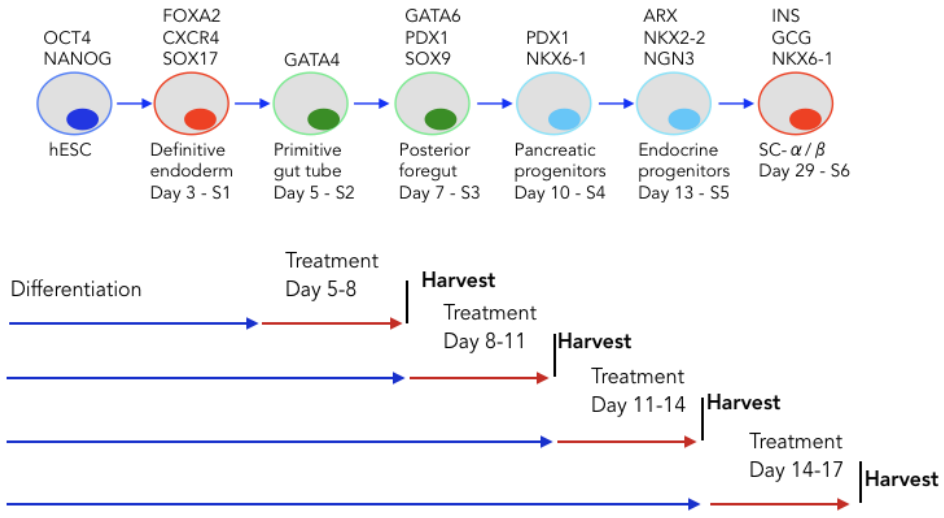

Table 4. Schematic Representation of the Suspension Protocol for the 20-Factor Screening.
This table provides a schematic representation of the suspension protocol used during the screening of 20 factors. It includes the treatment and harvest times of the samples, illustrating the experimental timeline and the specific stages at which the factors were administered and the samples were collected.

Our standard differentiation procedures involved the use of six-well low binding plates on an orbital shaker, with established parameters for medium volume per well, aggregate number per well, and orbital shaker speed. However, given the extensive array of factors and the quantity of material necessitated for this experiment, we could no adhere to the six-well plate format. Consequently, we adapted our methodology by modifying the aforementioned parameters to accommodate differentiation within a 24-well low binding plate format while simultaneously conducting treatment (see Table 4). Upon completion of the four-day treatment period, we harvested the aggregates and conducted gene expression analyses to assess endocrine induction and α- and β-cell fate determination. This experimental design enabled the evaluation of various triggering molecules' impacts on the differentiation process, offering valuable insights into their influence on endocrine cell development.

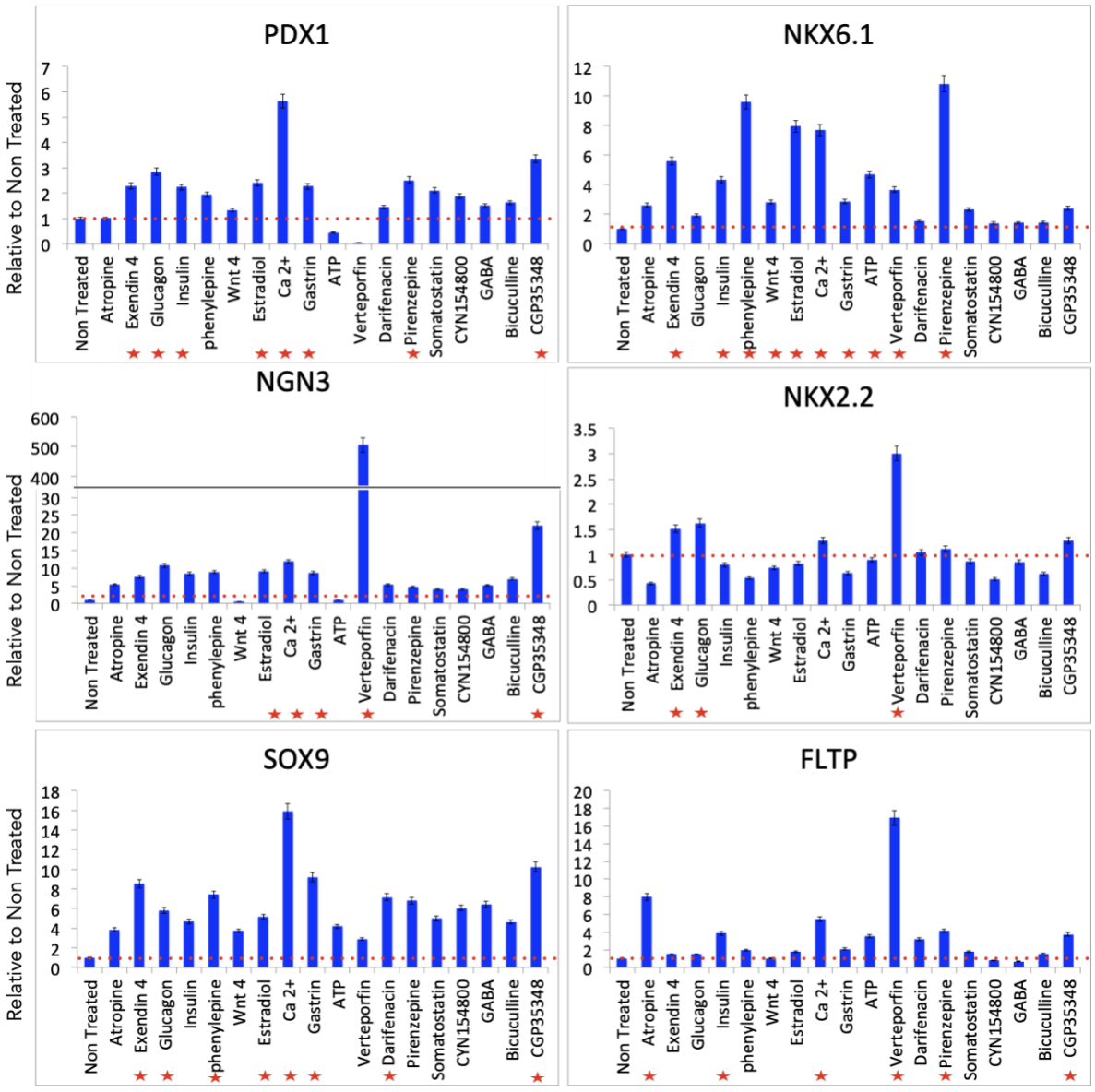

Figure 27. Screening results of treatment from day 5 to day 8; harvesting the samples at day 8 of the differentiation for qPCR analysis using 3 biological and 4 technical replicates (S.E.M.). Factors triggering the highest RNA expression are represented with a (red star). The treated samples were normalized relative to the non-treated samples from the differentiation.

Pancreatic islet cell differentiation is regulated by various signaling pathways and molecular factors. Understanding the impact of these factors on the differentiation process can provide valuable insights for optimizing *in vitro* differentiation protocol. The current challenge is to identify the optimal conditions for promoting endocrine differentiation and β-cell fate allocation *in vitro* by examining the effects of various factors on gene expression during the differentiation process. We performed a screening using qPCR analysis to measure the effect of different compounds and molecules on the expression of various

TFs and markers. The TFs *PDX1* and *NKX6-1* were used as markers for pancreatic progenitors, *NGN3* and *NKX2-2* as endocrine progenitor markers, and *SOX9* for ductal identity. Finally, we used the expression of the WNT/planar cell polarity effector and reporter gene Flattop (*FLTP*) as another marker for endocrine induction (Bader et al., 2016). The screening was carried out between day 5 and day 8 of treatment. Our results on day 5 through day 8 of treatment showed a significant increase of *PDX1* expression under Ca^{2+}(1 mM), GCG (2.8 mM), Estradiol (10 nM), Exendin 4 (10 nM), and gastrin (100 nM) exposure (Figure 27). Similarly, factors like pirenzepine (1 µM), estradiol, Ca^{2+}, Exendin 4, and gastrin increased *NKX6-1* expression. Verteporfin (5 µM), a Yap-inhibitor, also induced an increase in *NKX2-2* and *NGN3* levels. The treatment with pirenzepine (Acetylcholine-inhibitor) and gastrin showed a rise in *NKX2-2* and *NGN3* expression (Figure 27). Interestingly, factors like Verteporfin (5 µM), a Yap-inhibitor, showed high expression in *NGN3, NKX2-2,* and *FLTP,* all markers for endocrinogenesis, and decreased expression of *SOX9*, an ductal marker. Several other studies found that YAP inhibitor induces endocrinogenesis (Rosado-Olivieri et al., 2019), thus, our results were consistent with previous findings. Although gastrin treatment did not increase *NGN3* expression as much as Verteporfin, we observed gastrin enhancing the expression of *NGN3, PDX1* and *NKX6-1* when compared to the untreated control sample. Our results demonstrated the influence of various factors on endocrine differentiation and progenitor marker expression. The YAP inhibitor (Verteporfin), showed promising effects on inducing endocrinogenesis. Additionally, gastrin treatment enhanced the expression of key endocrine progenitors TFs.

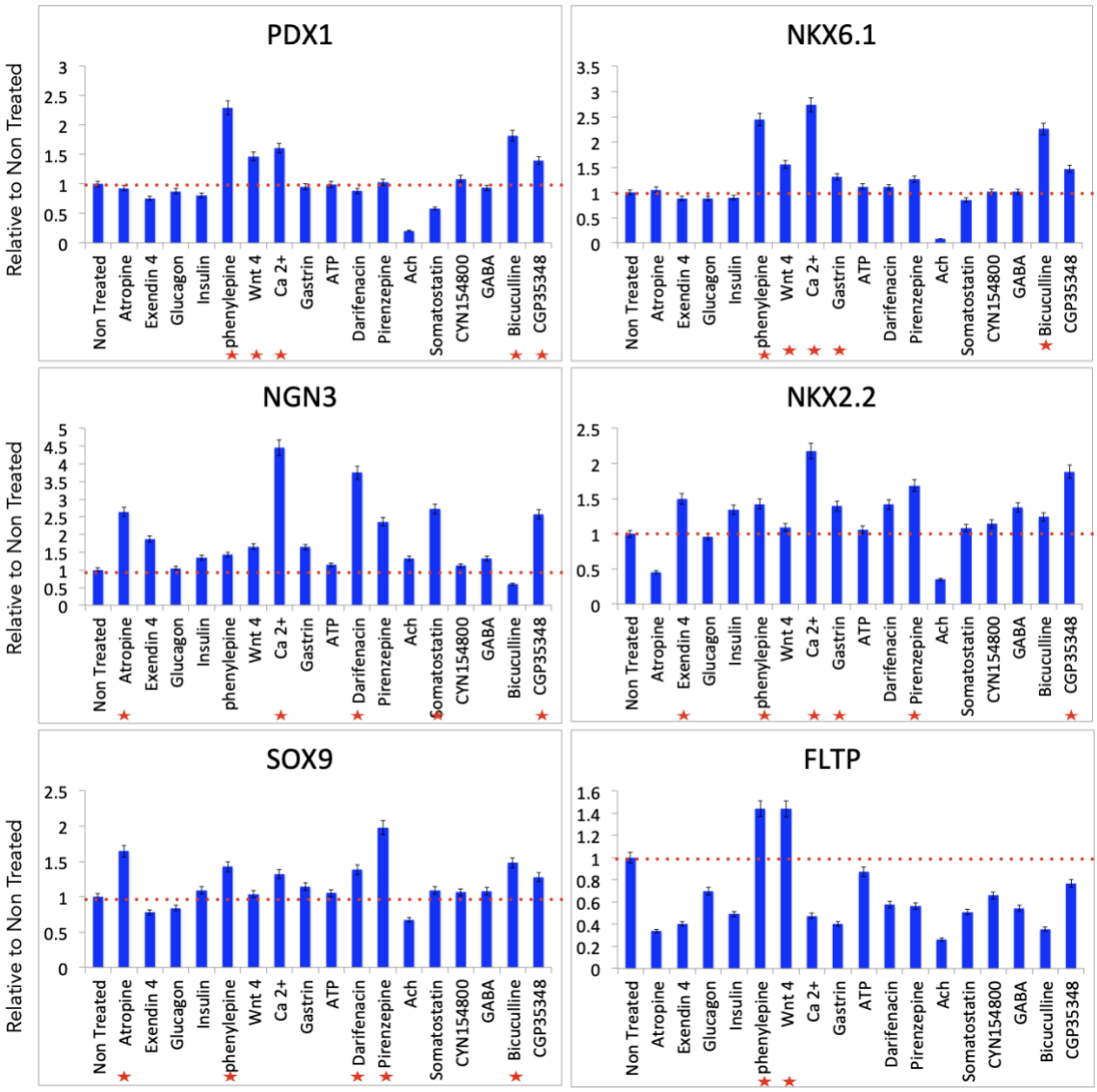

Figure 28. Screening results of treatment from day 8 to day 11; harvesting the samples at D11 of the differentiation for qPCR analysis, using 3 biological and 4 technical replicates (S.E.M). Factors triggering the highest RNA expression are represented with a (red star). The treated samples were normalized relative to the non-treated samples from the differentiation.

The specification of pancreatic progenitors from the foregut endoderm and their subsequent differentiation into endocrine and exocrine cells is a crucial stage in pancreatic development. Various TFs play essential roles in this process, including PDX1, GATA6, NKX6-1, and SOX9. Understanding how different factors modulate gene expression during the posterior foregut and pancreatic progenitor stage can provide valuable insights for optimizing *in vitro* differentiation protocols. The current challenge is to determine whether the treatment with various factors has an influence on gene expression during the posterior foregut and pancreatic progenitor stage and assess their potential on the

differentiation process. During day 8 to day 11 of the treatment, which coincide with the posterior foregut and pancreatic progenitor stage, the biological mechanism underlying these stages is characterized by the specification of dorsal and ventral pancreatic buds from foregut endoderm around mouse embryonic day E9. Later, these two pancreatic buds elongate alongside the duodenum and stomach, eventually fusing into a single organ at E12.5, giving rise to pancreatic endocrine and exocrine cells. (Herrera, 2000). Several TFs control pancreas induction and formation from multipotent progenitors in the foregut endoderm and pancreatic progenitor. Among the earliest TFs that mark the pancreatic region are *PDX1, GATA6, NKX6-1* and *Sox9* (Ahlgren et al., 1998). To determine whether the treatment with any of the factors from table 3 has an influence during the posterior foregut and pancreatic progenitor stage, we conducted a screening and assessed their potential. Factors such as gastrin, phenylepine (0.1 nM), pirenzepine, Ca^{2+}, and somatostatin (100 µM) increased the expression of *PDX1* and *NKX6-1.* In the case of *NGN3* and *NKX2-2*, treatments with Ca^{2+}, pirenzepine, and gastrin were effective. The screening also revealed an increased *FLTP* expression in samples treated with Wnt and phenylepine (see Figure 28). We concluded that the screening during the posterior foregut and pancreatic progenitor stage demonstrated the influence of various factors on the expression of key TFs and markers. Notably, Ca^{2+} treatment increased the expression of *PDX1, NKX6-1,* and *NGN3.* These findings contribute to our understanding of the molecular factors regulating pancreatic progenitor differentiation and can be used to optimize *in vitro* differentiation protocols.

To synthesize the screening results and identify a single triggering factor, we thoroughly analyzed the gene expression patterns throughout the treatment periods. Our analysis revealed that Acetylcholine (Ach) inhibitors, Yap Inhibitor and gastrin consistently induced the expression of TFs responsible for endocrine induction. Notably, these three factors increased the expression of pancreatic and endocrine TFs, such as *PDX1, NKX6-1, NKX2-2,* and *NGN3,* before and during the endocrine induction stage. Furthermore, these factors exhibited minimal to no cell toxicity at the concentrations required for TF induction. Gastrin was particularly intriguing, as it specifically increased endocrine progenitor markers (Veres et al., 2019; Memon et al., 2021). We considered factors such as the ion Ca^{2+}, however, at very low concentrations, it induced toxicity and cell death. Estradiol was also ruled out, as it only increased the expression of *PDX1* and *NKX6-1* without affecting *NGN3* and *NKX2-2,* markers for endocrine induction. While Verteporfin (a Yap-Inhibitor) demonstrated the most significant increase in the expression of TFs related to endocrine

induction, several research groups were already investigating this compound's biological effects during endocrine induction. Consequently, we decided to focus on gastrin, a hormone with very limited information available concerning its role in human endocrine and islet cell development. Investigating gastrin's involvement in these processes offers a unique opportunity to advance our understanding of endocrine development and optimized *in vitro* differentiation protocols.

4.7 Gastrin, CCK, and CCKBR expression in early islet-like aggregates

Gastrin and cholecystokinin (CCK) are well-known gastrointestinal peptide hormones. Their biosynthesis, molecular structures, and intestinal secretory patterns have been extensively characterized, with a notable feature being the high homology of their receptor active sites. Consequently, gastrin and CCK act as agonist for the same receptor, CCKBR (Rehfeld et al., 2019). In human islets, the upregulation of GAST and CCK appears to be associated with β-cell dedifferentiation and loss of function during diabetes progression (Rehfeld et al., 2019; Dufresne et al., 2006; Berna et al., 2007). Thus, we aimed to elucidate the functional role of gastrin and CCK in human endocrinogenesis and determine whether administering gastrin could improve current iPSC differentiation protocols. To understand the functional role of GAST and CCK, which can stimulate the seven transmembrane G-protein-coupled receptors, CCKAR and CCKBR, we first conducted gene expression studies to determine when and where endogenous GAST and CCK are expressed. After analyzing the screening results, we decided to focus on understanding the potential function of gastrin during human endocrinogenesis and test the hypothesis that administering this hormone could improve current iPSC differentiation protocols.

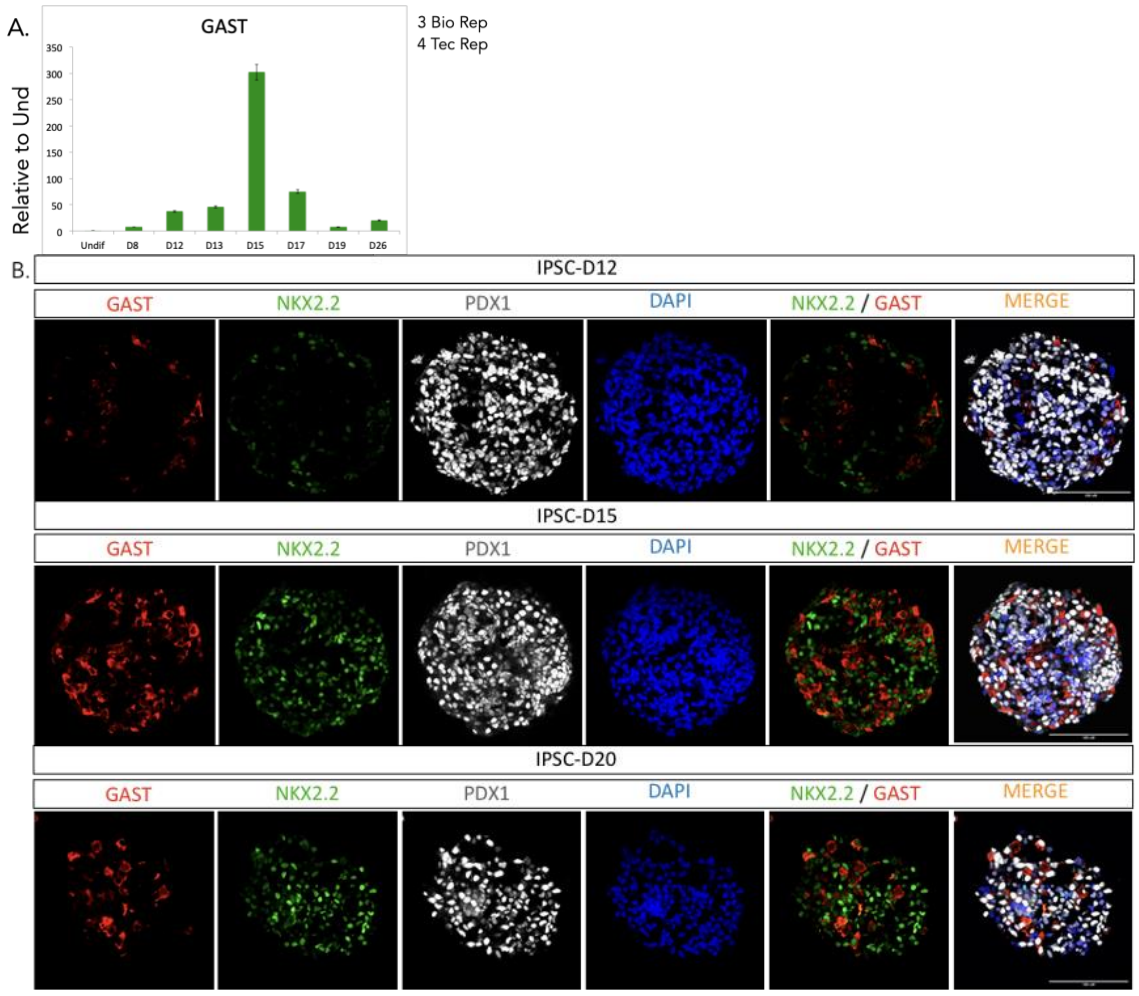

Figure 29. Representative immunofluorescence images of aggregates expressing the endogenous expression of gastrin during the formation of islet-like aggregates. (A) qPCR representing the *GAST* mRNA induction with peak expression at day 15 during the *in vitro* differentiation, relative to undifferentiated iPSC. (B) Immunostaining on day 12, day 15, and day 20 showed gastrin and NKX2-2 progression (n=30 aggregates). Scale bars, 100 µm.

We conducted pancreatic and endocrine differentiation and collected samples at different time points in order to perform mRNA expression profiling of the key components of the GAST and CCK signaling system. These results revealed an increase in *GAST* mRNA expression from day 8 with peak levels at day 15. After the endocrine induction process on day 15, *GAST* mRNA expression gradually decreased towards the end differentiation of hormone-positive α- and β-cells. For single cell resolution, we performed immunostaining on samples collected on day 12, 15 and 20 that showed increased expression levels of gastrin and the pan-endocrine marker NKX2-2 from day 12 through 20 (see Figure 29). Our findings indicate that gastrin hormone is transiently expressed during β-cell differentiation, with peak levels at endocrine induction stage. This suggests

a potential function for gastrin in endocrine lineage induction or segregation. Further investigation into the role of gastrin and CCK in endocrine development could provide valuable insights for improving iPSC differentiation protocols and advancing our understanding of the molecular mechanisms underlying endocrinogenesis.

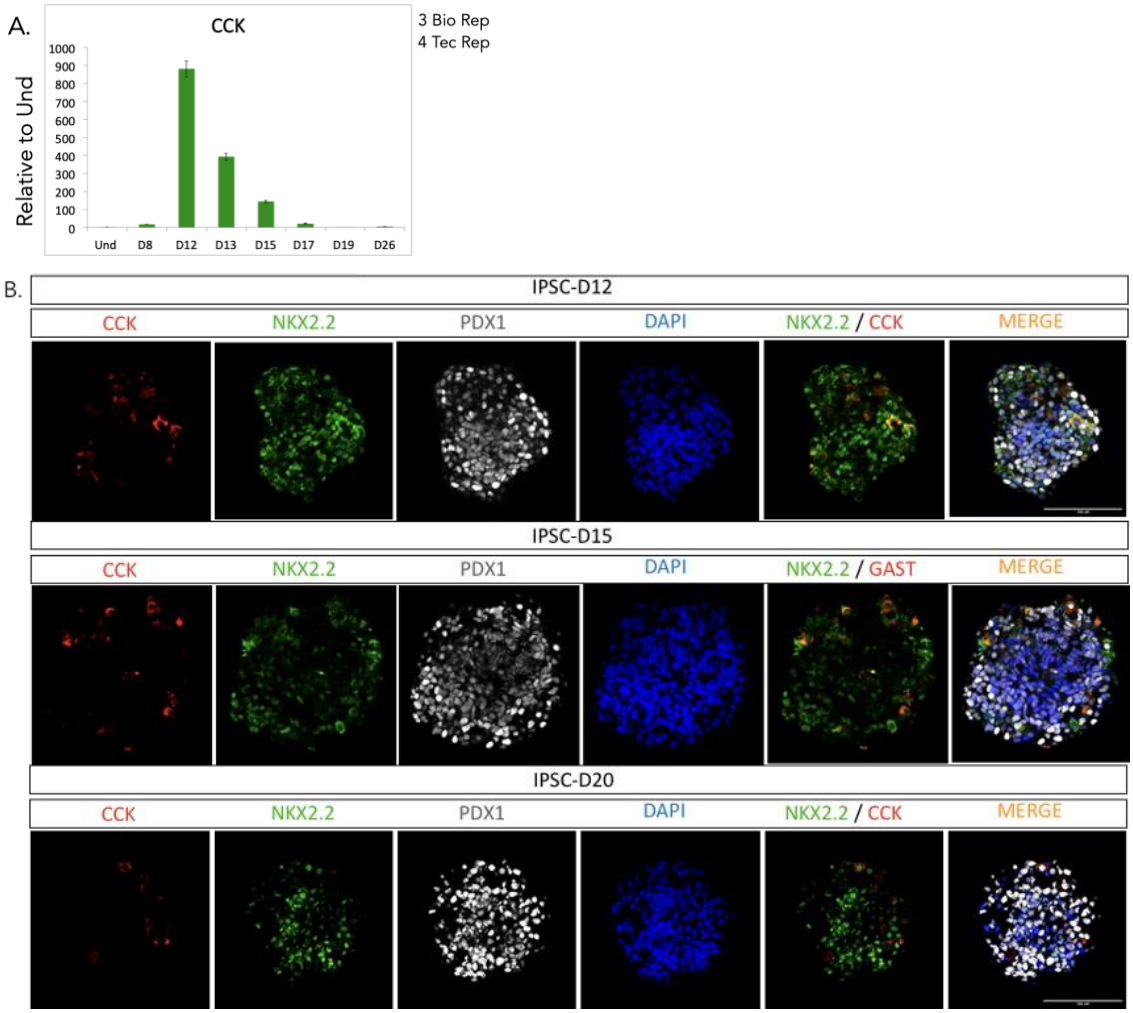

Figure 30. Representative immunofluorescence images of aggregates expressing the endogenous expression of CCK during the formation of islet-like aggregates. (A) qPCR representing the *CCK* induction during the differentiation, relative to undifferentiated. (B) Immunostaining on day 12, day 15, and day 20 showed CCK and NKX2-2 progression (n=30 aggregates). This observation was based on an analysis of 60 pictures taken of the aggregates. Scale bars, 100 µm.

In our investigation, we have incorporated the hormone/neurotransmitter cholecystokinin (CCK) into our analysis, owing to its intricate association with gastrin. Gastrin and CCK, among the earliest discovered gastrointestinal hormones, continue to have ambiguous and debated physiological roles as well as contributions to clinically significant gastrointestinal diseases (Berna et al., 2007; Dufresne et al., 2006). Subsequently, we

analyze the temporal and spatial expression patterns of the CCK mRNA and hormone. Quantitative polymerase chain reaction (qPCR) analysis indicated elevated *CCK* mRNA expression on day 12 and 13. A comparison of *CCK* and *GAST* mRNA expression revealed a marginally earlier expression of *CCK*, with both mRNAs exhibiting transient expression during endocrine induction. We further corroborated the mRNA expression analysis through immunostaining performed on day 12, 15, and 20, which mirrored the mRNA expression patterns and demonstrated the presence of CCK hormone. Intriguingly, on day 15 of the differentiation, CCK-positive cells were fewer in number than gastrin cells (see Figure 30). We concluded that CCK protein expression commences prior to the endocrine induction stage. Moreover, qPCR analysis revealed high CCK gene expression around day 12.

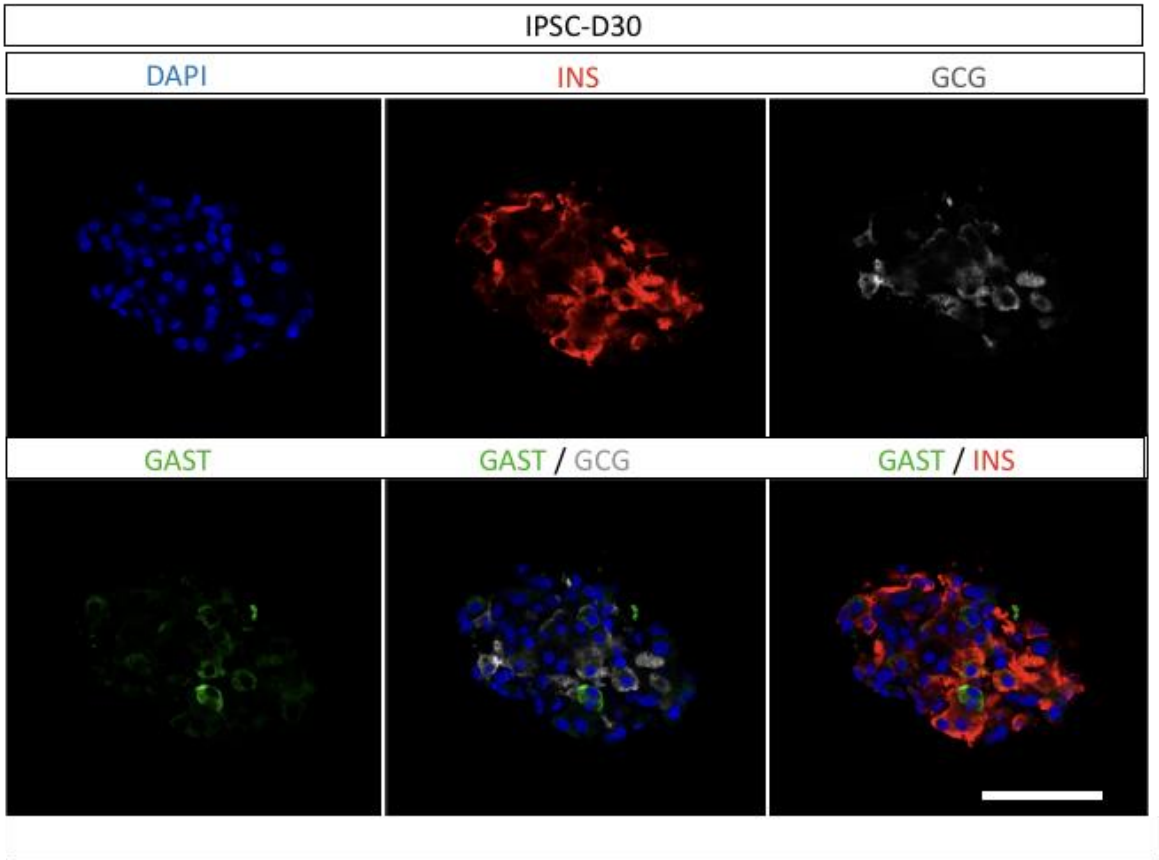

Figure 31. Representative immunofluorescence images of day 30 aggregates expressing the endogenous gastrin cells. Immunostaining revealed cells co-expressing gastrin with the hormone insulin (INS) and glucagon (GCG). A subset of gastrin-expressing cells did not colocalize with either insulin or glucagon-expressing cells (n=30 aggregates). Scale bars, 100 µm.

Gastrin has been reported to emerge in the adult pancreas in correlation with diabetes and malignant tumors (Yuval Dor et al., 2016). To gain deeper insights into the protein expression of gastrin during the advanced stages of α- and β-cell differentiation and in association with insulin and glucagon hormones, we conducted extended differentiation of aggregates until day 30. Immunostaining results revealed co-expression of $GAST^+$ and INS^+. Concurrently, $GAST^+$ cells were observed to co-express with GCG^+ cells. Notably, some gastrin cells did not exhibit co-expression with either insulin or glucagon (see Figure 31). We concluded that, during the later stages of the differentiation, gastrin cells may manifest in mono-hormonal or polyhormonal configuration.

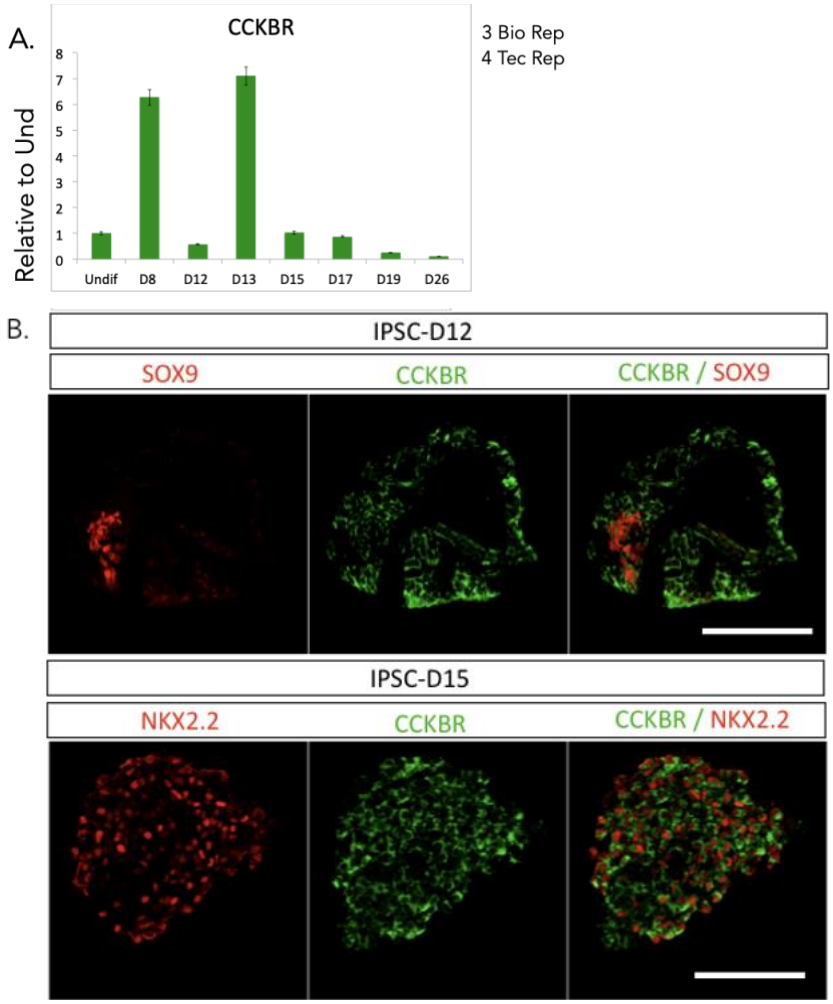

Figure 32. Representative immunofluorescence images of aggregates displaying endogenous expression of CCKBR during islet-like differentiation. (A) qPCR exhibited induction of the *CCKBR* early in the differentiation, relative to undifferentiated cells. (B) Immunostaining on day 12 revealed CCKBR co-localizing with TF SOX9, a marker for the exocrine compartment. Additionally, on day 15, CCKBR was expressed in the same cells as NKX2-2, a marker for the endocrine compartment (n=30 aggregates). Scale bars, 100 µm.

Gastrin and CCK are gastrointestinal hormones whose roles in human endocrinogenesis remain to be elucidated. A comprehensive understanding of their function and relationship to their corresponding receptor, CCKBR, is essential to shed light on their involvement during endocrine cell differentiation. This study aimed to investigate the expression patterns of CCKBR during endocrine cell differentiation in *in vitro*. We performed a detailed analysis of the temporal expression patterns of these hormones and their corresponding receptor CCKBR during the various stages of endocrine cell differentiation. The expression of CCKBR, as the common receptor for both gastrin and CCK, preceded the expression of both hormones. From the pancreatic progenitor period (day 8) to early endocrine progenitor stage (day 13) the receptor *CCKBR* mRNA was highly expressed. Interestingly, *CCKBR* expression exhibited downregulation on day 12, followed by a marked decrease in *CCKBR* mRNA expression thereafter (see Figure 32). Our findings suggest that the receptor CCKBR may account for some of gastrin or CCK stimulations during the early stage of pancreatic progenitor development. The most pronounced effects of the two hormones are expected to occur when their corresponding receptor is expressed. The role of CCKBR diminishes as cells transition into the endocrine progenitor stage and an adequate number of gastrin and CCK cells are present.

4.8 PDX1^{low} cells expressed gastrin^{+} and CCK^{+} during endocrine induction

In our screen, gastrin treatment was found to regulate the expression of the TF PDX1, a pivotal regulator of the pancreatic progenitor stage (Zeng et al., 2020). PDX1, an early pancreatic progenitor cell marker that remains expressed in β- and δ-cells and is essential for insulin gene transcription in β-cells (Suissa et al., 2013). Understanding the interplay between PDX1 expression and GAST and CCK hormones is essential to elucidating their roles in pancreatic endocrine cell development. This study aimed to investigate whether PDX1^{+} cells express GAST and CCK hormones and to identify any associations between PDX1 expression levels and gastrin and CCK expression patterns during islet-like aggregates differentiation. Therefore, we specifically examined the co-expression of PDX1^{+} cells with GAST and CCK hormones. The induction of PDX1 occurred during the differentiation of the islet-like aggregates in particular during the early part of pancreatic progenitor stage, around day 7. PDX1^{+} cells formed two distinct sub-populations, PDX1^{low} and PDX1^{high}. These two subpopulations were present from day 7 through day 30 of the

differentiation. Limited knowledge exists regarding the rationale for high and low PDX1 expression in pancreatic progenitor subpopulations and the islet cell subtypes they correspond to. During our differentiation, we observed gastrin and CCK expression in the PDX1^{low} subpopulation (see Figure 33). Our findings suggests that GAST and CCK expression occurs in cells exhibiting downregulated PDX1 expression, likely corresponding to non-β- and δ-cells.

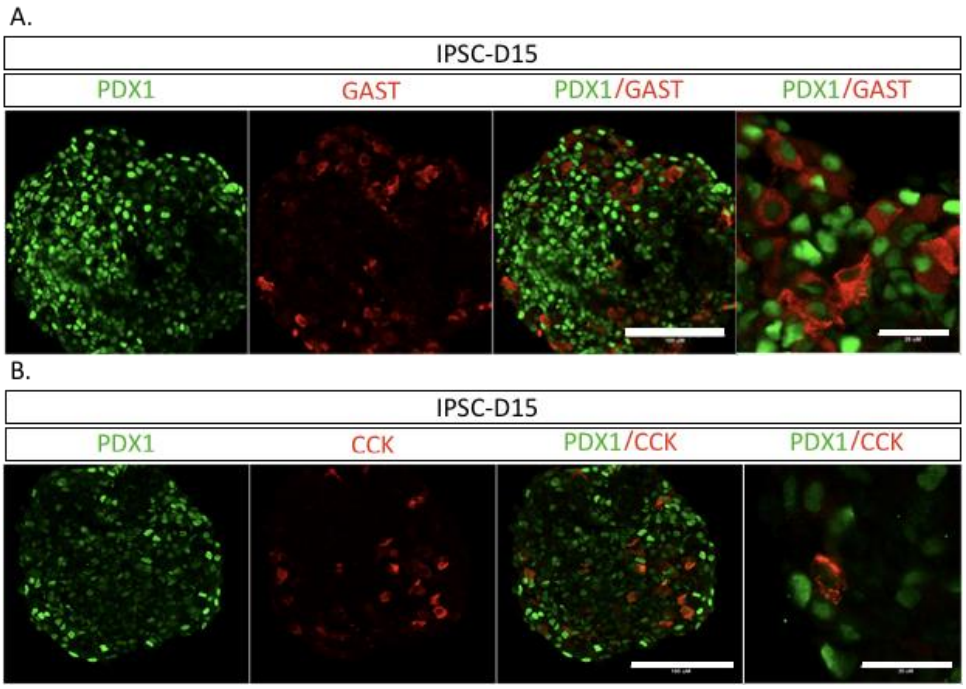

Figure 33. Representative immunofluorescence images of aggregates expressing TF PDX1 in relation to gastrin and CCK expression. (A) Immunostaining of the differentiation on day 15 showed that the majority of gastrin-positive cells were found in the PDX1 ^{low} subpopulation (n=30 aggregates). (B) Immunostaining on day 15 revealed that the hormone CCK expressed in PDX1 ^{low} cells (n=30 aggregates). Scale bars, 100 µm.

4.9 Gastrin treatment increases the number of PDX1^{low} cells

The hormone gastrin and cholecystokinin (CCK) act on the CCKB receptor (CCKBR), a G protein-coupled receptor featuring seven transmembrane domains (Rehfeld et al., 2019). Receptor activation by gastrin stimulates intracellular Ca^{2+} mobilization and protein kinase C via the inositol trisphosphate (IP3) pathway. Furthermore, CCKBR activates MAPK and PI3K pathways. The role of gastrin during the pancreatic progenitor stage is not well understood in either mice or human. To elucidate the function of gastrin during pancreatic and endocrine differentiation and its relationship with PDX1, we investigated the influence of gastrin treatment on PDX1 expression. Accordingly, we differentiated aggregates

towards islet-like cells and treated them with gastrin from day 5 to day 8, when CCKBR is expressed (see Figure 32), coinciding with the primitive gut tube and posterior foregut stages of the differentiation.

In cooperation with Carolin Daniel's group at Helmholtz institute for diabetes research, we conducted fluorescence-activated cell sorting (FACS) analysis. To perform this analysis, we differentiated large quantities of islet-like aggregates until day 20, followed by simultaneous staining with eight different antibodies and then FACS. Although multicolor FACS employs multiple fluorescent markers to characterize cellular subpopulations, enabling the analysis and isolation of viable cells, this technique only allows for the display of two axes simultaneously.

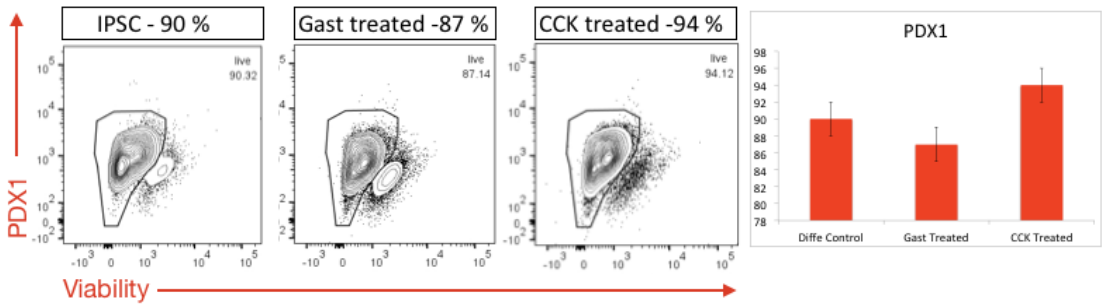

Figure 34. Multicolor FACS results demonstrating the effects of gastrin and CCK treatments on PDX1 expression. The Y-axis represents to cell viability, determined by measuring the number of live, healthy cells in the sample. Cell viability was assessed using nuclear staining of dead cells. PDX1 quantification was performed exclusively on healthy cells (n-4, S.E.M.). The results indicate that gastrin and CCK treatments do not significantly alter the total percentage of PDX1 expression (n=30 aggregates).

The FACS analysis demonstrated that on day 20 of the differentiation, there was no significant difference in the total PDX1 expression between control aggregates and those treated with gastrin and CCK. We conclude that gastrin and CCK treatment do not alter the expression of the total PDX1 at day 20 (see Figure 34).

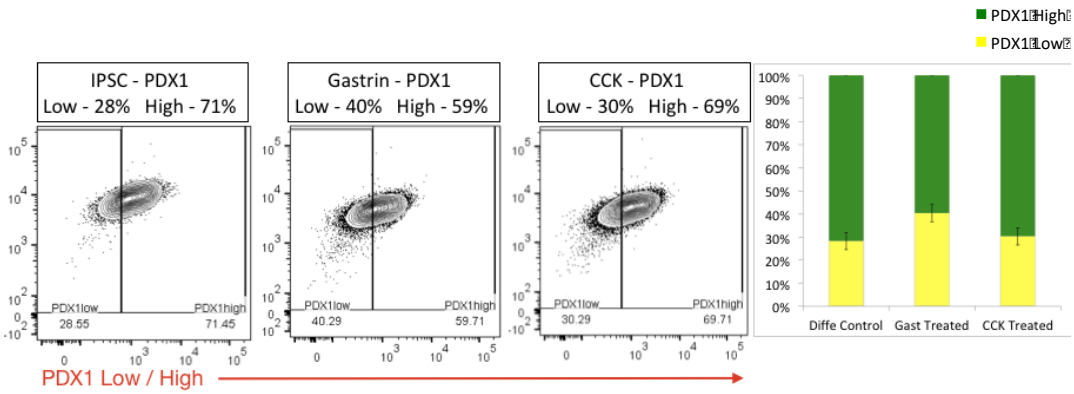

Figure 35. FACS analysis demonstrating the effects of gastrin and CCK treatments on PDX1 low and high subpopulations at day 20 of the differentiation (n-4, S.E.M.). The results indicate that gastrin treatment increases the percentage of PDX1 low **progenitor cells** (n=30 aggregates).

However, we evaluated the percentage of PDX1^{low} and PDX1^{high} cells on day 20 of the differentiation. We discovered that samples treated with gastrin from day 5 to day 8 exhibited a higher percentage of cells expressing PDX1^{low} compared to the control sample. Interestingly, the gastrin-treated population had fewer PDX1^{high} cells than the non-treated IPSC control population. In contrast, the sample treated with CCK during the same period showed no difference compared to the control sample. We concluded that treatment with gastrin and CCK influenced the expression balance of the two PDX1 populations (low and high) (see Figure 35).

4.10 Gastrin/CCK treatment reduces the number of polyhormonal cells

We compared the ratio of INS^{+} and GCG^{+} monohormonal and polyhormonal cells using FACS analysis at day 20 during the immature endocrine stage of the differentiation. The rationale behind this was to understand how polyhormonal cells are thought to be α-cell progenitors, which resolve under extended culture (Veres et al., 2019; Peterson et al., 2020). We found that aggregates treated with gastrin exhibited a higher percentage of insulin-positive cells and fewer glucagon/polyhormonal cells than the control aggregates. Similarly, we also observed an increase in insulin positive cells concomitant with a decrease in polyhormonal cells upon treatment with CCK (see Figure 36 A). We compared images of aggregates treated with gastrin and the control. These images revealed that gastrin-treated samples displayed fewer polyhormonal cells. We also observed an increased number of insulin-expressing cells in gastrin-treated aggregates (see Figure 36

B). This data suggests that gastrin and CCK likely influence the α- and β-cell lineage decision.

A.

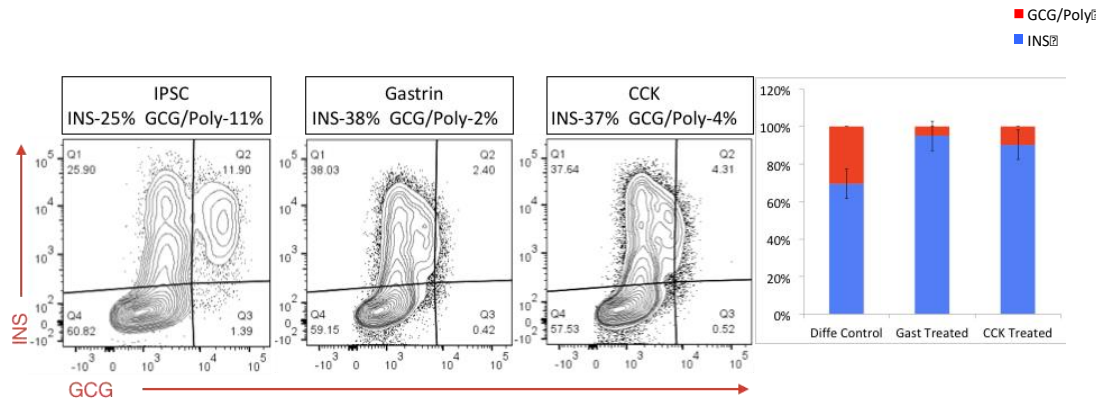

B.

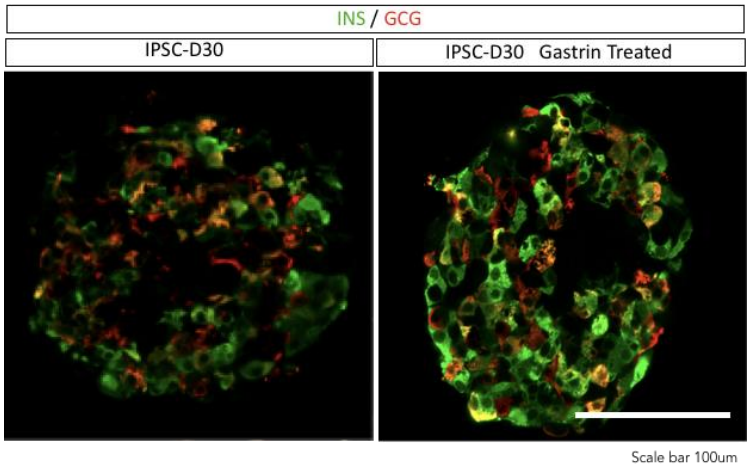

Figure 36. Effects of gastrin and CCK treatments on the proportions of α, β , and poly-hormonal cells at day 20 of the differentiation. (A) Multicolor FACS results indicate that gastrin and CCK treatment increase the percentage of β cells while reducing the percentage of α/poly-hormonal cells (n-4, S.E.M.). (B) Immunostaining of islet-like aggregates on day 30 of the differentiation reveals a decrease in poly-hormonal cells and an increase in insulin induction in gastrin-treated aggregates compared to the control. A total of 20 samples were imaged at day 30 of the differentiation to compare gastrin-treated aggregates with the control. Scale bars, 100 µm.

4.11 C-peptide-mCherry-hiPSC reporter line response to Gastrin and CCK

Our lab generated the C-peptide-mCherry-hiPSC reporter line using CRISPR/Cas9 to knock-in a T2A-H2B-mCherry cassette, replacing the translational C-peptide stop codon. This strategy facilitated the co-transcription of the mCherry cassette and the C-peptide gene, as well as T2A-peptide-mediated co-translational cleavage of C-peptide-T2A and mCherry (HMGUi001-A-8)" (Siehler et al., 2020). The line differentiated effectively using

our modified suspension protocol. Unlike the previous insulin reporter line that expressed fluorescence in the nucleus, the C-peptide expressed the reporter in the cytoplasm.

We used the C-peptide-mCherry-hiPSC reporter line to test the previous results obtained with the hiPSC line upon gastrin and CCK treatment. We differentiated the C-peptide-mCherry-hiPSC reporter line and treated with gastrin, CCK, and a combination of gastrin and CCK. We added the gastrin/CCK treatment combination based on the rationale that the two hormones appeared simultaneously during the differentiation. We collected samples on day 18 of the differentiation, followed by the disintegration of clusters into single cells and FACS analysis.

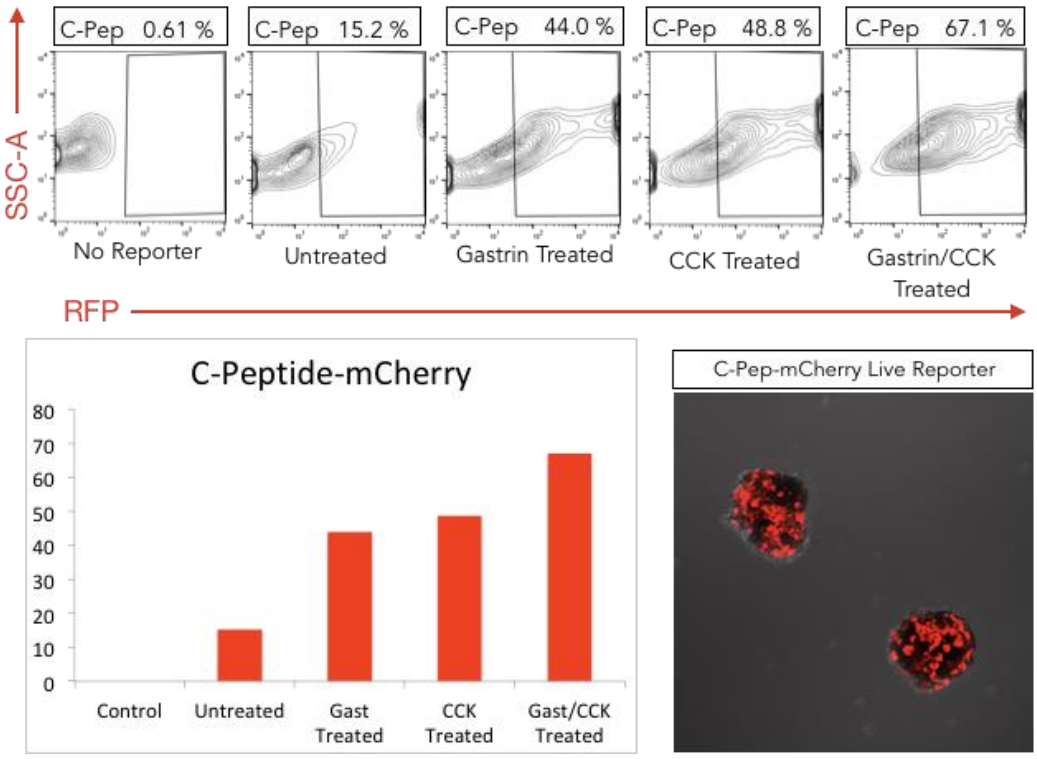

Figure 37. FACS analysis of C-peptide-mCherry-hiPSC reporter line following Gastrin, CCK, and the combined Gastrin/CCK treatments. Samples were harvested and analyzed on day 18 of the differentiation. The figure shows the live imaging of the C-Peptide mCherry reporter aggregates before FACS (n=30 aggregates).

Aggregates from the untreated control C-peptide-mCherry-hiPSC reporter line showed 15.2% C-peptide-mCherry positive iPSC-derived β-cells. Gastrin and CCK treatments generated 44% and 48% C-peptide-mCherry positive β-cells, respectively, considerably higher than the untreated control sample. The sample treated with both gastrin and CCK

yielded a 67% positive for C-peptide-mCherry (see Figure 37). Thus, CCK and gastrin appear to increase endocrine induction as well as β-cells lineage allocation. These results align with the observation of fewer α-cells progenitors from the polyhormonal result above (see Figure 36 A).

4.12 *ARX*$^{nCFP/nCFP}$ hiPSC reporter cell line response to Gastrin and CCK

To investigate the impact of gastrin and CCK on α-cell lineage induction and segregation, we utilized the *ARX*$^{nCFP/nCFP}$ hiPSC reporter cell line, following a similar approach as with the C-peptide-mCherry-hiPSC reporter. We subjected the aggregates to a differentiation and treatment with gastrin, CCK, and a combination of both gastrin and CCK.

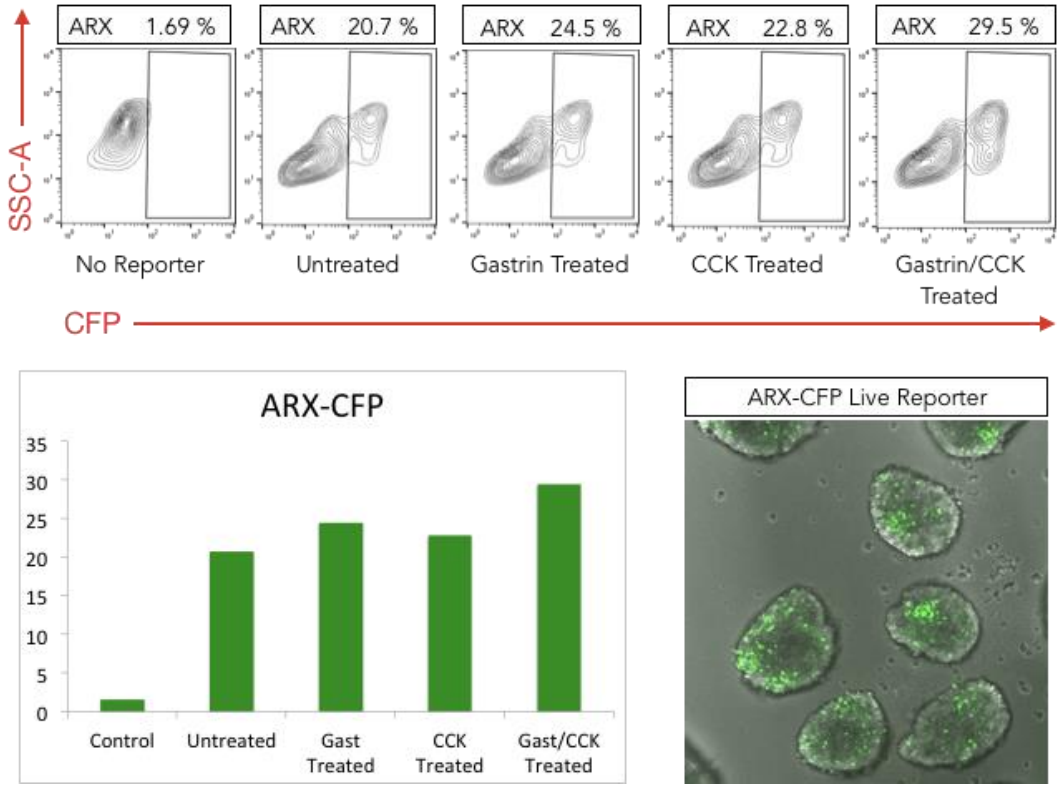

Figure 38. FACS analysis of *ARX*$^{nCFP/nCFP}$ hiPSC reporter line following Gastrin, CCK, and the combined Gastrin/CCK treatments. Samples were harvested and assessed on day 18 of the differentiation. The figure shows the live imaging of the *ARX*$^{nCFP/nCFP}$ hiPSC reporter aggregates before FACS (n=30 aggregates).

Subsequent FACS analysis of the treated samples revealed distinct outcomes. In the untreated samples, 20% of the cells were ARX-CFP positive. Upon gastrin treatment, the proportion of ARX-CFP positive cells increased to 24%, while the CCK-treated sample

exhibited a 22% ARX-CFP positive rate. Notably, the combined treatment of gastrin and CCK resulted in a further increase, with 29% of the cells expressing ARX-CFP (see Figure 38). In summary, our findings indicate that gastrin and CCK effectively promote β-cell lineage formation. However, their impact on α-cell lineage induction appears to be less pronounced. This observation warrants further investigation into the mechanisms underlying the differential effects of gastrin and CCK on α-cell lineage commitment.

4.13 Gastrin antagonist and NGN3 expression

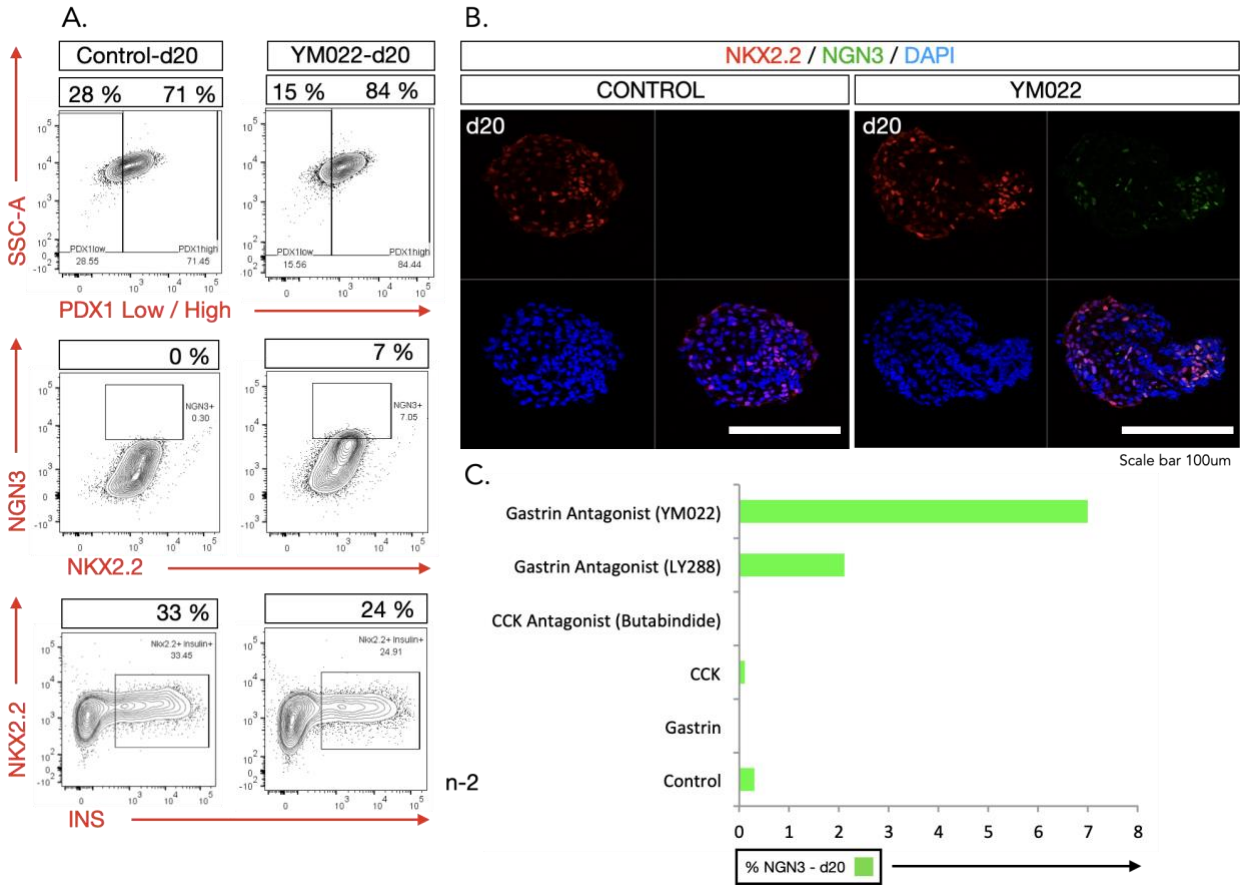

Figure 39. Effect of Gastrin Antagonist YM022 on NGN3 Expression during Differentiation.
This figure demonstrates the impact of YM022, a gastrin antagonist, on NGN3 expression during differentiation. Treatment with YM022 from day 5 to day 8 resulted in the presence of NGN3 on day 20 of the differentiation (Immature endocrine cells). (A) Multicolor FACS analysis was performed to compare control and treated samples, examining PDX1^{high} and PDX1^{low} populations, NGN3 expression, and insulin induction. The analysis included a total of 30 aggregates. (B) Immunostaining revealed NGN3 expression in both control and treated samples. (C) The column chart presents the results of multicolor FACS analysis for control cells as well as cells treated with gastrin, CCK, CCK-antagonist, and two gastrin antagonists. The chart illustrates the percentage of NGN3 TF expression at day 20 of the differentiation. Scale bars in all images represent a length of 100 µm.

To elucidate the role of gastrin and CCK in endocrine lineage induction versus α- and β-cell lineage segregation, we analyzed the induction of the master regulator of endocrinogenesis, NGN3. NGN3 knockout results in the failure of endocrine induction in both mice and humans (Jenny et al., 2002; Schonhoff et al., 2004). Specifically, we employed treatments with two gastrin antagonists to investigate their effects on differentiation. We treated samples from day 5 to day 8 and conducted multicolor FACS analysis on day 20. The samples treated with the gastrin antagonist (YM022) exhibited a lower number of $PDX1^{low}$ and a higher $PDX1^{high}$ cells compared to the control. The number of $NGN3^{+}$ cells on the same day was 7% higher than the control in the sample treated with YM022. Notably, NGN3 should not be present on day 20 of the differentiation, as its transient presence occurs during day 15 of the differentiation. The early treatment with YM022 altered the ratio of PDX1 (low and high) compared to the control. We postulate that the samples treated with YM022 displayed fewer $PDX1^{low}$ than control, which could explain the presence of some NGN3-positive cells later in the differentiation. The delayed presence of NGN3 reduced the expression of the hormone insulin (see Figure 39 A, C).
Immunostaining analysis revealed the presence of NGN3-positive cells in the sample treated with YM022 on day 20 of differentiation, while the control sample displayed no detectable NGN3-expressing cells at this stage. Furthermore, the samples treated with gastrin, CCK, CCK antagonist, and control showed no expression of NGN3 on day 20 of the differentiation. In contrast, the two gastrin antagonists exhibited 2% and 7% expression of NGN3 on day 20 (see Figure 39 B). Based on these observations, we can deduce that gastrin agonists treatment promotes the expression of $PDX1^{high}$ and NGN3, thereby potentially influencing endocrine lineage commitment and differentiation.

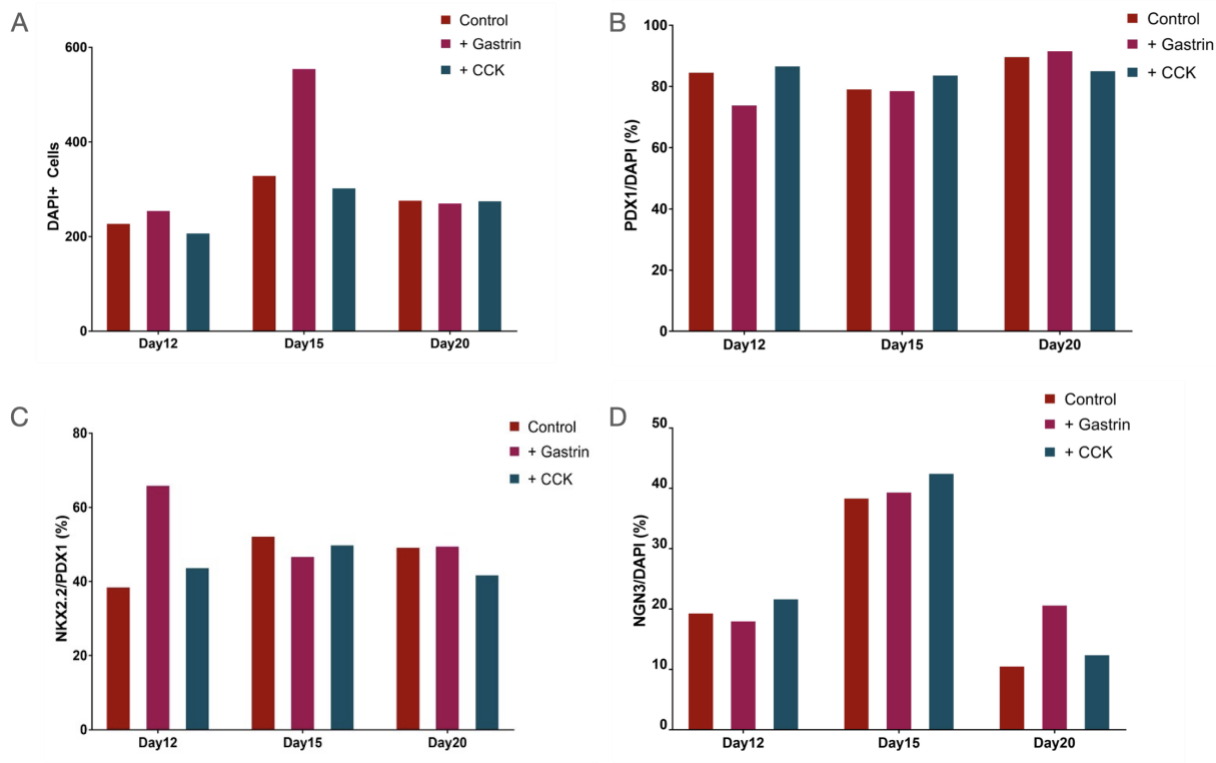

Figure 40. Quantification of control, gastrin, and CCK treated aggregates at pancreatic progenitor stage (day 12), endocrine progenitor stage (day 15), and immature islet stage (day 20). Graphs depict the analysis of 30 aggregates, conducted with the Imaris cell imaging software. Percentages of DAPI, NKX2-2, and NGN3 were calculated based on the number of PDX1 expressing cells as 100%, considering PDX1 cells are pancreatic cells. (A) Represents the quantification of DAPI-positive cells during day 12,15, and 20 of differentiation. (B) Displays the percentage of DAPI-positive cells relative to PDX1-positive cells during day 12, 15, and 20 of differentiation. (C) Illustrates the percentage of the NKX2-2-positive cells relative to the PDX1-positive cells during day 12, 15, and 20 of differentiation. (D) Depicts the percentage of NGN3-positive cells relative to PDX1-positive cells during days 12, 15, and 20 of the differentiation.

To directly investigate the impact of gastrin and CCK on pancreatic progenitors, endocrine progenitors and immature islet-like aggregate cells, we executed quantification analyses by differentiating aggregates treating them with gastrin and CCK. The aggregates were then harvested on day 12, 15, and 20 of the differentiation, immunostained and quantified using the IMARIS cell imaging software. By quantifying 30 aggregates per sample, we generated graphs (see Figure 40). We postulated that gastrin and CCK treatment would modulate the expression of the pan-endocrine TF NKX2-2 and the key endocrine progenitor regulator NGN3. Based on the quantification, we concluded that gastrin treatment augmented the number of cells during the endocrine progenitor stage (day 15). We also observed an upregulation of NKX2-2-positive cells during the pancreatic progenitor stage (day 12) in gastrin-treated samples. Finally, gastrin-treated cells exhibited elevated NGN3 expression during the immature islet stage (day 20). Assessment of

endogenous gastrin and CCK expression during pancreatic progenitor, endocrine progenitor, and immature islet stages in gastrin and CCK-treated samples enabled us to ascertain that during the pancreatic progenitor stage, CCK-treated samples demonstrated enhanced signal intensity of TF NKX2-2. We also observed mutual exclusivity between cells expressing TFs NKX2-2 and NKX6-1. Gastrin-treated samples presented an increased overall cell count (day 12). Additionally, we detected elevated endogenous gastrin expression in CCK-treated aggregates during the endocrine progenitor stage. During the endocrine induction stage, gastrin-treated aggregates displayed more CCK-positive cells than the control and CCK-treated groups. Aggregates exposed to gastrin until day 20 of the differentiation manifested increased NGN3 expression at the later stage.

4.14 Gastrin and CCK treatments to assess INS (C-Pep) and GCG expression

4.14.1 Endocrine Progenitor Stage

The transient expression of the TF NGN3 is a characteristic feature of the endocrine progenitor stage. Prior research has indicated varying levels of NGN3 expression, ranging from low to high, in cells during this stage. The activation of NGN3 expression is instrumental in initiating the formation of hormone-producing cells within pancreatic islets (Villasenor et al., 2008). In our differentiation protocol, aimed at generating islet-like aggregates, we observed a similar transient expression pattern of the TF NGN3 during the endocrine induction phase. To investigate the implications of gastrin and CCK treatment on the development of insulin-and glucagon-producing cells, we designed an experiment involving the differentiation of aggregates and their treatment with gastrin and CCK. We postulated that the early presence of gastrin and CCK might modulate the allocation of α- and β-cells progenitors in islet-like aggregates. To evaluate the efficacy of our experimental design, we directed the differentiation of aggregates toward the endocrine progenitor stage. The treatment commenced on day 8 of the differentiation and continued until day 15, at which point the aggregates were harvested and subjected to cryo-sectioning. Subsequently, immunostaining was employed to assess and compare C-peptide, glucagon, and NGN3 expression levels in gastrin-treated, CCK-treated, and control samples.

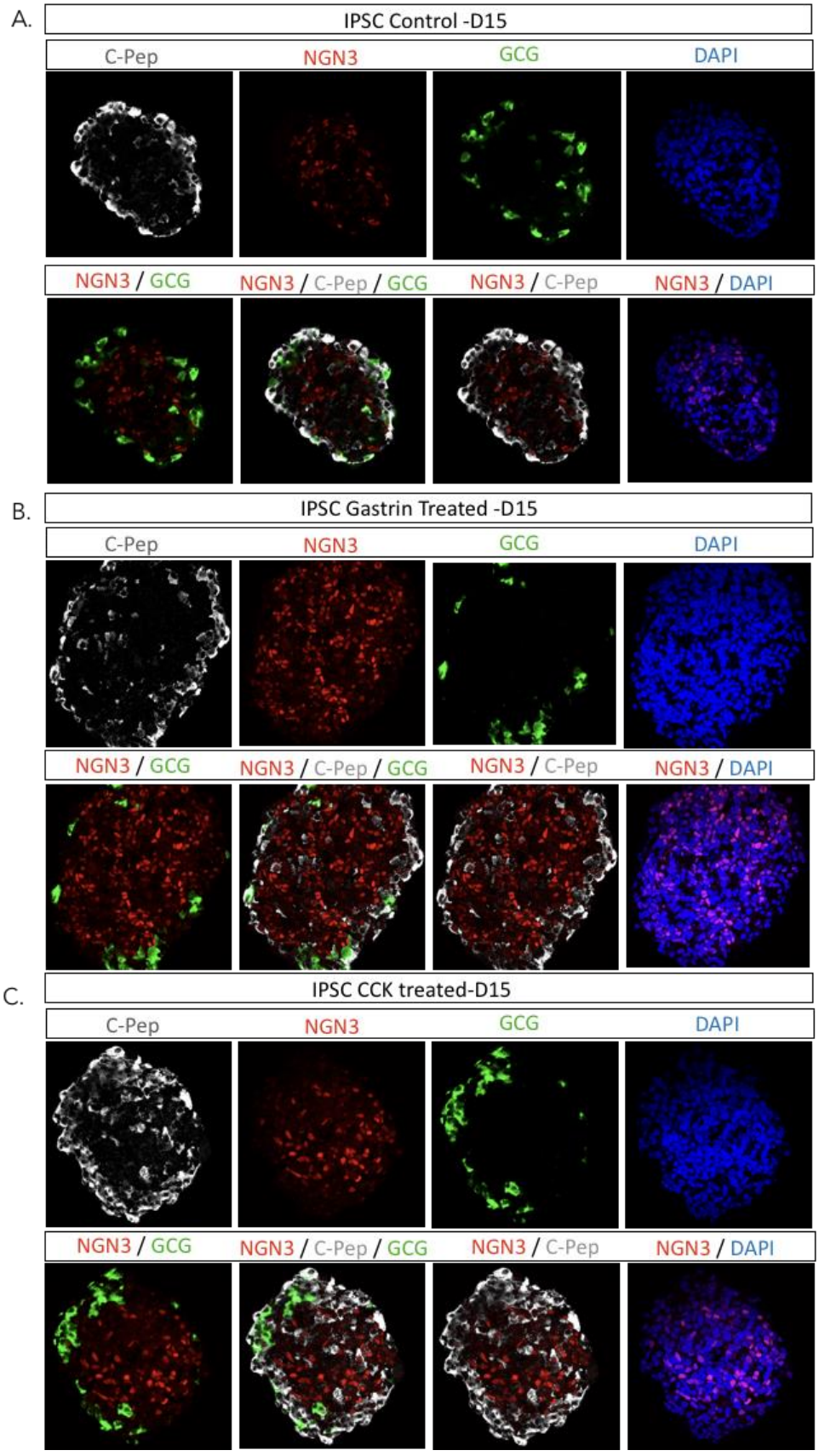
A.
IPSC Control -D15
C-Pep
NGN3
GCG
DAPI
NGN3 / GCG
NGN3 / C-Pep / GCG
NGN3 / C-Pep
NGN3 / DAPI
B.
IPSC Gastrin Treated -D15
C-Pep
NGN3
GCG
DAPI
NGN3 / GCG
NGN3 / C-Pep / GCG
NGN3 / C-Pep
NGN3 / DAPI
C.
IPSC CCK treated-D15
C-Pep
NGN3
GCG
DAPI
NGN3 / GCG
NGN3 / C-Pep / GCG
NGN3 / C-Pep
NGN3 / DAPI

Figure 41. Immunostaining of aggregates at the endocrine progenitor stage, displaying the expression of TF NGN3 and hormones C-peptide and glucagon. (A) Aggregates differentiated to day 15, untreated control. (B) Aggregates at day 15 treated with the hormone gastrin. (C) Aggregates at day 15 treated with the hormone CCK.

During the endocrine progenitor stage, a marked upregulation of NGN3 expression was observed in samples treated with gastrin and CCK compared control samples. Nevertheless, no significant disparities were detected in the early expression of C-peptide and glucagon between treated and control samples. A prominent observation was that, at day 15, NGN3 expression consistently emanated from the center of the aggregates, whereas the initial presence of hormones was localized to the periphery of the aggregates. This observation held true for more than 80 analyzed aggregates (see Figure 41). In conclusion, the administration of gastrin and CCK treatments from day 8 to day 15 of the differentiation augments the expression of the TF NGN3 during the endocrine progenitor stage. Despite this increase, no discernible alterations in early INS and GCG producing cells were detected, suggesting a more complex relationship between NGN3 expression and hormone-producing cell development.

4.14.2 Immature Islet Stage

During the final stage of the differentiation, a subset of cells does not adopt an endocrine fate. These non-endocrine cells exhibit characteristics similar to pancreatic-progenitor cell types from earlier stages, expressing key transcription factors while lacking endocrine markers. The TF NGN3, a transiently expressed master regulator of *in vivo* endocrine induction, is expressed by cells bridging the endocrine stage, and its expression subsequently diminishes following the endocrine induction stage (Veres et al., 2019). Our aim was to elucidate whether gastrin and CCK treatment enhances endocrine cell production and leads to the generation of more hormone-producing cells, while maintaining the transient expression of NGN3 unaltered. We designed this experiment anticipating that early treatment with gastrin and CCK would yield a substantial difference in the number of α and β-cells produced by the aggregates.

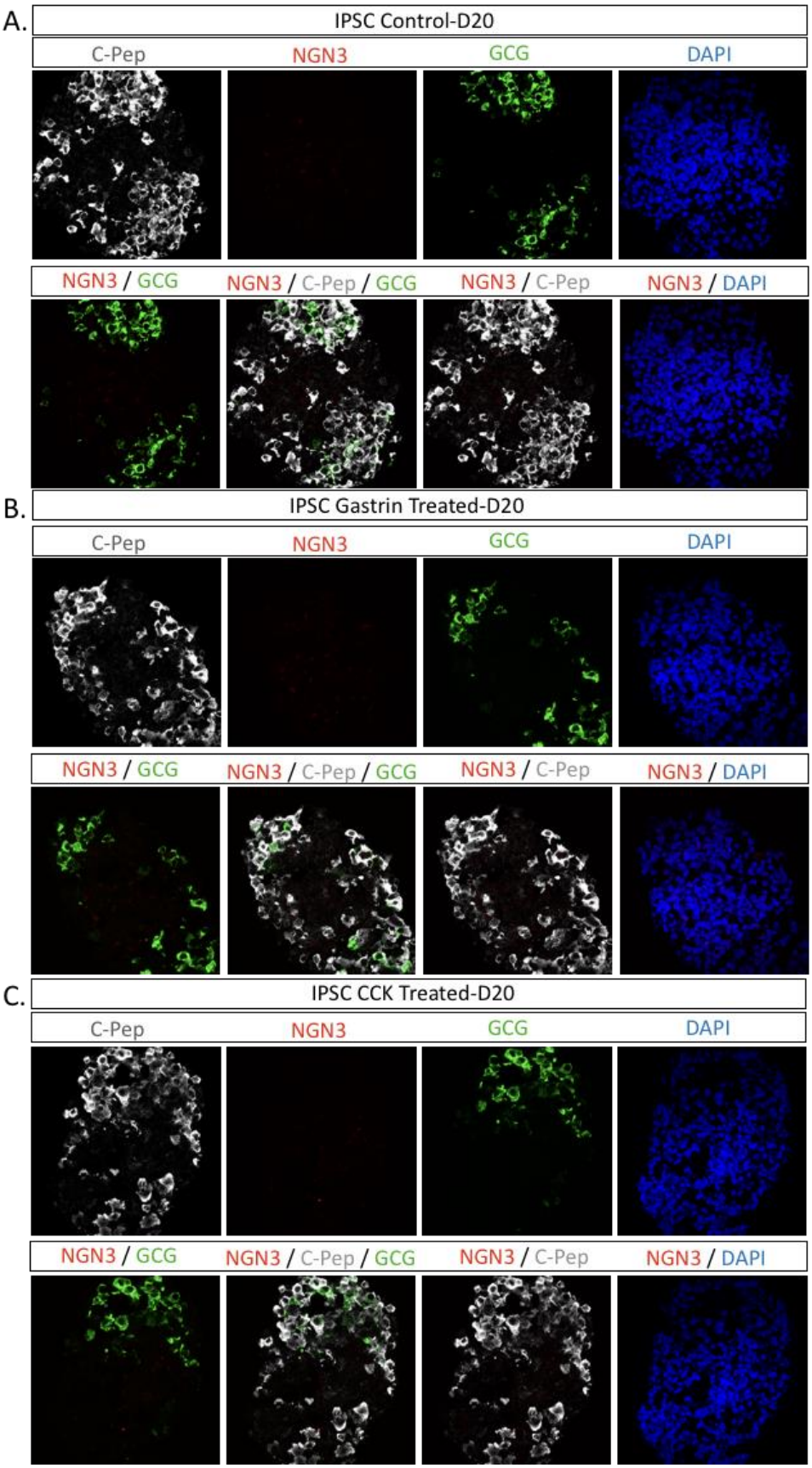
A.
IPSC Control-D20
C-Pep
NGN3
GCG
DAPI
NGN3 / GCG
NGN3 / C-Pep / GCG
NGN3 / C-Pep
NGN3 / DAPI
B.
IPSC Gastrin Treated-D20
C-Pep
NGN3
GCG
DAPI
NGN3 / GCG
NGN3 / C-Pep / GCG
NGN3 / C-Pep
NGN3 / DAPI
C.
IPSC CCK Treated-D20
C-Pep
NGN3
GCG
DAPI
NGN3 / GCG
NGN3 / C-Pep / GCG
NGN3 / C-Pep
NGN3 / DAPI

Figure 42. Immunostaining of aggregates at the immature islet stage, displaying the expression of TF NGN3 and the hormones C-peptide and glucagon. (A) Aggregates differentiated to day 20 untreated control. (B) Aggregates at day 20 treated with the hormone gastrin. (C) Aggregates at day 20 treated with the hormone CCK.

During the immature islet stage, we observed a surge in α and β-cells within the aggregates compared to the preceding pancreatic progenitor stage. Furthermore, we noted the absence of NGN3 expression following the completion of its transient expression phase. We evaluated insulin, glucagon, and NGN3 expression at day 20 of the differentiation in islet-like aggregates treated with gastrin and CCK. Upon analysis of 80 scanned aggregates, we concluded that gastrin and CCK treatment from day 8 to day 15 of differentiation did not result in an increased number of α and β-cells at day 20 of the differentiation. Additionally, we determined that gastrin and CCK treatment during this time period did not influence the transient expression of the TF NGN3 (see Figure 42).

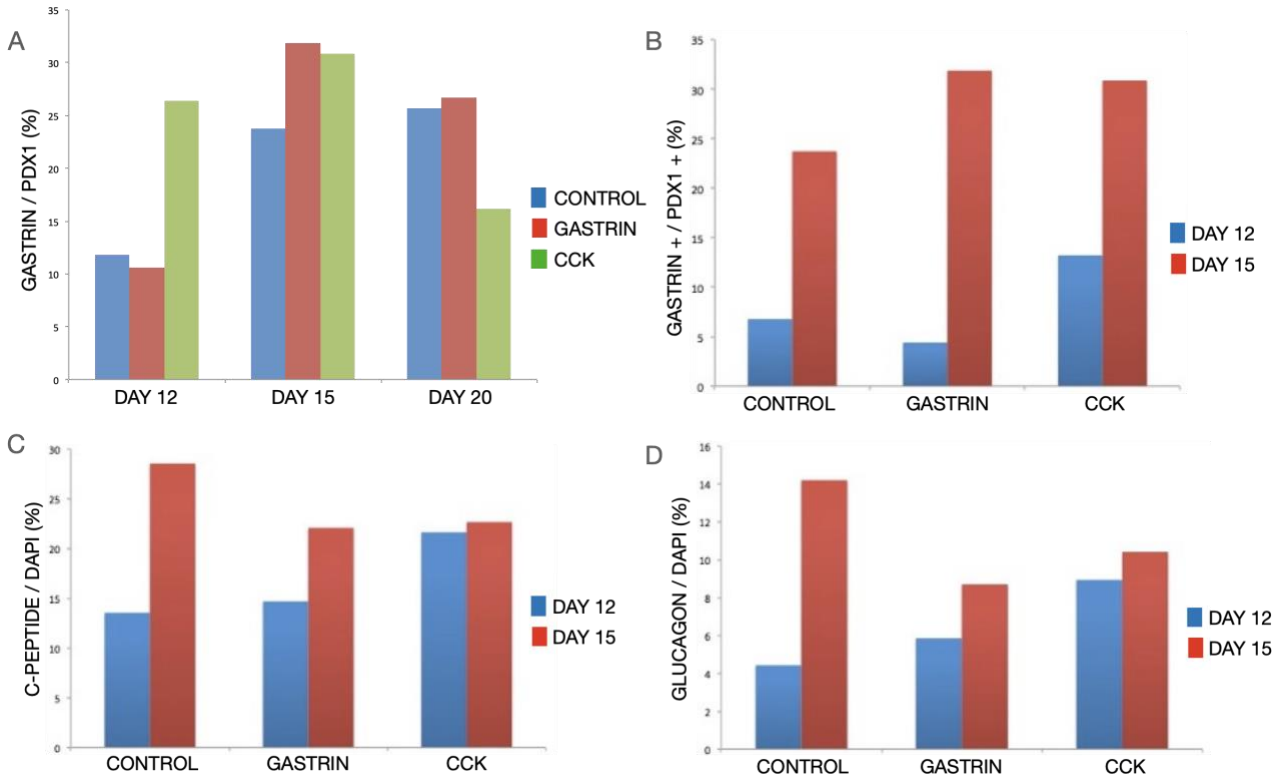

Figure 43. Quantification analysis of control, gastrin, and CCK treated aggregates at pancreatic progenitor stage (day 12), endocrine progenitor stage (day 15), and immature islet stage (day 20). Data were obtain by counting 30 aggregates using Imaris cell imaging software, with the percentage of gastrin, C-peptide, and glucagon calculated based on the number of DAPI-expressing cells as 100%. (A) The graph displays the proportion of endogenous gastrin-expressing cells relative to the PDX1 population at day 12,15,

and 20 of the differentiation, with PDX1-expressing cells serving as the 100% reference. (B) The graph depicts the percentage of cells gastrin and PDX1 double-positive cells at days 12 and 15. (C) The chart illustrates the proportion of C-peptide-expressing cells relative to the DAPI population at days 12 and 15 of differentiation. (D) The graphic represents the percentage of GCG-expressing cells in relation to the DAPI population at days 12 and 15 of differentiation.

Utilizing image analysis of 30 aggregates per sample enabled the elucidation of cell distribution, colocalization, and the mutual exclusivity of cells. The objective was to quantify the aggregates at distinct time points to uncover the impact of gastrin and CCK during isle-like aggregate formation. Consistent with prior experiments, aggregates underwent differentiation, harvesting, immunostaining, and quantification using IMARIS cell imaging software. It was hypothesized that gastrin and CCK treatment would alter the quantity of the C-peptide and glucagon producing cells. Quantification results (see Figure 43 A) indicated that gastrin and CCK treatment enhanced the expression of these hormones during the endocrine progenitor stage. Additionally, gastrin and CCK treatment until harvesting on day 15 and day 20 did not yield increased INS (C-Pep) or glucagon expression (see Figure 43 C, D). Gastrin and CCK treatment augmented endogenous gastrin and CCK expression on day 12 and 15, with a substantial population of gastrin and CCK being endocrine, as evidenced by PDX1 positive cells (see Figure 43 B). By evaluating endogenous expression INS (C-Pep) and GCG expression during endocrine progenitor and immature islet stages in gastrin and CCK-treated samples, it was concluded that gastrin and CCK treatment from day 8 of the differentiation to day 15 increased the expression of TF NGN3 during the endocrine progenitor stage. It was consistently observed that NGN3 positive cells emerged from the center of the aggregates during the endocrine progenitor stage, while hormones manifested on the aggregate periphery. As the differentiation progressed, the hormone-producing cells were located both in the center and periphery of the aggregates.

5. Discussion

While the production of large quantities of stem cells offers the potential for unlimited material, the efficient generation of mature β-cells remains a significant challenge (Russ et al., 2015; Rezania et al., 2014; Nair et al., 2019; Balboa et al., 2019). Therefore, the overarching aims of this PhD thesis were: 1) to develop a more efficient islet-like aggregates differentiation protocol, thereby advancing novel therapeutic approaches to replenish the functional β-cell mass using hiPSCs and ultimately overcoming diabetes (Pagliuca et al., 2014; de Klerk et al., 2021); 2) to identify novel factors that regulate endocrinogenesis, as understanding the factors involved in specifying early human pancreatic lineages is crucial for generating β-cells with physiological functions similar to mature human islets; and 3) to investigate the impact of gastrin and CCK on β-cell generation, as the limited understanding of the molecular pathways orchestrating pancreatic islet development contributes to the current protocol's inability to generate β-cells that replicate *in vivo* development (Krentz et al., 2021; Veres et al., 2019).

Prior to the commencement of this project, the regenerative medicine field primarily generated β-cells through monolayer protocols or protocols initiated as monolayers and continued in air-liquid interface or suspension. Most of these protocols emerged from Novocell later renamed to Viacyte company and represented significant breakthroughs at the time (D'Amour et al., 2005; D'Amour et al., 2006; Kroon et al., 2008; Rezania et al., 2014). Additionally, several other suspension protocols with a more 3D approach have surfaced in the years since we began our studies (Pagliuca et al., 2014; Nair et al., 2019; Russ et al., 2015; Velazco-Cruz et al., 2019). Therefore, the parallel development of more effective 3D β-cell differentiation protocol, including our attempts, addresses some of the major limitations of previous studies and advances the field of stem cell generated β- and islet cell development for regenerative medicine. Furthermore, the novel discoveries regarding gastrin and CCK treatment and their impact on endocrinogenesis will enable future research and applications aimed at curing diabetes.

5.1 Development of a scaled-up 3D islet-like aggregates protocol

The generation of functional pancreatic β-cell in sufficient quantities remains a considerable challenge in regenerative medicine, despite advances in monolayer and suspension differentiation protocols (Pagliuca et al., 2014; Balboa et al., 2022; Nair et al.,

2019; Russ et al., 2015; Triolo et al., 2021). Our study aimed to overcome the limitations associated with existing protocols for differentiating β-cells, focusing on the development of an improved strategy that generates clinically relevant quantities of functional β-cells.
Our laboratory has identified four main concerns that could have an impact on the efficacy and reliability of islet-like aggregates and β-cells in monolayer protocols. These concerns include inadequate cell yields, which limit the suitability of islet-like aggregates for transplantation and screening experiments. Pronounced variability between wells raises questions about the reproducibility and consistency of these protocols across different experimental contexts. The generation of heterogeneous cell populations, including unintended cell types, may compromise the overall function of the islet-like aggregates and affect transplantation outcomes. Furthermore, there is an insufficiency in recapitulating the differentiation and maturation processes observed in adult human β-cells, potentially limiting their functionality (Siehler et al., 2021; Nair et al., 2019; Rezania et al., 2014; Triolo et al., 2021). Simultaneously, we identified three key issues with existing suspension protocols that emerged concomitant with the development of our modified differentiation protocol. Firstly, precocious endocrine induction during 3D differentiation, which may adversely affect maturation and functionality of the resultant β-cells. Secondly, the generation of polyhormonal cells using 3D differentiation protocols, leading to concerns about the purity and functionality of the resulting cell populations. Lastly, there was a dependence on bioreactors for 3D aggregates generation, which, despite potential benefits, introduce additional complexity and may not be universally practical (Russ et al., 2015; Velazco-Cruz et al., 2019; Nair et al., 2019; Balboa et al., 2022). By addressing these concerns and modifying the β-cell protocol to generate larger quantities of islet-like aggregates and enhance their insulin secretion in response to glucose fluctuations, our work holds great potential to make a significant impact in the field of regenerative medicine. This progress will drive the development of novel therapeutic strategies for diabetes, aiming to generate functional β-cells in abundant quantities and with high reproducibility. Ultimately, these advancements will facilitate successful clinical applications and lead to improved outcomes for patients.

The pioneering monolayer protocols developed by Novocell, later renamed Viacyte, have made significant advancements in the generation of *in vitro* β-cells and have provided a comprehensive analysis of β-cell production specifically targeted for human therapeutic applications (Pagliuca et al., 2014; Krentz et al., 2021; Rezania et al., 2014; Nair et al.,

2019; D'Amour et al., 2006; Kroon et al., 2008). However, these methods were unable to yield large quantities of cell populations suitable for screening or transplantation experiments, necessitating further optimization (Triolo et al., 2021). To address this limitation, we modified the monolayer differentiation protocol from (Rezania et al., 2014), which initially employed a monolayer and transitioned to an air-liquid interface culture system following the pancreatic progenitor stage. Our modified all-suspension protocol was based on the extant research and developmental cues guiding the formation of mature islet-like aggregates. This novel approach facilitated the achievement of our objective: generating over 400 aggregates per individual well at the end of the differentiation process (see Figure 10 and Table 1). In comparison, the established monolayer protocol from Rezania et al. yielded approximately 20 to 40 aggregates per single well at the end of differentiation. These findings demonstrate that our modified all-suspension protocol successfully addresses the challenges associated with generating adequate quantities of well-characterized β-cells for screening assays and transplantation, ameliorating several significant shortcomings of previous studies. Our cells typically exhibit $PDX1^{+}/NKX6\text{-}1^{+}/NGN3^{+}$ expression and post-NGN3 markers such as NEUROD1 or NKX2-2 at later *in vitro* stages. Furthermore, we observed the expression of $insulin^{+}$ and $glucagon^{+}$ cells (see Figures 11,12,13 and 14).

Well-to-well variability arises when differentiating cells using multiple plates and subsequently combining them to obtain large quantities of cells for screening or transplantation experiments. This variability stems from the distinct microenvironments created by cell numbers, heterogeneity, and the factors added during differentiation. Furthermore, the absence of standard operating procedures and checkpoints during critical stages of differentiation exacerbates well-to-well variability (Siehler et al., 2021; Krentz et al., 2021). It became evident that well-to-well variability at every stage of the differentiation was a significant issue faced by monolayer protocols (Pagliuca et al., 2014; de Klerk et al., 2021; Triolo et al., 2021; Balboa et al., 2022). To address this concern, our modified protocol increased the production of islet-like aggregates. Due to the large number of aggregates generated, our approach allowed for harvesting of aggregates from the same well for specific experiment. These aggregates were exposed to identical factors throughout the differentiation process (see Figure 10 and Table 1). Additionally, the implementation of standard operating procedures, standardized protocols, and culturing methods facilitated regular quality control during the differentiation, which helped minimize

differentiation batch variability. These findings demonstrate that enhancing the production of islet-like aggregates and implementing checkpoints for quality control during key stages of differentiation significantly reduce well-to-well variability.

A critical concern with current monolayer protocols is the generation of heterogeneous cell populations, as these unintended cells impair the function of the islet-like aggregates. The low reproducibility levels observed when performing these protocols with various stem cell lines suggest that cell-intrinsic factors have not been adequately considered, potentially could compromising cell usage. Although monolayer cell cultures are a prevalent method, their lack of complexity and tissue architecture does not accurately reflect *in vivo* biological process. The advent of 3D cell culture techniques has revolutionized *in vitro* culture for biological research by recapitulating cell heterogeneity, structure, and functions of primary tissues, thereby increasing the reproducibility of the protocols across different cell lines (Cacciamali et al., 2022; Escalada et al., 2019). Our all-suspension protocol, which generates 3D aggregates, addressed this issue (see Figures 10, 11, 12). We propose that the spherical structure contributes to islet architecture, closely related to islet physiology and function (Cacciamali et al., 2022). While the monolayer protocol from Rezania and colleagues is valuable for monolayer studies, our modified protocol offers a more physiologically relevant platform due to its resemblance to native 3D islet formation. The absence of matrices, such as exogenous growth factor like Matrigel, confers advantages over previous monolayers protocols in terms of generating heterogeneous cell populations and unintended cells (Velazco-Cruz et al., 2019; Veres et al., 2019; Balboa et al., 2022; Peterson et al., 2020; Augsornworawat et al., 2023). Furthermore, the scalable 3D protocol described herein enables the differentiation of multiple iPSC lines, including the parental line HMGUi001-A (see Figure 14), INS-H2B-mCherry reporter line (see Figure 16), *ARX*$^{nCFP/nCFP}$ hiPSC reporter cell line (see Figure 23), and C-peptide-mCherry-hiPSC reporter line (see Figure 37). All lines differentiated using our 3D suspension protocol consistently generate islet-like aggregates and express PDX1^{+}/NKX6-1^{+}/NGN3^{+}, insulin^{+} and glucagon^{+} cells. However, a 10 to 15 % difference in the generation of insulin-expressing β-like cells between iPSC lines remains. These findings demonstrate that our protocol offers advantages over monolayer protocols and a significant increase in reproducibility when performed with different human PSCs. Nevertheless, addressing the cell heterogeneity issue remains a challenge to be resolved.

Despite the significant advancements in β-cells differentiation protocols, the glucose-stimulated insulin secretion (GSIS) of stem cell-derived β-cells remains suboptimal when compared to native pancreatic islets (Velazco-Cruz et al., 2019; Balboa et al., 2022; Triolo et al., 2021; Krentz et al., 2021). Our objective was to generate β-cells that demonstrate improved responsiveness to GSIS by leveraging the benefits of our suspension protocol. We hypothesized that the 3D spherical structure would positively influence the cell physiology and function, ultimately leading to the production of more mature β-cells with enhanced GSIS responsiveness (see Figure 10, 14). Our rationale was based on the utilization of 3D aggregates, which provide several advantages by enhancing cell-to-cell interactions and influencing cell differentiation. E-Cadherin, a cell adhesion molecule, plays a crucial role in mediating these interactions within 3D structures by facilitating the formation of tight junctions and adherens junctions, thereby promoting cellular cohesion and communication (Bader et al., 2016). Moreover, WNT/PCP signaling is of particular importance for endocrine differentiation within the 3D environment, as it regulates cell polarity, migration, and tissue patterning. The three-dimensional architecture plays a pivotal role in facilitating the activation and maintenance of WNT/PCP signaling, thereby contributing to effective endocrine differentiation. Notably, β-cells possess gap junctions that enable rapid and synchronized responses during insulin secretion (Bader et al., 2016; Russ et al., 2015). These gap junctions facilitate direct cell-to-cell communication, ensuring coordinated insulin release and an efficient response to glucose levels. However, our findings reveal that the islet-like aggregates generated using our protocol fail to produce mature cell types and do not exhibit the desired first and second-phase insulin secretion, as demonstrated in our GSIS test (Fig. 14). It is possible that the functionality of these cells is less dependent on the tissue architecture (2D or 3D) and more reliant on other niche factors derived from tissues such as vascular endothelial cells, neurons and mesenchymal cells. Alternatively, cell-to-cell interactions within the niche might play a more significant role in determining functionality. A more effective approach may involve generating a multilineage system composed of endocrine cells, endothelial cells, and neurons in order to better access factors that are likely to influence the generation of functional, mature islet-like aggregates (Latres et al., 2019, Balboa et al., 2022; Siehler et al., 2019; Migliorini et al., 2021; Nair et al., 2019). Future research should focus on identifying key factors and conditions that contribute to the maturation of stem cell-derived β-cells, as well as refining the suspension protocol to more closely mimic the *in vivo* environment of pancreatic islets. By addressing these limitations and enhancing our

understanding of β-cell maturation, we can improve the therapeutic potential of stem cell-derived β-cells for the treatment of diabetes.

The issue of precocious endocrine induction has been a significant concern for groups working with 3D suspension protocol (Russ et al., 2015; Nair et al., 2019; Balboa et al., 2022; Krentz et al., 2021; Triolo et al., 2021). Many of these 3D studies have reported similar findings, where populations of C-peptide/insulin-positive cells lack the expression of the TF NKX6-1. Russ and colleagues demonstrated that this population resulted from precocious endocrine induction in PDX1-positive pancreatic progenitors, which lacked NKX6-1 expression. Furthermore, they showed that the absence of TF NKX6-1 expression could be avoided by excluding BMP inhibitors during the pancreas specification stage (Russ et al., 2015; Velazco-Cruz et al., 2019). In our 3D differentiation protocol, we also observed the generation of precocious endocrine cells that lacked the expression of the TF NKX6-1, a critical marker for β-cells. We addressed this issue early in the differentiation process by not including BMP inhibitors during the pancreas specification stage. As a result, the majority of our NKX6-1-expressing cells gave rise to β-cells (see Figure 11, 12). The interplay between BMP inhibitors and NKX6-1 during pancreatic formation encompasses intricate interactions that involve the modulation of signaling pathways and TFs. BMP inhibitors, by inhibiting the activity of bone morphogenetic proteins, play a crucial role in regulating the development and differentiation of pancreatic cells. NKX6-1, a key TF, involved in the specification and maturation of pancreatic endocrine cells. The dynamic interplay between BMP inhibitors and NKX6-1 plays a pivotal role in regulating the delicate balance of signaling cascades and transcriptional regulation, which ultimately contributes to the precise orchestration of pancreatic development. By excluding BMP inhibitors, we have successfully addressed the challenge of precocious endocrine induction, leading to an improved generation of β-cells that closely resemble their *in vivo* counterparts. Furthermore, our findings suggest that NKX6-1, as a β-cell specific TF, may induce the expression of NGN3 in PDX1-positive and NKX6-1-negative cells, potentially promoting α-cell fate determination. These discoveries provide valuable insights into the regulatory mechanisms governing pancreatic development and offer potential avenues for further investigation.

The generation of polyhormonal cells during β-cell differentiation has been a significant concern in the field. Recent studies have revealed that a substantial proportion of these polyhormonal cells are pre-α-cells, yet the factors influencing their formation and effective methods for prevention remain unclear. Pancreatic differentiation protocols have identified the presence of polyhormonal cells that co-express both insulin and glucagon, highlighting the need for further research to elucidate the mechanisms underlying their development and to optimize differentiation protocols for the generation of pure β-cells (Veres et al., 2019; Augsornworawat et al., 2023). These polyhormonal cells exhibited several markers of α-cells in addition to glucagon. Veres and colleagues demonstrated these cells to be pre-α-cells (Veres et al., 2019). *In vitro*-derived polyhormonal cells typically become monohormonal glucagon-expressing cells, aligning with previous findings (Kelly et al., 2011). Cells co-expressing glucagon and insulin have been identified in two contexts: 1) human fetal pancreatic development, where $INS^{+}GCG^{+}ARX^{+}$ cells are α-cell precursors (Riedel et al., 2012), and 2) type 2 diabetes, where $INS^{+}GCG^{+}$ cells represent dedifferentiated β-cells (Spijker et al., 2015). In our study utilizing a suspension differentiation protocol, we observed the presence of a population of polyhormonal cells. Interestingly, we discovered that the percentage of polyhormonal cells varied depending on the treatment with gastrin and CCK in our cultures, as depicted in (Figure 36). We propose a hypothesis that suggests the influence of gastrin and CCK on the proportion of the $PDX1^{low}$ population during the pancreatic progenitor stage. Additionally, we speculate that ARX/PAX4 double positive cells may transition into ARX^{+} single α-cells over time, and the presence of CCK and gastrin could potentially impact this process. Notably, once ARX is activated, it functions as a dominant repressor of β-cell fate, while PDX1 is known as a TF associated with β-cells. Therefore, modulation of PDX1 expression levels may have the potential to bias the fate determination between α- and β-cells. We postulate that modulating $PDX1^{low}$ levels early in the differentiation process could significantly impact endocrine progenitor cell lineage allocation. Our findings highlight that the generation of polyhormonal cells is impacted by the presence of gastrin and CCK, suggesting that modulation of these factors could help optimize differentiation protocols. Further research is warranted to elucidate the precise mechanisms underlying these observations and to develop targeted strategies for improving β-cells differentiation protocols.

5.2 Generation and application of ARX reporter for studying glucagon-producing α-cells development and function.

We successfully generated the *ARX*$^{nCFP/nCFP}$ hiPSC reporter cell line, which signifies a substantial advancement in the study of glucagon-producing α-cells, as the aristaless-related homeobox (ARX) TF plays a crucial role in the α-cells formation. *In vitro* differentiation of these reporter cells towards the endocrine lineage confirmed the specific co-expression of the reporter protein in human glucagon^{+} cells, providing a powerful tool for monitoring human α-cell progenitor formation and differentiation (see Figure 23, 24). At the time of generating this line, existing hPSC reporter cell lines for the study of α-cell precursor were not available. Only a limited number of hiPSC reporter cell lines have been generated to report glucagon, including a double reporter for both insulin and glucagon (Labonne et al., 2021). Therefore, the *ARX*$^{nCFP/nCFP}$ hiPSC reporter cell line represents a significant advantage to investigate the differentiaiton and function of α-cells and their precursors. Additionally, the design of this reporter cell line offers additional benefits. The inclusion of the 2A-peptide approach for co-translational cleavage ensures the separation of *ARX* from H2B-CFP, allowing for independent activity of *ARX*. Consequently, this strategy preserves the functionality of *ARX* without interference, while still enabling the translation of equal amounts of *ARX* and H2B-CFP-Flag protein by the reporter line. Several potential applications emerge from the development of this reporter cell line.

Firstly, the enrichment of α/β-cell precursors at early stages is facilitated. The isolation of ARX^{+} cells enables to explore the process of endocrine specification and examine the differentiation towards various hormone-producing cell lineage. Secondly, the enrichment of ARX^{+} cells at late stages of differentiation is supported. The reporter cell line facilitates the study of pure α-cell populations, providing valuable insights into α-cell function and development. Thirdly, the generation of more purified β-cell populations is made possible. The isolation and study of ARX^{+} cells can enhance our understanding of the differentiation process and potentially lead to improvements in the purity of β-cell populations generated *in vitro*. Finally, the investigation of *ARX* target genes is facilitated. The isolation of specific ARX^{+} cells using this line will allows for the analysis of *ARX* target genes through techniques such as chromatin immunoprecipitation sequencing (ChIP-seq) (Jaini et al., 2014) or cleavage under targets and release using nuclease (CUT&RUN) assays (Skene et al., 2017). In summary, the creation of the *ARX*$^{nCFP/nCFP}$ hiPSC reporter cell line offers an invaluable resource for the scientific community to study α-cells development,

differentiation, and function. This reporter line allows for the generation of double reporter cells, enabling the monitoring of α-cell formation in comparison to β-cell formation. Moreover, this reporter cell line not only enhances our understanding of the cellular and molecular mechanisms underlying endocrine lineage specification, but also holds great potential for advancing research in the field.

5.3 Identification of novel soluble factors that regulate endocrinogenesis

The understanding of endocrinogenesis, the process through which pancreatic endocrine cells develop from endocrine progenitors during the prenatal stage, still requires further elucidation. Specifically, the intricate process of endocrinogenesis and the roles of various factors involved in this process need to be clarified. A better understanding of this developmental process could guide the generation of mature hormone-producing cells from iPSCs (Staels et al., 2021). Numerous factors, including neurotransmitters and hormones, have been identified as essential during endocrinogenesis (Molina et al., 2014). For example, the work of Phillips and Ballian highlighted the presence and influence of acetylcholine and somatostatin during endocrinogenesis (Phillips et al., 2010; Ballian et al., 2006). Furthermore, the studies conducted by the research groups of Banerjee and Feng explored the influence of gastrin on pancreatic cancer through the targeted delivery of nanotherapeutics to human endocrine cells and the modulation of paracrine GABA signaling in pancreatic α-cells proliferation within a murine model of T1D (Feng et al., 2017; Banerjee et al., 2018). These studies collectively contribute to a deeper understanding of the various factors involved in the development of pancreatic endocrine cells and provide valuable insight for generating mature hormone-producing cells from iPSCs. The question persists as to whether factors, extensively documented in the literature as present during both human and mouse endocrinogenesis yet not employed in established β-cell differentiation protocols, will influence the formation and functionality of islet-like aggregates.

To address these questions, we conducted a low-throughput screening with 20 different factors selected based on literature research, describing compounds that increase pancreatic progenitors, endocrine progenitors, and the maturation of islet-like aggregates (Phillips et al., 2010, Feng et al., 2017; Banerjee et al., 2018; Petersen et al., 2018; Wu et al., 2017; Ballian et al., 2006). The primary goal of the screening was to identify factors that regulate endocrine induction and lineage segregation, potentially improving the

differentiation and maturation of islet-like aggregates (see Table 3). Our low-throughput screening identified three main targets: the Yap-inhibitor (Verteporfin), the Acetylcholine M1 antagonist (Pirenzepine), and the hormone gastrin. These compounds were chose based on their increased expression profile of pancreatic progenitors and early endocrine genes such as PDX1, NKX6-1, NKX2-2, and NGN3 (see Figures 27, 28). Our screening results align well with the existing literature (Banerjee et al., 2018; Petersen et al., 2018; Wu et al., 2017). Among the compounds investigated, the Yap-inhibitor demonstrated the most promising endocrine induction results. Previous studies by Melton and colleagues indicated that the Hippo pathway is responsible for regulating the proliferation and specification of pancreatic progenitors into the endocrine lineage. They also found that the downregulation of YAP, an effector of the pathway, enhances endocrine progenitor differentiation, ultimately leading to the generation of stem cell-derived-β cells with improved insulin secretion capabilities (Rosado-Oliveri et al., 2019). In line with these findings, the Ferrer group reported that TEAD and its coactivator YAP activate pancreatic signaling mediators and transcription factors, thereby regulating the expansion of pancreatic progenitors (Cebola et al., 2015). Although the Yap-inhibitor yielded the most relevant results during our screening, several publications emerged that explored the pivotal role of Yap-inhibitor during human islet development (Rosado-Oliveri et al., 2019). In conclusion, the reviewed publications not only shifted our focus towards investigating the relationship between YAP-inhibitor and endocrinogenesis, but also validated our screening results (Cebola et al., 2015; Mamidi et al., 2018). The roles of the Acetylcholine M1 antagonist and gastrin in islet development have not been extensively studied. However, we believe they play a role in human pancreatic islet formation. We postulate that they contribute to human pancreatic islet formation. We opted not to investigate the acetylcholine M1 antagonist due to our laboratory's limited experience with neurotransmitters in the context of pancreatic islet development. Among the three potential targets, we determined that examining gastrin's role in islet formation to be the most appropriate, considering our expertise and laboratory capabilities.

5.4 Impact of gastrin and CCK signaling on endocrinogenesis

The importance of hormones such as gastrin and CCK in the pancreas cannot be overstated, particularly in the context of pancreatic islet development, function, and their potential involvement in diabetes. While existing research on gastrin's role in islet

development is limited (Khan et al., 2018; Suissa et al., 2013), a large body of literature addresses its involvement in pancreatic cancer and diabetes (Smith et al., 2016; Rehfeld et al., 2019; Nadella et al., 2019). However, gastrin's function in islet organogenesis remains to be elucidated. To fill this knowledge gap, our research investigated gastrin and CCK's role during the early stages of endocrine formation. Notably, there are no prior publications regarding CCK's contribution to pancreatic islet development, rendering our findings novel and significant. Nevertheless, questions remain regarding the specific functions of gastrin and CCK during human endocrinogenesis, warranting further investigation.

In our investigations, we determined the endogenous timepoints of gastrin and CCK expression during pancreatic islet development (see Figures 29, 30). Our results indicate that gastrin is present throughout α- and β-cell differentiation, particularly during the endocrine induction stage. In parallel, CCK protein expression commences prior to the endocrine induction stage. We also observed that gastrin potentially influences both PDX1^{low} expression and NGN3, which may contribute to endocrine lineage allocation. Additionally, our findings suggest the possibility of a cooperative interaction between gastrin and CCK, indicating that these hormones might operate synergistically to modulate islet development and endocrine differentiation.

Glaser and colleagues, demonstrated high gastrin expression in embryonic pancreas and its subsequent decline postnatally (Suissa et al., 2013). Our results align with Glaser's findings regarding gastrin-positive cells co-expressing glucagon (seen Figure 31). However, unlike their murine model, we observed gastrin co-localization with insulin-expressing cells as well, in iPSC-derived pancreatic islets. The differences between our iPSC-based system and Glaser group murine model may account for this discrepancy. Furthermore, our data corroborate the expression of TFs, such as NKX2-2, and PDX1^{low}, in gastrin-positive cells (seen Figure 29), reinforcing the distinction between PDX1^{low} and PDX1^{high} expressions (Suissa et al., 2013). Interestingly, CCK-positive cells in our study also expressed PDX1^{low} (seen Figure 30, 33). Nevertheless, the relationship between gastrin-positive cells and NGN3 positive cells remains to be confirmed. Kaestner's group (Lee et al., 2002) previously demonstrated the relationship between NGN3 and gastrin in Ngn3 (-/-) mice, which exhibit intestinal metaplasia of the gastric epithelium. Based on these findings, we postulated that similar events might occur during pancreatic islet development. Our experiments involving gastrin and CCK treatment during differentiation revealed altered NGN3 expression levels. Our data demonstrate that gastrin antagonist

directly modulate PDX1^{low} and PDX1^{high} expressions, prolonging NGN3 expression and reducing INS-positive cells (seen Figure 38 A). We hypothesize that an increase in PDX1^{high} expression might affect NGN3 regulation, consequently determining insulin induction. In our study, aggregates treated with gastrin antagonist (YM022) from day 5 to day 8 of differentiation continued to express NGN3 at day 20 compared to untreated aggregates, while insulin expression was reduced. In support of these observations, additional experiments using another gastrin antagonist (LY288) showed similar NGN3 expression patterns at day 20 of differentiation (seen Figure 38 C). Thus, we conclude that activation of CCKBR by gastrin antagonists influences NGN3, the master regulator of endocrine cell fate, extending its expression later in differentiation and decreasing insulin expression in developing pancreatic islets. Additional experiments are also necessary to elucidate the molecular mechanisms underlying the observed effects of gastrin and CCK on NGN3 expression and the modulation of the PDX1^{low} and PDX1^{high} expressions.

The observed simultaneous expression patterns of gastrin and CCK during differentiation, as well as their shared affinity for the CCKBR receptor, suggest the possibility of a cooperative interaction between these two hormones in context of pancreatic islet development (Zeng et al., 2020; Aly et al., 2004; Konturek et al., 1991). Our findings, which demonstrate an increase in insulin expression in aggregates treated with a combination of gastrin and CCK (see Figure 37), further support this hypothesis. However, these initial observations warrant further investigation to establish a mechanistic understanding of the potential synergistic relationship between gastrin and CCK during islet organogenesis. Future studies should focus on elucidating the molecular pathways and mechanisms by which gastrin and CCK may exert their cooperative effects on pancreatic islet development. For instance, investigating the activation of downstream signaling cascades and TFs in response to combined gastrin and CCK treatment could provide valuable insights into the molecular basis of their interplay. Moreover, single-cell RNA sequencing (scRNA-seq) and single-cell proteomics could be employed to explore the heterogeneity of cell populations within the aggregates and determine the specific cell types that are most responsive to gastrin and CCK treatment. In addition to exploring the molecular mechanisms, optimizing the concentrations and treatment durations of gastrin and CCK may be crucial for enhancing the potential benefits of their combined application. Dose-response and time-course experiments could help identify the optimal conditions for achieving maximal insulin expression and improving the overall efficiency of the

differentiation process. Furthermore, assessing the functionality of the derived pancreatic islet cells, such as glucose-stimulated insulin secretion and calcium influx, will be essential for determining the physiological relevance of the observed effects.

CCKBR, a G-protein-coupled receptor, is targeted by both gastrin and CCK, which are structurally related peptides. These peptides appear in the pancreatic islet following NGN3 expression, during early endocrine induction phase. There are two subtypes of these receptors, CCKBR and CCKAR, with only CCKBR expressed in pancreatic islets (Marjorie et al., 2002; Lee et al., 2002). Gastrin receptor activation prompts CCKBR signaling, leading to calcium release and PKC activation, essential for β-cell insulin release and pancreatic development (Zanner et al., 2002; Klec et al., 2019). Additionally, CCKBR coupling with Gq and $G\alpha_{12/13}$ proteins promotes cell proliferation and inhibits apoptosis via multiple cascades and EGFR transactivation (Zeng et al., 2020). Akt and EGFR pathways contribute to pancreatic β-cells survival and cell cycle progression (Elghazi et al., 2009). Intriguingly, our experimental findings have revealed crucial insights into the temporal dynamics of gastrin and CCK expression during the pancreatic islet differentiation process. We observed that endogenous protein expression of these hormones occurs on day 12 of the differentiation, coinciding with the pancreas progenitor stage. Furthermore, our low-throughput screening results demonstrated a notable increase in PDX1 and NKX6-1 expression upon treatment of aggregates from day 5 to day 8 of differentiation. However, treating the aggregates with gastrin and CCK after day 8 did not yield a similar increase in PDX1/NKX6-1 expression, raising questions regarding the optimal treatment timepoint for achieving the most significant outcomes. The reconcile these seemingly conflicting results, we postulate that during day 5 to day 8 of the differentiation, the high expression of CCKBR receptors in the absence of endogenous gastrin or CCK suggests a functional receptor pathway amenable to ligand binding. Consequently, we speculate that an external source of gastrin and CCK might be responsible for stimulating the CCKBR receptor during early islet formation, subsequently triggering the onset of gastrin and CCK production within the pancreatic tissue. Supporting this hypothesis, previous studies have reported the presence of minimal amounts of gastrin and CCK in the stomach bud and nearby tissues during the formation of pancreatic buds (Shulkes et al., 1997), which aligns with our day 5 to day 8 treatment window. It is plausible that these trace amounts of hormones could activate the highly expressed CCKBR receptor, thereby initiating a cascade of events that result in the increased production of gastrin and CCK

within the developing pancreatic buds (Aly et al., 2004). In light of these findings, further investigation into the spatiotemporal dynamics of gastrin and CCK expression, as well as their interaction with CCKBR receptors during pancreatic islet development, is warranted. The genetic deletion of CCKBR could provide valuable insights into this phenomenon, enhancing our understanding. Similarly, investigating the effects of Gastrin and CCK knockout (KO) in relevant models would further complement the ongoing pharmacological studies. A more comprehensive understanding of these molecular mechanisms could elucidate novel strategies for optimizing differentiation protocols and improving the therapeutic potential of *in vitro*-generated pancreatic islet cells.

Collectively, our findings point to gastrin and CCK as potential modulators of endocrine lineage allocation, though a comprehensive understanding of their roles in human islet development has not yet been achieved. Nonetheless, the preliminary evidence allows us to explore the possible functions of gastrin and CCK during islet formation. The expression patterns of these peptides during islet formation and their disappearance prior to birth suggest a critical role within this specific developmental timeframe (Konturek et al., 199; Aly et al., 2004; Zeng et al., 2020). Moreover, our data indicate that the roles of gastrin and CCK in the differentiation process are time-dependent (see figures 29, 30), leading us to hypothesize that these peptides have multiple distinct roles contingent on differentiation stages, hormone concentration, and receptor-binding patterns.

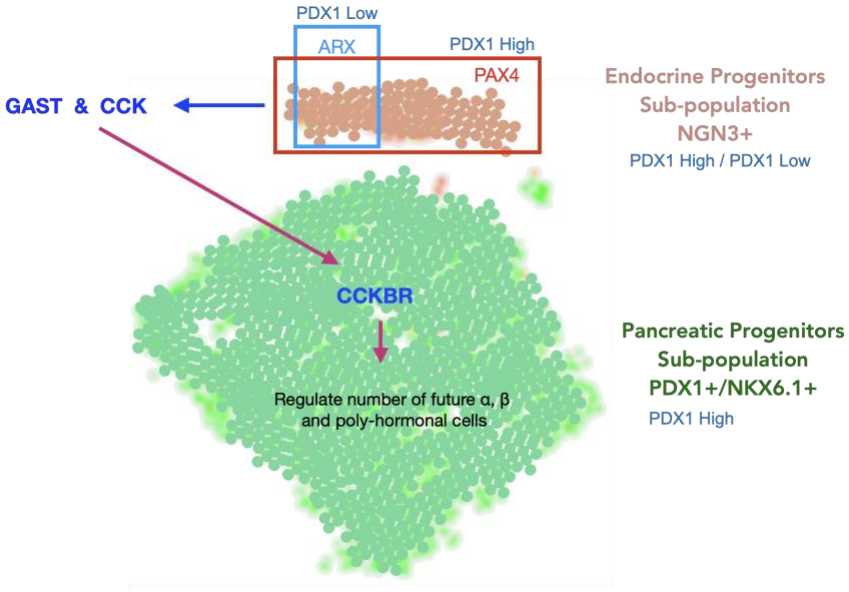

Figure 44. Schematic representation of pancreatic progenitor population at day 12 of the differentiation (S4). Model showing the possible role of gastrin and CCK activating CCKBR and downstream components. PDX1^{high} characterizes the pancreatic progenitor sub-population, where the endocrine progenitor sub-population is characterized by PDX1$^{low\ /\ high}$, subdivided by PAX4 / PDX1^{high} and ARX / PDX1^{low}. We

hypothesize that the small endocrine progenitor subpopulation in the pancreatic progenitor stage expresses ARX, PAX4, gastrin, and CCK. We believe that signals by ARX and PAX4 in conjunction with gastrin and CCK reached the main pancreatic progenitor sub-population, activating the CCKBR receptors. These signals regulated the number of α, β, and poly-hormonal cells generated at this early stage of the differentiation.

We propose that gastrin and CCK may play a critical role in regulating endocrine lineage formation. According to our model, a small subpopulation of endocrine cells, expressing ARX, PAX4, gastrin, and CCK, coexists with a large pancreatic progenitor subpopulation, which exhibits high CCKBR expression. It likely that gastrin and CCK, secreted from endocrine cells, exert signals through a feedback loop mechanism to pancreatic progenitors, thereby governing their induction towards endocrine lineage and controlling islet cell numbers. Moreover, this signaling may also regulate the allocation of progenitor cells toward α-, β- and poly-hormonal cells, ensuring optimal islet functionality (seen Figure 44). Overall, our findings contribute to the understanding of gastrin and CCK's involvement in pancreatic islet development and their potential roles in endocrine lineage induction. Further studies will be necessary to elucidate the precise mechanisms by which these hormones function during islet organogenesis.

6. Materials and Methods

6.1 Material

6.2 Consumables

50 ml / 15 ml tubes	Becton and Dickinson and Company
2 ml / 1.5 ml / 0.2 ml tubes	Eppendorf (safe-lock reaction tubes)
15 cm/ 10 cm/ 6 cm dishes	Thermo Scientific Fisher (nunc) 6-well/ 12-well/ 24-well/
48-well plates/ 96-well plates	Thermo Scientific Fisher (nunc) (straight/conical)
10 cm bacterial plates	Becton Dickinson GmbH (BD Falcon™)
8 well chambers	Ibidi (uncoated and coated 8-well imaging plates)
Embedding moulds	Leica (Peel-a-way embedding molds)
50 ml / 25 ml / 10 ml	Greiner bio-one
5 ml / 2 ml / 1 ml	Plastic pipettes Greiner bio-one
Pasteur pipettes, plastic	Carl Roth GmbH & Co. KG
Blotting paper	GE Healthcare Buchler GmbH & Co (Whatman paper)
Cell strainer	Falcon (Nylon cell stainer 70 µm)
Counting chambers	Biorad (counting slides dual chamber for cell counter)
Embedding molds	Sigma (Peel-a-way embedding molds, S-22)
FACS tubes	Falcon (5 ml polystyrene round bottom tube with cell strainer cap)
	Falcon (5 ml polypropene round bottom tube)
Films	Sigma-Aldrich (Kodak BioMax MS), Amersham GE Healthcare Buchler GmbH & Co (Hyperfilm ECL)
Glass slides	Thermo Scientific (Menzel Gläser superfrost plus)
Needles	Sterican 27G ½ ``, Sterican 30G ½ ``
Parafilm	Pechiney Plastic Packaging

PVDF membrane	Biorad
Scalpels	Aesculap AG & Co
Spacer	Life Technologies (Secure-Sela, 9mm 0.12 mm deep)
Syringes	Braun (Omnifix 30 ml / 3 ml)
Syringe filter	Millex-GP (Filter unit fast flow and low binding 0.22 µm)
TEM tubes	Ted Pella, Inc. (BEEM® capsules)
qPCR 96-well plates	Life Technologies (MicroAmp Fast optcal 96-well reaction plate)
Adhesive covers	Life Technologies (optical adhesive covers)
Protein ladder	Life Technologies (PageRuler Plus Pre-Stained)
RNA ladder	NEB (RNA ladder 100 bp)
Goat serum	Biozol
Donkey serum	Millipore
Human serum	Sigma

6.3 Equipments

Agarose gel chamber	Midi 450 (neolab)
Balances	ABS, EWB (Kern & Sohn GmbH)
Bioanalyzer	Agilent 2100 Bioanalyzer (Agilent)
Centrifuges	5417R, 5430C, 5804 R (Eppendorf)
	Microcentrifuge (Roth), Micro 220 (Hettich)
	Universal 320R (Hettich), 6767 (Corning)
Cell counter	TC20™ Automated cell counter (Biorad)
Cryostat	Ag Protect (Leica)
Cytospin equipment	Cyto chambers, filter, rotor (Hettich)
Developing machine	AGFA Curix 60 developing machine (AGFA HealthCare GmbH)

ddH_2O	QPod (Millipore)
FACS	BD FACSAria III
Film cassettes	Hypercassette (Amersham)
Freezer	-20°C Medline, premium nofrost (Liebherr)
	-80°C (Thermo Scientific)
Fridge	4°C comfort (Liebherr)
Gel documentation system	UVsolo TS Imaging System (Biometra)
Glassware	Schott-Duran (Schott)
Glucometer	Accu-Check Avia (Roche)
Ice machine	AF103 (Scotsman)
Incubation systems/ovens	Thermomixer comfort, Thermomixer 5436 (Eppendorf)
	Oven (Thermo Scientific)
Incubator	BBD6220 (Thermo Scientific)
	Inkubator C16 (Labortect)
Microscopes	Axiovert 200M (Carl Zeiss AG)
	MS5 (Leica)
	TCS SP5 (Leica) and Cube (heating), Brick (CO_2)
	M80 (Leica) and Dissection light (Leica)
Microwave	700W (Severin)
N_2 tank	Biostore systems (Cryo Anlagenbau GmbH)
PCR machines	Personal Thermocycler, Professional Trio Thermocycler (Biometra)
pH meter	Mettler Toledo (Hanna Instruments)
Photometer	NanoDrop 2000 c (Thermo Fisher Scientific)
	HERAstar FS (BMG Labtech)
Pipettes	1000 µl/ 200 µl / 20 µl/ 10 µl (Eppendorf)

Pipettboy	Accu-jet® pro (Brand GmbH)
Polyacrylamid gel chamber	Mini Trans-Blot® Cell (Biorad)
Power supply (agarose gel)	Power Source 300V (VWR)
qPCR cycler	ViiA7 Real-time PCR system (life technologies)
	AB 7300 unit (BD)
Roller/Mixer	VSR 23 (VWR international), Shaker DOS-10L (neolab), RMS (Assistent), Rocker 247 (Everlast)
Sterile hoods	MSC Advantage (Thermo Scientific)
Stirrer	D-6011 (neolab)
Timer	Roth
Tissue Homogenizer	Ultra Turrax T25 (IKA)
Ultrasonic bath	Ultrasonic cleaner (VWR)
Vortexer	LSE Vortex Mixer (Corning), IKA Vortex
Water bath	Memmert
Western Blot semi-dry	Trans-Blot® SD, Semi-Dry Transfer cell (Biorad)

6.4 Chemicals

(If not indicated chemicals were purchased from Sigma-Aldrich, Merck or Carl Roth)

A 7-AAD (eBioscience)

Acrylamide/bisacrylamide (Rotiphorese)

Agarose (Biozym Scientific)

APS

L-Arginine

B BCA

Bromophenol blue

BrdU

BSA

C Calcium chloride

Chloroform, 99+%

D DAPI

Developer G135 A/B (AGFA)

1,4-Diazabicyclo[2.2.2]octane (Dapco)

Dimethylsulfoxide (DMSO), >99,9%

Dithiothreitol (DTT)

Dithizone

DNAZap (Thermo Fisher Scientific)

dNTPs (Fermentas)

E EDTA

EdU (Life Technologies)

Ethanol, 96%

Ethidiumbromide

G L-Glutamine

Glucose

Glutaraldehyde

Glycerol

Glycin

H 10N HCl

HEPES (powder)

Hoechst 33342 (Thermo Fisher Scientific)

Human serum albumin

I Isopropanol, 100%

M Magnesium chloride

Methanol, 100%

Milk powder (Becton Dickinson)

Mounting medium – Jung Tissue Freezing medium (Leica)

N Nitrogen(l) (Linde AG, München)

NP40 (Life Technologies)

P Paraformaldehyde

Polyacrylamide

Polyvinyl-alcohol

Potassium chloride (KCl)

Potassium hydrogenphosphate (KH_2PO_4)

ProLong Gold antifade reagent (Invitrogen)

R Rapid fixer G356 (AGFA)

RNaseZAP

S Sodium chloride

Sodium desoxycholate

Sodium dodecylsulphate (SDS)

Sodium hydrogenic phosphate (Na_2HPO_4)

Sodium hydroxide

Sodium tetraborate ($Na_2B_2O_7$)

T TEMED

Tris

Triton X-100

Tween-20

6.5 Mastermix and kits

Agilent RNA 6000 Pico kit (Agilent Technologies)

Dynamo Color Flash SYBR Green qPCR kit (Life Technologies)

ECL Detection Kit (Millipore)

Human ultrasensitive Insulin ELISA kit (Mercodia)

Primer (Eurofins MWG Operon)

QIamp DNA Blood Mini kit (Qiagen)

QIAquick PCR Purification Kit (Qiagen)

RNeasy Mini Kit, RNeasy Micro Kit, miRNA Micro Kit (Qiagen)

Sodium calcodylate buffer pH7.4 (0.1 M) 2% paraformaldehyde 2.5% glutaraldehyde (Electron Microscopy Sciences)

SuperScript Vilo cDNA synthesis kit (Life Technologies)

SuperSignal West femto maximum sensitivity substrate (Life Technologies)

TaqMan Fast Advanced Master Mix (Life Technologies)

TaqMan Universal Master Mix II, no UNG (Life Technologies)

6.6 Solutions and buffers for immunostainings

10x PBS:	1.37 M NaCl, 26.8 mM KCl, 0,101 M Na_2HPO_4, 13.8 mM KH_2PO_4
PBST:	1x PBS + 0.1% Tween20 (adjust to pH7.4)
4% PFA:	1.3 M PFA in 1x PBS (adjust to pH7.2-7.4)
Permeabilisation (sections):	0.2% TritonX-100, 100 mM Glycin in dH_2O
Permeabilisation (islets):	0.5% TritonX-100, 100 mM Glycin in dH_2O
Blocking solution:	5% FCS, 1% serum (goat or donkey) in PBST
DAPI:	5 mg DAPI in 25 ml PBS
Elvanol (embedding):	0.015 mM Polyvinyl-alcohol, 24 mM Tris pH 6.0, 2 g DABCO in 90 ml H_2O and 37.8 ml Glycerol
Antigen retrieval:	10 N HCl in H_2O
10x Tris-Borat-Buffer:	10 mM $Na_2B_2O_7$ in dH_2O

Glucose stimulated insulin secretion

10x Krebs buffer:	1.2 M NaCl, 48 mM KCl, 25 mM $CaCl_2$*$2H_2O$, 12 mM $MgCl_2$ in dH_2O
1x Modified Krebs buffer:	1x Krebs buffer, 5 mM HEPES, 0.025 mM $NaHCO_3$, 0.1% BSA in H_2O (adjust to pH7.4)
FACS buffer:	1x PBS (-Ca/Mg), 3% FCS, 5 mM EDTA
DNA lysis buffer:	100 mM Tris pH 8.0, 5 mM EDTA pH 8.0, 200 mM NaCl, 0.2% SDS in H_2O

6.6 Solutions and buffers for cell culture

DPBS (-Ca/-Mg)	Gibco
DPBS	Lonza
Trypsin-EDTA Gibco	0.05% or 0.25% Trypsin, 0.53 mM EDTA•4Na,
DMEM (4.5 g/l glucose)	Gibco
DMEM (1 g/l glucose)	Gibco
RPMI1640	Lonza
HBSS	Lonza
Penicillin/Streptomycin (100x)	Gibco
OptiPrep Density gradient medium	Sigma
FCS	PAN
β-mercaptoethanol (50mM)	Gibco / Life Technologies
HEPES (1 M)	Gibco
Matrigel	BD Bioscience / Neolab
CMRL1066	Gibco / Thermo Fisher Scientific

6.8 Small molecules, drugs and reagents

WNT4	R&D systems

Wnt5a (mouse)	R&D systems
WNT5A (human)	R&D systems
EdU	Life Technologies
BrdU	Sigma
Murine Noggin	Peprotech
Y-27632	Santa Cruz
Gastrin	Tocris
CCK Octapeptide	Tocris
Caerulein Acetate	Sigma
LY288	Tocris
YM022	Sigma
CI988	Tocris
L-365260	Sigma
Activin A	R&D systems
CHIR	R&D systems
KGF	R&D systems
Retinoic Acid	R&D systems
SANT-1	R&D systems
TPB	Tocris
ALK5 Inh II	R&D systems
Heparin	Peprotech
Zinc Sulfate	Tocris
Trolox	Peprotech
Caerulein	Tocris
LY288	Tocris
YM022	Sigma

CI988	Tocris
Butabindide oxalate	Tocris
Proglumide	Tocris

6.9 Primary and secondary antibodies

Table 6.9.1 Primary antibodies

ID	Protein Name	Generated in	Dilution	Company
26	GFP	chicken	IF 1:1000	Aves Labs
48	Glucagon	guinea pig	IF 1:500	Millipore
53	β -Catenin	mouse	IF 1:1000	BD
82	Ki67	rabbit	IF 1:300	Novocastra
121	Insulin	guinea pig	IF 1:300	Thermo Fisher Scientific
123	Pdx1	rabbit	IF 1:300	NEB
125	Glut2	rabbit	IF 1:500	Millipore
192	Nkx6-1	goat	IF 1:200	R&D systems
193	Somatostatin	Goat	IF 1:500	Santa Cruz
197	Nkx6-1	rabbit	IF 1:300	Acris/Novus
199	Ki67	rabbit	IF 1:300	Abcam
214	Neurogenin 3	mouse	IF 1:100	DSHB Hybridoma
215	Insulin	rabbit	IF 1:300	Thermo Fisher Scientific
216	Glucagon	guinea pig	IF 1:500	TAKARA
221	SOX2	goat	IF 1:500	Santa Cruz
227	OCT-3/4	goat	IF 1:500	Santa Cruz
257	CCKBR	rabbit	IF 1:200	LS Bio
277	FOXA2	rabbit	IF 1:500	Cell Signaling
302	SOX17	goat	IF 1:500	Neuromics
315	Nestin	mouse	IF 1:500	Abcam
546	Gastrin	rabbit	IF 1:100	Abcam
503	CCK	rabbit	IF 1:300	Abcam

Table 6.9.2 Secondary antibodies

ID	Name	Conjugated	Dilution	Company
11	Alexa Fluor phalloidin	546	IC 1:40	Invitrogen
18	Donkey anti-goat IgG	633	IC 1:500	Invitrogen
23	Donkey anti-mouse IgG	488	IC 1:500	Invitrogen
24	Donkey anti-rabbit IgG	555	IC 1:500	Invitrogen
28	Donkey anti-chicken IgY	488	IC 1:500	Dianova
45	donkey anti-rat IgG	649	IC 1:500	Dianova
46	donkey anti-guineapig	649	IC 1:500	Dianova
56	Donkey anti-mouse IgG	594	IC 1:500	Invitrogen
62	Donkey anti-rat IgG	647	IC 1:500	Dianova
63	Donkey anti-goat IgG	594	IC 1:500	Invitrogen
64	Donkey anti-rabbit IgG	594	IC 1:500	Invitrogen

6.10 Taqman primers

Table 6.10.1 Taqman primers

Box-Position	Gene	Order Information	Box-Position	Gene	Order Information
A-A5	*Ins1*	Mm01950294_s1	A-G9	*Ghrl*	Mm00445450_m1
A-A9	*Nkx6-1*	Mm00454961_m1	A-G10	*Amy2a3*	Mm02342486_mh
A-A10	*Bace2*	Mm00517138_m1	A-H12	*MafA*	Mm00845206_s1
A-B9	*Hadh*	Mm0130384_m1	B-A4	*Ucn3*	Mm00453206_s1
A-B11	*Gcg*	Mm01269055_m1	B-A7	*Npy*	Mm03048253
A-C4	*Actb*	Mm00607939_s1	B-A8	*Cfap126/Fltp*	Mm01290541_m1
A-D1	*Wnt4*	Mm01194003_m1	B-C12	*Slc2a2*	Mm00446229_m1
A-D3	*Gapdh*	Mm99999915_g1	B-D1	*Dvl2*	Mm00432899_m1
A-D4	*Ins2*	Mm00731505_Gh	B-D3	*Celsr1*	Mm00464808_m1
A-D5	*GFP*	Mr04329676_mr	B-D4	*Fzd6*	Mm00433387_m1
A-D6	*Wnt5b*	Mm01183986_m1	B-E9	*Grb10*	Mm01180443_m1

A-E11	*Sst*	Mm00436671_m1	B-E10	*Alpk1*	Mm01319946_m1
A-F12	*18S*	Mm03928990_g1	C-B1	*Pcsk1*	Mm00479023_m1
A-G2	*mKi67*	Mm01278817_m1	C-B10	*Gipr*	Mm01316344_m1
A-G6	*Ppy*	Mm01250509_g1	IDO	*Atp5b*	Mm01160389_g1

TaqMan primer were purchased from Life Technologies

6.11 Methods

6.12 Cell culture

The hiPSCs culture was maintained under a feeder-free system on Geltrex (Invitrogen) in StemMACS iPS-Brew XF, human (Miltenyi Biotec). Cells were passaged at 70% confluency, washed once with 1x DPBS without Mg^{2+} and Ca^{2+} (Invitrogen, Cat#14190), and incubated for 5 minutes with StemPro Accutase Cell Dissociation Reagent (Thermo Fisher Scientific). After dissociation, cells were rinsed with iPS-Brew XF medium and spun at 1000 rpm for 5 minutes. The resulting pellet was re-suspended in iPS-Brew XF medium, and single cells were seeded in iPS-Brew medium plus 10 µM Y-27632 (Sigma-Aldrich; MO, Cat#Y0503) at a concentration of 1.0 $x10^6$ cells in a 10 cm Geltrex-coated surface plate. The cultures were fed daily with the iPS-Brew medium.

6.13 Pancreatic lineage differentiation protocol

6.13.1 S1: definitive endoderm (3 days)

The suspension-based differentiation was carried out as follows. Confluent cultures were rinsed with 1× DPBS without Mg^{2+} and Ca^{2+} (Invitrogen, Cat#14190) followed by incubation with StemPro Accutase (1×) for 5 min at 37 °C. Released single cells were rinsed with iPS-Brew XF and spun at 1,000 r.p.m. for 5 min. The resulting cell pellet was re-suspended in iPS-Brew XF medium supplemented with Y-27632 (10 µM; Sigma-Aldrich; MO, Cat#Y0503). The single-cell suspension was counted, and each well of a 6-well low-binding plate were seeded with 2.0 $x10^6$ cells in 4 ml of MCDB 131 medium (Life, Cat# 10372-019) further supplemented with 1.5 g/l sodium bicarbonate (Sigma, MO, Cat# S6297), 1× Glutamax (Life, Cat#35050-079), 10 mM final glucose (Sigma, Cat# G8769) concentration, 0.5% BSA (fatty acid-free BSA, Proliant, IA, Cat#68700), 100 ng/ml Activin-A (Pepro-Tech), and 1.5 µM of CHIR-99021 (GSK3β inhibitor, SelleckChem, Cat#S2924) for day 1 only. The plate was placed in an orbital shaker at 110 RPM. For day 2, cells were

cultured in MCDB with 0.5% BSA, 1.5 g/l sodium bicarbonate, 1× Glutamax, 10 mM glucose, 100 ng/ml Activin-A and 0.1 μM of CHIR-99021. On day three, cells were cultured in MCDB with 0.5% BSA, 1.5 g/l sodium bicarbonate, 1× Glutamax, 10 mM glucose, and 100 ng/ml Activin-A.

6.13.2 S2: primitive gut tube (2 days)

Cells were exposed to MCDB 131 medium further supplemented with 1.5 g/l sodium bicarbonate, 1× Glutamax, 10 mM final glucose concentration, 0.5% BSA, 0.25 mM ascorbic acid (Sigma, Cat# A4544) and 50 ng/ml of FGF7 (R & D Systems, Cat#251-KG) for 2 days.

6.13.3 S3: posterior foregut (2 days)

Cultures were continued for 2 d in MCDB 131 medium further supplemented with 2.5 g/l sodium bicarbonate, 1× Glutamax, 10 mM final glucose concentration, 2% BSA, 0.25 mM ascorbic acid, 50 ng/ml of FGF7, 0.25 μM SANT-1 (Sigma, Cat# S4572), 1 μM retinoic acid (RA; Sigma, Cat#R2625), 100 nM LDN193189 (LDN; BMP receptor inhibitor, Stemgent, CA, Cat#04-0019), 1:200 ITS-X (Life, Cat#51500056), and 200 nM TPB (PKC activator, custom synthesis, ChemPartner).

6.13.4 S4: pancreatic endoderm, PDX1$^+$/NKX6-1$^+$ cells (3 days)

MCDB 131 medium supplemented with 2.5 g/l sodium bicarbonate, 1× Glutamax, 10 mM final glucose concentration, 2% BSA, 0.25 mM ascorbic acid, 2 ng/ml of FGF7, 0.25 μM SANT-1, 0.1 μM retinoic acid, 200 nM LDN193189, 1:200 ITS-X, and 100 nM TPB for 3 days.

6.13.5 S5: pancreatic endocrine precursors, PDX1$^+$/NKX6-1$^+$/NEUROD1$^+$ (3 days)

The cells were exposed to MCDB 131 medium supplemented with 1.5 g/l sodium bicarbonate, 1× Glutamax, 20 mM final glucose concentration, 2% BSA, 0.25 μM SANT-1, 0.05 μM retinoic acid, 100 nM LDN193189, 1:200 ITS-X, 1 μM T3 (3,3′,5-Triiodo-L-thyronine sodium salt, Sigma, T6397), 10 μM ALK5 inhibitor II (Enzo Life Sciences, NY, Cat# ALX-270-445), 10 μM zinc sulfate (Sigma, Z0251) and 10 μg/ml of heparin (Sigma, H3149) for 3 days.

6.13.6 S6: NKX6-1^{+}/insulin^{+} cells (7–15 days)

MCDB 131 medium further supplemented with 1.5 g/l sodium bicarbonate, 1× Glutamax, 20 mM final glucose concentration, 2% BSA, 100 nM LDN193189, 1:200 ITS-X, 1 µM T3, 10 µM ALK5 inhibitor II, 10 µM zinc sulfate, 100 nM gamma secretase inhibitor XX for the first 7 d only (EMD MilliPore, MA, Cat# 565789) and 10 µg/ml of heparin for 7–15 days.

6.13.7 S7: NKX6-1^{+}/insulin^{+}/MAFA^{+} cells (7–15 days)

MCDB 131 medium supplemented with 1.5 g/l sodium bicarbonate, 1× Glutamax, 20 mM glucose concentration, 2% BSA, 1:200 ITS-X, 1 µM T3, 10 µM ALK5 inhibitor II, 10 µM zinc sulfate, 1 mM N-acetyl cysteine (N-Cys, Sigma, Cat# A9165), 10 µM Trolox (Vitamin E analogue, EMD, Cat#648471), 2 µM R428 (AXL inhibitor, SelleckChem, Cat# S2841) and 10 µg/ml of heparin for 7–15 d. Unless otherwise specified, for all stages, the cultures were fed daily.

6.14 Generation of clonal hiPSCs mutant lines using gRNA /ssDNA

The plasmid pU6-BbsI sgRNA-CAG-venus-bpA (Addgene) containing a BbsI site and multiple sites for gRNA, venus, and Cas9 genes was utilized. The iPSCs were cultured regularly for 3 days until reaching 60% confluence, and then dissociated using StemPro Accutase. Single cells were plated on Geltrex (Invitrogen) coated plates. After 20 minutes, they were transfected with gRNA/ssDNA using Lipofectamine RNAiMAX (Thermo Fisher Scientific, Cat # 13778-150). The gRNA/ssDNA and Lipofectamine RNAiMAX were separately diluted in Opti-MEM (Thermo Fisher Scientific, Cat # 31985070) for 20 minutes, followed by mixing the buffers for 5 minutes at room temperature. Finally, the mixture was added to the hiPSCs. After 4 hours of transfection, the medium was replaced.

6.15 Establishment of clonal hiPSCs mutant lines

The hiPSCs were dissociated into single cells using StemPro Accutase two days after transfection. Using the FACS Aria, cells expressing Venus were sorted and plated at different densities ranging from 2,000 to 10,000 cells per 10 cm plate. After one week, individual colonies were mechanically selected and re-plated in Geltrex-coated 24-well plates with iPS-Brew medium supplemented with 10 µM Y-27632 (Sigma-Aldrich; MO, Cat#Y0503). PCR analysis using Herulase II Fusion DNA Polymerase (Agilent Technologies, Cat#600679) was performed to screen for positive clones. Subsequently, Sanger sequencing was conducted to identify mutant clones.

6.16 FACS sorting and flow cytometric analysis

Aggregates were collected and allowed to settle by gravity. They were washed once in PBS and dissociated by gentle pipetting after 15-min incubation in StemPro Accutase. For sorting, the cell suspension was filtered and re-suspended in FACS buffer consisting of PBS containing 2 mM EDTA (Ambion) and 1% BSA (Sigma). For flow-based analysis, dissociated cells were fixed with 2% paraformaldehyde (Electron Microscopy Science) for 20 min at room temperature, followed by two washes in PBS. Samples were either stored at 4 °C or immediately to the blocking step for 30 min. Followed by stained with directly conjugated antibodies or primary antibodies for 30 min, two washes were performed with PBS. The secondary antibodies were added for 30 min, and cells were washed twice with PBS and filtered. Cell sorting was performed on a FACS Aria II (BD Bioscience). The data analysis was performed with FlowJo software. In general, the single cells were gated according to their FSC-A (front scatter area) and SSC-A (side scatter area), excluding dead cells and debris. Singlets were gated dependent on the FSC-W (front scatter width) and FSC-H (front scatter height), excluding double cells.

6.17 Immunofluorescence analysis

For the sectioning of clusters, aggregates were fixed for 30 min at room temperature with 2% paraformaldehyde, followed by 2 washes in PBS and embedded in 2% agar (Sigma), followed by dehydration, paraffin embedding, and sectioning. Cut sections were rehydrated and blocked for 2h at room temperature in blocking buffer (in house) with 0.2% Triton X-100 (Fisher). Primary antibodies were incubated overnight at 4 °C in a blocking buffer. The next day, sections were washed three times with PBS containing 0.1% Tween-20 (PBS-T, Sigma) and incubation in appropriate secondary antibodies diluted in blocking buffer for 4h at room temperature. Slides were washed in PBS-T and PBS before incubation with DAPI diluted in PBS for 30 min. Followed by 3 washes in PBS-T and mounted with Evanol on glass slides. Nuclei were visualized with DAPI. Images were acquired using a Leica SP5 and Zeiss microscopes.

6.18 GSIS assays

For the dynamic GSIS assay, aggregates of the same size were manually selected and subjected to various glucose concentrations, following established protocols. Modified Krebs-Ringer phosphate Hepes (KRPH) buffer supplemented with 0.1% BSA was utilized. The aggregates were incubated in KRPH containing 2.8 mM glucose for 30 minutes,

followed by sequential incubation with different glucose concentrations as specified. Assessment of pancreatic insulin and glucagon concentrations was carried out using acid ethanol extraction. Human insulin concentrations were determined using an Ultrasensitive Insulin ELISA kit (Mercodia).

6.19 Electrophoresis

The PCR products were loaded on an agarose gel (1 – 1.5%) and separated by size using gel electrophoresis. The agarose gel was prepared by dissolving agarose in TAE (Tris-acetate, EDTA) buffer in the microwave. After cooling the solution, EtBr (1:20000) was added to the solution, which was then mixed and poured into a gel tray. The solid gel was transferred into a TAE buffer filled gel chamber. The PCR products were mixed with Orange G (1:4), loaded on the gel, separated by applying voltage, and the DNA fragments were detected using a gel documentation system.

6.20 Islet-like aggregates re-aggregation

To re-aggregate islet-like aggregates, the differentiated cells were FACS-sorted and separated by the emission of Venus. The sorted islet-like cells were cultured 6 well low binding plates, shaking in differentiation medium corresponding with the day of FACS-sorting. The culture was supplemented by 10 µM Y-27632 (Santa Cruz) for the first 1 day.

6.21 Image analysis

The images were analyzed using Imaris™ (Bitplane) and Fiji software (Fiji). In detail, the islet-like aggregates volume was determined by the surface rendering of the backscatter image. In our studies, we analyzed 10 aggregates per conditions in z-stacks of 10 µm distance. Hormone's quantification was analyzed by eye-counting.

6.22 Cryopreservation

If needed, IPSCs were thawed fast in a 37°C warm water bath and transferred into a culture dish containing culture medium. After one day, the medium was changed, and the cells were usually cultured for four days prior to an experiment. To cryopreserve IPSCs, the cells were accutased as described before and re-suspended in freezing medium (DMSO and FCS 1:1). After transferring the cells into cryovials, the cells were frozen in freezing boxes overnight at -80°C and then transferred into liquid N_2.

6.23 CRISPR/Cas9 design and plasmid building

The web toll CRISPETa (crispeta.crg.eu) was used to design sgRNAs capable of targeted specific genes in the genomic DNA. The sgRNAs binding site in the genome was sequence initially sequence due to genome variation. The sequence of CACCGGG was added to the 5' site of sense oligo, and sequences of AAAC and CCC were added to 5' and 3' anti-sense oligo sites, respectively, to increase the expression. Addgene PU6-(BbsI) sgRNA_CAG-Cas9-GFP-bpA (ID86985) plasmid containing the BbsI site was used to clone single and multiple gRNAs. Following the cloning, single and multiples gRNAs expression cassette was subjected to Sanger sequencing.

6.24 hiPSCs culture and CRISPR/Cas9 plasmid transfection

The hiPSCs were maintained Geltrex (Life-Technologies)-coated plates in human StemMACS iPS-Brew XF medium (Miltenyi Biotec). The medium was daily renewed; 5 min incubation with StemPro Accutase Cell Dissociation Reagent (Thermo Fisher Scientific) was used to dissociate and passage the confluent hiPSCs. Cellular stress was reduced by adding 10 μM ROCK inhibitor (Y-27632, Santa Cruz Biotechnology) for the first 24 h after dissociation. Cells with a density of 2 x 105 were seeded in 6 well plates one day before plasmid transfection. Each well 2.5 μg dual sgRNA vector was transfected into the hiPSCs using 5 μl LipofectamineTM Stem Transfection Reagent (Fisher Scientific) and 200 μl OptiMEM medium (Fisher Scientific) according to manufacture instruction.

6.25 FACS enrichment of transfected hiPSCs

After transfection, the cells were incubated for 48 hours before being dissociated and prepared for FACS experiment. The cell suspension was filtered and re-suspended in FACS buffer, which consisted of 2 mM EDTA and 1% BSA (Sigma) in PBS. The cells were sorted based on high GFP signal levels using the FACS Aria III (BD Bioscience). Approximately four thousand cells were then seeded in 10 cm dishes. After one week, single-cell-derived clones were selected, expanded, and screened by PCR. Flow cytometry was performed to quantify the expression of pluripotency markers (OCT4 and SOX2) in the clones. The resulting data were analyzed using FlowJo software.

6.26 Clone screening for CRIPR/Cas9-mediated genomic deletion

The appropriate PCR primers for sequencing and clones screening were designed using Clone Manager Molecule Software. Long Amp Taq DNA Polymerase enzyme (NEB) was

used for PCR reactions. The PCR products were cloned into a TA vector (NEB) and followed by sequencing to confirm the deletion's authenticity at both alleles.

6.27 RNA isolation

According to the kit manual, RNA isolation was carried out using the miRNA kit (Qiagen). Also, the DNA was degraded by performing an on-column DNase I treatment. The RNA was eluted in 130 µl of nuclease-free water for immediate use or stored at -80°C.

6.28 RNA amplification

The amplification was performed according to the kit manual using 50 ng RNA. The procedure was conducted in a strictly RNase-free environment. Furthermore, all cDNAs have to be degraded by DNAZap to prohibit primer contaminations.

6.29 Reverse transcription

The reverse transcription transcribes RNA into cDNA. For cDNA preparation, the SuperScript Vilo cDNA synthesis kit (Life Technologies) was used. Thereby, the solution of RNA (100 – 500 ng RNA), 5x VILO™ reaction mix, and 10x SuperScript™ enzyme mix were incubated at 25°C for 10 min before 120 min at 85°C. Afterward, the cDNA was stored at -20°C or -80°C.

6.30 Determination of the DNA or RNA concentration

The DNA or RNA concentration in solution was measured by a NanoDrop using the extinction at 260 nm. The cDNA resulting from amplified RNA was determined using the ssDNA program of the Nanodrop. The purity of the DNA and RNA was assessed by the quotient of E_{260nm}/E_{280nm} and E_{260nm}/E_{230nm} which had to be around 2.0.

6.31 Cryosections

The dissected islet-like aggregates were fixed in 2% paraformaldehyde (PFA) for 20 min at RT. After washing the pancreas 2x in PBS, the tissue was cryoprotected in a sequential gradient of 15%, 30% sucrose in PBS (2 hr each). After overnight incubation in 30% sucrose in PBS and tissue embedding medium (Leica) (1:1), the islet-like aggregates were placed in 100% tissue embedding medium, in an embedding mold, frozen using dry ice and stored at -80°C. To prepare cryosections, the embedded and frozen islet-like

aggregates were cut in 20 µm sections using a cryostat (Leica), mounted on a glass slide (Thermo Fisher Scientific), and dried for 30 min at RT before use or storage at -20°C.

6.32 Quantitative PCR (qPCR)

The qPCR was conducted using TaqMan™ probes (Life Technologies) and 50 ng of cDNA per reaction. TaqMan probes are hydrolysis probes that consist of a fluorophore attached to the 5'-end, an oligonucleotide, and a quencher at the 3'-end. The probe binds to the cDNA between the forward and reverse primers and is degraded by the exonuclease activity of the Taq Polymerase. This enzymatic cleavage disrupts the interaction between the quencher and fluorophore, resulting in a fluorescence signal. Each reaction contained a total volume of 10 µl, consisting of 2.5 µl of cDNA in nuclease-free water, 5 µl of TaqMan™ Advanced master mix (Life Technologies), and 2.5 µl of TaqMan probe™ (Life Technologies) in nuclease-free water. After sealing the 96-well plates (Life Technologies) and centrifuging them at 1000 rpm for 1 minute, the qPCR was performed using the Viia7 instrument (Thermo Fisher Scientific). The data were analyzed using Excel. The Ct-values, which represent the point of linear fluorescence slope, were normalized across samples, transformed into linear expression values, and further normalized to reference genes and control samples.

Relative expression (gene) = $(2^{Ct\ (mean\ genes) - Ct\ (gene)})$ / $(2^{Ct\ (mean\ references) - Ct\ (reference)})$

Normalized expression (gene) = Relative expression (gene) / Relative expression $_{control}$ (gene)

The normalized gene expression was represented using bar graphs ± s.e.m. Statistical significance was determined using a two-tailed unpaired t-test with Welch correction. The expression level of each gene transcript was calculated by normalizing it to the expression of the respective housekeeping gene. Undifferentiated iPSC mRNA was used as the reference for normalizing gene expression. The relative gene expression was presented as the ratio of the target gene concentration to the concentration of the housekeeping gene, 18S. P-values were calculated using a two-tailed Student's t-test.

6.33 Statistics

The statistical analysis was carried out using Graphpad Prism. If not otherwise indicated, a two-sided and unpaired Welch-corrected *t*-test was used. * Indicated *P*-values smaller than 0.05, ** > 0.01, *** > 0.001 and **** > 0.0001.

7. References

Aamodt, K. I., & Powers, A. C. (2017). Signals in the pancreatic islet microenvironment influence β-cell proliferation. *Diabetes, Obesity and Metabolism*, *19*, 124–136. https://doi.org/10.1111/dom.13031

Aguayo-Mazzucato, C., Koh, A., El Khattabi, I., Li, W.-C., Toschi, E., Jermendy, A., Juhl, K., Mao, K., Weir, G. C., Sharma, A., & Bonner-Weir, S. (2011). Mafa expression enhances glucose-responsive insulin secretion in neonatal rat beta cells. *Diabetologia*, *54*(3). https://doi.org/10.1007/s00125-010-2026-z

Aguayo-Mazzucato, C., van Haaren, M., Mruk, M., Lee, T. B., Crawford, C., Hollister-Lock, J., Sullivan, B. A., Johnson, J. W., Ebrahimi, A., Dreyfuss, J. M., Van Deursen, J., Weir, G. C., & Bonner-Weir, S. (2017). β Cell Aging Markers Have Heterogeneous Distribution and Are Induced by Insulin Resistance. *Cell Metabolism*, *25*(4). https://doi.org/10.1016/j.cmet.2017.03.015

Ahlgren, U., Jonsson, J., Jonsson, L., Simu, K., & Edlund, H. (1998). beta -Cell-specific inactivation of the mouse Ipf1/Pdx1 gene results in loss of the beta -cell phenotype and maturity onset diabetes. *Genes & Development*, *12*(12). https://doi.org/10.1101/gad.12.12.1763

Ahlqvist, E., Storm, P., Käräjämäki, A., Martinell, M., Dorkhan, M., Carlsson, A., Vikman, P., Prasad, R. B., Aly, D. M., Almgren, P., Wessman, Y., Shaat, N., Spégel, P., Mulder, H., Lindholm, E., Melander, O., Hansson, O., Malmqvist, U., Lernmark, Å., … Groop, L. (2018). Novel subgroups of adult-onset diabetes and their association with outcomes: a data-driven cluster analysis of six variables. *The Lancet Diabetes & Endocrinology*, *6*(5), 361–369. https://doi.org/10.1016/S2213-8587(18)30051-2

Alonso-Magdalena, P., Ropero, A. B., Carrera, M. P., Cederroth, C. R., Baquié, M., Gauthier, B. R., Nef, S., Stefani, E., & Nadal, A. (2008). Pancreatic Insulin Content Regulation by the Estrogen Receptor ERα. *PLoS ONE*, *3*(4). https://doi.org/10.1371/journal.pone.0002069

Aly, A., Shulkes, A., & Baldwin, G. S. (2004). Gastrins, cholecystokinins and gastrointestinal cancer. *Biochimica et Biophysica Acta (BBA) - Reviews on Cancer*, *1704*(1). https://doi.org/10.1016/j.bbcan.2004.01.004

Andrali, S. S., Sampley, M. L., Vanderford, N. L., & Özcan, S. (2008). Glucose regulation of insulin gene expression in pancreatic β-cells. *Biochemical Journal*, *415*(1). https://doi.org/10.1042/BJ20081029

Ang, S.-L., & Rossant, J. (1994). HNF-3β is essential for node and notochord formation in mouse development. *Cell*, *78*(4), 561–574. https://doi.org/10.1016/0092-8674(94)90522-3

Anık, A., Çatlı, G., Abacı, A., & Böber, E. (2015). Maturity-onset diabetes of the young (MODY): an update. *Journal of Pediatric Endocrinology and Metabolism*, *28*(3–4). https://doi.org/10.1515/jpem-2014-0384

Apelqvist, Å., Li, H., Sommer, L., Beatus, P., Anderson, D. J., Honjo, T., de Angelis, M. H., Lendahl, U., & Edlund, H. (1999). Notch signalling controls pancreatic cell differentiation. *Nature*, *400*(6747). https://doi.org/10.1038/23716

Arda, H. E., Benitez, C. M., & Kim, S. K. (2013). Gene Regulatory Networks Governing Pancreas Development. *Developmental Cell*, *25*(1). https://doi.org/10.1016/j.devcel.2013.03.016

Auerbach, A., Cohen, A., Ofek Shlomai, N., Weinberg-Shukron, A., Gulsuner, S., King, M.-C., Hemi, R., Levy-Lahad, E., Abulibdeh, A., & Zangen, D. (2020). NKX2-2 Mutation Causes Congenital Diabetes and Infantile Obesity With Paradoxical Glucose-Induced Ghrelin Secretion. *The Journal of Clinical Endocrinology & Metabolism*, *105*(11). https://doi.org/10.1210/clinem/dgaa563

Augsornworawat, P., Hogrebe, N. J., Ishahak, M., Schmidt, M. D., Marquez, E., Maestas, M. M., Veronese-Paniagua, D. A., Gale, S. E., Miller, J. R., Velazco-Cruz, L., & Millman, J. R. (2023). Single-nucleus multi-omics of human stem cell-derived islets identifies deficiencies in lineage specification. *Nature Cell Biology*. https://doi.org/10.1038/s41556-023-01150-8

Bader, E., Migliorini, A., Gegg, M., Moruzzi, N., Gerdes, J., Roscioni, S. S., Bakhti, M., Brandl, E., Irmler, M., Beckers, J., Aichler, M., Feuchtinger, A., Leitzinger, C., Zischka, H., Wang-Sattler, R., Jastroch, M., Tschöp, M., Machicao, F., Staiger, H., … Lickert, H. (2016). Identification of proliferative and mature β-cells in the islets of Langerhans. *Nature*, *535*(7612). https://doi.org/10.1038/nature18624

Balboa, D., Barsby, T., Lithovius, V., Saarimäki-Vire, J., Omar-Hmeadi, M., Dyachok, O., Montaser, H., Lund, P.-E., Yang, M., Ibrahim, H., Näätänen, A., Chandra, V., Vihinen, H., Jokitalo, E., Kvist, J., Ustinov, J., Nieminen, A. I., Kuuluvainen, E., Hietakangas, V., … Otonkoski, T. (2022). Functional, metabolic and transcriptional maturation of human pancreatic islets derived from stem cells. *Nature Biotechnology*, *40*(7), 1042–1055. https://doi.org/10.1038/s41587-022-01219-z

Balboa, D., Saarimäki-Vire, J., & Otonkoski, T. (2019). Concise Review: Human Pluripotent Stem Cells for the Modeling of Pancreatic β-Cell Pathology. *Stem Cells*, *37*(1), 33–41. https://doi.org/10.1002/stem.2913

BALDWIN, G. S. (1995). The role of gastrin and cholecystokinin in normal and neoplastic gastrointestinal growth. *Journal of Gastroenterology and Hepatology*, *10*(2). https://doi.org/10.1111/j.1440-1746.1995.tb01083.x

Balena, R., Hensley, I. E., Miller, S., & Barnett, A. H. (2013). Combination therapy with GLP-1 receptor agonists and basal insulin: a systematic review of the literature. *Diabetes, Obesity and Metabolism*, *15*(6). https://doi.org/10.1111/dom.12025

Ballian, N., Brunicardi, F. C., & Wang, X.-P. (2006). Somatostatin and its Receptors in the Development of the Endocrine Pancreas. *Pancreas*, *33*(1), 1–12. https://doi.org/10.1097/01.mpa.0000226894.16817.e8

Banerjee, S., & Saluja, A. K. (2018). A Theranostic Approach to Target Gastrin in Pancreatic Cancer. *Cellular and Molecular Gastroenterology and Hepatology*, *6*(1), 117-118.e1. https://doi.org/10.1016/j.jcmgh.2018.04.002

Bankaitis, E. D., Bechard, M. E., & Wright, C. V. E. (2015). Feedback control of growth, differentiation, and morphogenesis of pancreatic endocrine progenitors in an epithelial plexus niche. *Genes & Development*, *29*(20). https://doi.org/10.1101/gad.267914.115

Bastidas-Ponce, A., Scheibner, K., Lickert, H., & Bakhti, M. (2017). Cellular and molecular mechanisms coordinating pancreas development. *Development*, *144*(16). https://doi.org/10.1242/dev.140756

Bechard, M. E., Bankaitis, E. D., Hipkens, S. B., Ustione, A., Piston, D. W., Yang, Y.-P., Magnuson, M. A., & Wright, C. V. E. (2016). Precommitment low-level *Neurog3* expression defines a long-lived mitotic endocrine-biased progenitor pool that drives production of endocrine-committed cells. *Genes & Development*, *30*(16). https://doi.org/10.1101/gad.284729.116

Beucher, A., Gjernes, E., Collin, C., Courtney, M., Meunier, A., Collombat, P., & Gradwohl, G. (2012). The Homeodomain-Containing Transcription Factors Arx and Pax4 Control Enteroendocrine Subtype Specification in Mice. *PLoS ONE*, *7*(5), e36449. https://doi.org/10.1371/journal.pone.0036449

Bjerg, L., Hulman, A., Charles, M., Jørgensen, M. E., & Witte, D. R. (2018). Clustering of microvascular complications in Type 1 diabetes mellitus. *Journal of Diabetes and Its Complications*, *32*(4). https://doi.org/10.1016/j.jdiacomp.2018.01.011

Blöchinger, A. K., Siehler, J., Wißmiller, K., Shahryari, A., Burtscher, I., & Lickert, H. (2020). Generation of an INSULIN-H2B-Cherry reporter human iPSC line. *Stem Cell Research*, *45*. https://doi.org/10.1016/j.scr.2020.101797

Blum, B., Hrvatin, S., Schuetz, C., Bonal, C., Rezania, A., & Melton, D. A. (2012). Functional beta-cell maturation is marked by an increased glucose threshold and by expression of urocortin 3. *Nature Biotechnology*, *30*(3), 261–264. https://doi.org/10.1038/nbt.2141

Borden, P., Houtz, J., Leach, S. D., & Kuruvilla, R. (2013). Sympathetic Innervation during Development Is Necessary for Pancreatic Islet Architecture and Functional Maturation. *Cell Reports*, *4*(2), 287–301. https://doi.org/10.1016/j.celrep.2013.06.019

Brafman, D. A., Moya, N., Allen-Soltero, S., Fellner, T., Robinson, M., McMillen, Z. L., Gaasterland, T., & Willert, K. (2013). Analysis of SOX2-Expressing Cell Populations

Derived from Human Pluripotent Stem Cells. *Stem Cell Reports*, *1*(5), 464–478. https://doi.org/10.1016/j.stemcr.2013.09.005

Cacciamali, A., Villa, R., & Dotti, S. (2022). 3D Cell Cultures: Evolution of an Ancient Tool for New Applications. *Frontiers in Physiology*, *13*. https://doi.org/10.3389/fphys.2022.836480

Cebola, I., Rodríguez-Seguí, S. A., Cho, C. H.-H., Bessa, J., Rovira, M., Luengo, M., Chhatriwala, M., Berry, A., Ponsa-Cobas, J., Maestro, M. A., Jennings, R. E., Pasquali, L., Morán, I., Castro, N., Hanley, N. A., Gomez-Skarmeta, J. L., Vallier, L., & Ferrer, J. (2015). TEAD and YAP regulate the enhancer network of human embryonic pancreatic progenitors. *Nature Cell Biology*, *17*(5), 615–626. https://doi.org/10.1038/ncb3160

Churchill, A. J., Gutiérrez, G. D., Singer, R. A., Lorberbaum, D. S., Fischer, K. A., & Sussel, L. (2017). Genetic evidence that NKX2-2 acts primarily downstream of Neurog3 in pancreatic endocrine lineage development. *ELife*, *6*. https://doi.org/10.7554/eLife.20010

Collombat, P., Hecksher-Sørensen, J., Broccoli, V., Krull, J., Ponte, I., Mundiger, T., Smith, J., Gruss, P., Serup, P., & Mansouri, A. (2005). The simultaneous loss of *Arx* and *Pax4* genes promotes a somatostatin-producing cell fate specification at the expense of the α-and β-cell lineages in the mouse endocrine pancreas. *Development*, *132*(13), 2969–2980. https://doi.org/10.1242/dev.01870

Da Silva Xavier, G. (2018). The Cells of the Islets of Langerhans. *Journal of Clinical Medicine*, *7*(3), 54. https://doi.org/10.3390/jcm7030054

Dassaye, R., Naidoo, S., & Cerf, M. E. (2016). Transcription factor regulation of pancreatic organogenesis, differentiation and maturation. In *Islets* (Vol. 8, Issue 1). https://doi.org/10.1080/19382014.2015.1075687

de Klerk, E., & Hebrok, M. (2021). Stem Cell-Based Clinical Trials for Diabetes Mellitus. *Frontiers in Endocrinology*, *12*. https://doi.org/10.3389/fendo.2021.631463

Decker, K., Goldman, D. C., L. Grasch, C., & Sussel, L. (2006). Gata6 is an important regulator of mouse pancreas development. *Developmental Biology*, *298*(2), 415–429. https://doi.org/10.1016/j.ydbio.2006.06.046

Doyle, M. J., & Sussel, L. (2007). NKX2-2 Regulates β-Cell Function in the Mature Islet. *Diabetes*, *56*(8). https://doi.org/10.2337/db06-1766

Dufresne, M., Seva, C., & Fourmy, D. (2006). Cholecystokinin and Gastrin Receptors. *Physiological Reviews*, *86*(3), 805–847. https://doi.org/10.1152/physrev.00014.2005

Ediger, B. N., Du, A., Liu, J., Hunter, C. S., Walp, E. R., Schug, J., Kaestner, K. H., Stein, R., Stoffers, D. A., & May, C. L. (2014). Islet-1 Is Essential for Pancreatic β-Cell Function. *Diabetes*, *63*(12). https://doi.org/10.2337/db14-0096

Elghazi, L., & Bernal-Mizrachi, E. (2009). Akt and PTEN: β-cell mass and pancreas plasticity. *Trends in Endocrinology & Metabolism*, *20*(5), 243–251. https://doi.org/10.1016/j.tem.2009.03.002

Feng, A. L., Xiang, Y.-Y., Gui, L., Kaltsidis, G., Feng, Q., & Lu, W.-Y. (2017). Paracrine GABA and insulin regulate pancreatic alpha cell proliferation in a mouse model of type 1 diabetes. *Diabetologia*, *60*(6), 1033–1042. https://doi.org/10.1007/s00125-017-4239-x

Gage, B. K., Baker, R. K., & Kieffer, T. J. (2014). Overexpression of PAX4 reduces glucagon expression in differentiating hESCs. *Islets*, *6*(2), e29236. https://doi.org/10.4161/isl.29236

Gage, B. K., Asadi, A., Baker, R. K., Webber, T. D., Wang, R., Itoh, M., Hayashi, M., Miyata, R., Akashi, T., & Kieffer, T. J. (2015). The Role of ARX in Human Pancreatic Endocrine Specification. *PLOS ONE*, *10*(12), e0144100. https://doi.org/10.1371/journal.pone.0144100

Gradwohl, G., Dierich, A., LeMeur, M., & Guillemot, F. (2000). *neurogenin3* is required for the development of the four endocrine cell lineages of the pancreas. *Proceedings of the National Academy of Sciences*, *97*(4), 1607–1611. https://doi.org/10.1073/pnas.97.4.1607

Grieco, G. E., Brusco, N., Licata, G., Fignani, D., Formichi, C., Nigi, L., Sebastiani, G., & Dotta, F. (2021). The Landscape of microRNAs in βCell: Between Phenotype Maintenance and Protection. *International Journal of Molecular Sciences*, *22*(2). https://doi.org/10.3390/ijms22020803

Hashimoto, T., Kawano, H., Daikoku, S., Shima, K., Taniguchi, H., & Baba, S. (1988). Transient coappearance of glucagon and insulin in the progenitor cells of the rat pancreatic islets. *Anatomy and Embryology*, *178*(6), 489–497. https://doi.org/10.1007/BF00305036

Haumaitre, C., Barbacci, E., Jenny, M., Ott, M. O., Gradwohl, G., & Cereghini, S. (2005). Lack of TCF2/vHNF1 in mice leads to pancreas agenesis. *Proceedings of the National Academy of Sciences*, *102*(5), 1490–1495. https://doi.org/10.1073/pnas.0405776102

Herrera, P. L. (2000). Adult insulin- and glucagon-producing cells differentiate from two independent cell lineages. *Development*, *127*(11), 2317–2322. https://doi.org/10.1242/dev.127.11.2317

Ionescu-Tirgoviste, C., Gagniuc, P. A., Gubceac, E., Mardare, L., Popescu, I., Dima, S., & Militaru, M. (2015). A 3D map of the islet routes throughout the healthy human pancreas. *Scientific Reports*, *5*(1), 14634. https://doi.org/10.1038/srep14634

Jain, C., Ansarullah, Bilekova, S., & Lickert, H. (2022). Targeting pancreatic β cells for diabetes treatment. *Nature Metabolism*, *4*(9), 1097–1108. https://doi.org/10.1038/s42255-022-00618-5

Jaini, S., Lyubetskaya, A., Gomes, A., Peterson, M., Tae Park, S., Raman, S., Schoolnik, G., & Galagan, J. (2014). Transcription Factor Binding Site Mapping Using ChIP-Seq. *Microbiology Spectrum*, *2*(2). https://doi.org/10.1128/microbiolspec.MGM2-0035-2013

Jenny, M. (2002). Neurogenin3 is differentially required for endocrine cell fate specification in the intestinal and gastric epithelium. *The EMBO Journal*, *21*(23), 6338–6347. https://doi.org/10.1093/emboj/cdf649

Jensen, J., Heller, R. S., Funder-Nielsen, T., Pedersen, E. E., Lindsell, C., Weinmaster, G., Madsen, O. D., & Serup, P. (2000). Independent development of pancreatic alpha- and beta-cells from neurogenin3-expressing precursors: a role for the notch pathway in repression of premature differentiation. *Diabetes*, *49*(2), 163–176. https://doi.org/10.2337/diabetes.49.2.163

Kanai-Azuma, M., Kanai, Y., Gad, J. M., Tajima, Y., Taya, C., Kurohmaru, M., Sanai, Y., Yonekawa, H., Yazaki, K., Tam, P. P. L., & Hayashi, Y. (2002). Depletion of definitive gut endoderm in *Sox17* -null mutant mice. *Development*, *129*(10), 2367–2379. https://doi.org/10.1242/dev.129.10.2367

Kaneto, H., & Matsuoka, T. (2015). Role of Pancreatic Transcription Factors in Maintenance of Mature β-Cell Function. *International Journal of Molecular Sciences*, *16*(12). https://doi.org/10.3390/ijms16036281

Kaneto, H., Matsuoka, T., Katakami, N., & Matsuhisa, M. (2009). Combination of MafA, PDX-1 and NeuroD is a Useful Tool to Efficiently Induce Insulin-Producing Surrogate β -Cells. *Current Medicinal Chemistry*, *16*(24). https://doi.org/10.2174/092986709788802980

Kawaguchi, Y., Cooper, B., Gannon, M., Ray, M., MacDonald, R. J., & Wright, C. V. E. (2002). The role of the transcriptional regulator Ptf1a in converting intestinal to pancreatic progenitors. *Nature Genetics*, *32*(1), 128–134. https://doi.org/10.1038/ng959

Kelly, O. G., Chan, M. Y., Martinson, L. A., Kadoya, K., Ostertag, T. M., Ross, K. G., Richardson, M., Carpenter, M. K., D'Amour, K. A., Kroon, E., Moorman, M., Baetge, E. E., & Bang, A. G. (2011). Cell-surface markers for the isolation of pancreatic cell types derived from human embryonic stem cells. *Nature Biotechnology*, *29*(8), 750–756. https://doi.org/10.1038/nbt.1931

Khan, D., Vasu, S., Moffett, R. C., Irwin, N., & Flatt, P. R. (2018). Expression of Gastrin Family Peptides in Pancreatic Islets and Their Role in β-Cell Function and Survival. *Pancreas*, *47*(2), 190–199. https://doi.org/10.1097/MPA.0000000000000983

Kim, A., Miller, K., Jo, J., Kilimnik, G., Wojcik, P., & Hara, M. (2009). Islet architecture: A comparative study. *Islets*, *1*(2), 129–136. https://doi.org/10.4161/isl.1.2.9480

Kim, J. B., Zaehres, H., Wu, G., Gentile, L., Ko, K., Sebastiano, V., Araúzo-Bravo, M. J., Ruau, D., Han, D. W., Zenke, M., & Schöler, H. R. (2008). Pluripotent stem cells

induced from adult neural stem cells by reprogramming with two factors. *Nature*, *454*(7204). https://doi.org/10.1038/nature07061

Klec, C., Ziomek, G., Pichler, M., Malli, R., & Graier, W. F. (2019). Calcium Signaling in ß-cell Physiology and Pathology: A Revisit. *International Journal of Molecular Sciences*, *20*(24), 6110. https://doi.org/10.3390/ijms20246110

Kodama, M., Tsukamoto, K., Yoshida, K., Aoki, K., Kanegasaki, S., & Quinn, G. (2009). Embryonic Stem Cell Transplantation Correlates With Endogenous Neurogenin 3 Expression and Pancreas Regeneration in Streptozotocin-injured Mice. *Journal of Histochemistry & Cytochemistry*, *57*(12). https://doi.org/10.1369/jhc.2009.954206

Koliaki, C., Liatis, S., le Roux, C. W., & Kokkinos, A. (2017). The role of bariatric surgery to treat diabetes: current challenges and perspectives. *BMC Endocrine Disorders*, *17*(1). https://doi.org/10.1186/s12902-017-0202-6

Konturek, S. J., Bilski, J., Hladij, M., Krzyzek, E., Cai, R.-Z., & Schally, A. V. (1991). Role of Cholecystokinin, Gastrin and Gastrin-Releasing Peptide in the Regulation of Pancreatic Secretion in Cats. *Digestion*, *49*(2). https://doi.org/10.1159/000200708

Kopp, J. L., Grompe, M., & Sander, M. (2016). Stem cells versus plasticity in liver and pancreas regeneration. *Nature Cell Biology*, *18*(3), 238–245. https://doi.org/10.1038/ncb3309

Kotaka, M., Toyoda, T., Yasuda, K., Kitano, Y., Okada, C., Ohta, A., Watanabe, A., Uesugi, M., & Osafune, K. (2017). Adrenergic receptor agonists induce the differentiation of pluripotent stem cell-derived hepatoblasts into hepatocyte-like cells. *Scientific Reports*, *7*(1), 16734. https://doi.org/10.1038/s41598-017-16858-5

Krentz, N. A. J., Shea, L. D., Huising, M. O., & Shaw, J. A. M. (2021). Restoring normal islet mass and function in type 1 diabetes through regenerative medicine and tissue engineering. *The Lancet Diabetes & Endocrinology*, *9*(10), 708–724. https://doi.org/10.1016/S2213-8587(21)00170-4

Labonne, T., Elefanty, A. G., Stanley, E. G., & Schiesser, J. V. (2021). An INSULIN-GFP/GLUCAGON-mCherry reporter line for the study of human pancreatic endocrine cell development. *Stem Cell Research*, *56*, 102547. https://doi.org/10.1016/j.scr.2021.102547

Latres, E., Finan, D. A., Greenstein, J. L., Kowalski, A., & Kieffer, T. J. (2019). Navigating Two Roads to Glucose Normalization in Diabetes: Automated Insulin Delivery Devices and Cell Therapy. *Cell Metabolism*, *29*(3), 545–563. https://doi.org/10.1016/j.cmet.2019.02.007

Lavine, J. A., Raess, P. W., Davis, D. B., Rabaglia, M. E., Presley, B. K., Keller, M. P., Beinfeld, M. C., Kopin, A. S., Newgard, C. B., & Attie, A. D. (2008). Overexpression of Pre-Pro-Cholecystokinin Stimulates β-Cell Proliferation in Mouse and Human Islets with Retention of Islet Function. *Molecular Endocrinology*, *22*(12). https://doi.org/10.1210/me.2008-0255

Le Lay, J., & Stein, R. (2006). Involvement of PDX-1 in activation of human insulin gene transcription. *Journal of Endocrinology*, *188*(2). https://doi.org/10.1677/joe.1.06510

Lee, C. S., Perreault, N., Brestelli, J. E., & Kaestner, K. H. (2002). Neurogenin 3 is essential for the proper specification of gastric enteroendocrine cells and the maintenance of gastric epithelial cell identity. *Genes & Development*, *16*(12), 1488–1497. https://doi.org/10.1101/gad.985002

Li, L., Cheng, W.-Y., Glicksberg, B. S., Gottesman, O., Tamler, R., Chen, R., Bottinger, E. P., & Dudley, J. T. (2015). Identification of type 2 diabetes subgroups through topological analysis of patient similarity. *Science Translational Medicine*, *7*(311). https://doi.org/10.1126/scitranslmed.aaa9364

Mamidi, A., Prawiro, C., Seymour, P. A., de Lichtenberg, K. H., Jackson, A., Serup, P., & Semb, H. (2018). Mechanosignalling via integrins directs fate decisions of pancreatic progenitors. *Nature*, *564*(7734), 114–118. https://doi.org/10.1038/s41586-018-0762-2

Mannucci, E. (2012). Insulin Therapy and Cancer in Type 2 Diabetes. *ISRN Endocrinology*, *2012*. https://doi.org/10.5402/2012/240634

Marc J. Berna, & Robert T. Jensen. (2007). Role of CCK/Gastrin Receptors in Gastrointestinal/Metabolic Diseases and Results of Human Studies Using Gastrin/CCK Receptor Agonists/Antagonists in these Diseases. *Current Topics in Medicinal Chemistry*, *7*(12), 1211–1231. https://doi.org/10.2174/156802607780960519

Mellitzer, G., Bonné, S., Luco, R. F., Van De Casteele, M., Lenne-Samuel, N., Collombat, P., Mansouri, A., Lee, J., Lan, M., Pipeleers, D., Nielsen, F. C., Ferrer, J., Gradwohl, G., & Heimberg, H. (2006). IA1 is NGN3-dependent and essential for differentiation of the endocrine pancreas. *The EMBO Journal*, *25*(6), 1344–1352. https://doi.org/10.1038/sj.emboj.7601011

Memon, B., Younis, I., Abubaker, F., & Abdelalim, E. M. (2021). PDX1-/NKX6-1+ progenitors derived from human pluripotent stem cells as a novel source of insulin-secreting cells. *Diabetes/Metabolism Research and Reviews*, *37*(5). https://doi.org/10.1002/dmrr.3400

Migliorini, A., Nostro, M. C., & Sneddon, J. B. (2021). Human pluripotent stem cell-derived insulin-producing cells: A regenerative medicine perspective. *Cell Metabolism*, *33*(4), 721–731. https://doi.org/10.1016/j.cmet.2021.03.021

Migliorini, A., Roscioni, S. S., & Lickert, H. (2016). Targeting insulin-producing beta cells for regenerative therapy. *Diabetologia*, *59*(9), 1838–1842. https://doi.org/10.1007/s00125-016-3949-9

Migliorini, F., Maffulli, N., Baroncini, A., Knobe, M., Tingart, M., & Eschweiler, J. (2021). Matrix-induced autologous chondrocyte implantation versus autologous matrix-

induced chondrogenesis for chondral defects of the talus: a systematic review. *British Medical Bulletin*, *138*(1), 144–154. https://doi.org/10.1093/bmb/ldab008

Miguel-Escalada, I., Bonàs-Guarch, S., Cebola, I., Ponsa-Cobas, J., Mendieta-Esteban, J., Atla, G., Javierre, B. M., Rolando, D. M. Y., Farabella, I., Morgan, C. C., García-Hurtado, J., Beucher, A., Morán, I., Pasquali, L., Ramos-Rodríguez, M., Appel, E. V. R., Linneberg, A., Gjesing, A. P., Witte, D. R., … Ferrer, J. (2019). Human pancreatic islet three-dimensional chromatin architecture provides insights into the genetics of type 2 diabetes. *Nature Genetics*, *51*(7). https://doi.org/10.1038/s41588-019-0457-0

Miranda, M. A., Macias-Velasco, J. F., & Lawson, H. A. (2021). Pancreatic β-cell heterogeneity in health and diabetes: classes, sources, and subtypes. *American Journal of Physiology-Endocrinology and Metabolism*, *320*(4). https://doi.org/10.1152/ajpendo.00649.2020

Mitchell, R. K., Nguyen-Tu, M.-S., Chabosseau, P., Callingham, R. M., Pullen, T. J., Cheung, R., Leclerc, I., Hodson, D. J., & Rutter, G. A. (2017). The transcription factor Pax6 is required for pancreatic β cell identity, glucose-regulated ATP synthesis, and Ca2+ dynamics in adult mice. *Journal of Biological Chemistry*, *292*(21), 8892–8906. https://doi.org/10.1074/jbc.M117.784629

Molina, J., Rodriguez-Diaz, R., Fachado, A., Jacques-Silva, M. C., Berggren, P.-O., & Caicedo, A. (2014). Control of Insulin Secretion by Cholinergic Signaling in the Human Pancreatic Islet. *Diabetes*, *63*(8), 2714–2726. https://doi.org/10.2337/db13-1371

Moon, S. Y., Park, Y. Bin, Kim, D.-S., Oh, S. K., & Kim, D.-W. (2006). Generation, culture, and differentiation of human embryonic stem cells for therapeutic applications. *Molecular Therapy*, *13*(1). https://doi.org/10.1016/j.ymthe.2005.09.008

Moya, N., Cutts, J., Gaasterland, T., Willert, K., & Brafman, D. A. (2014). Endogenous WNT Signaling Regulates hPSC-Derived Neural Progenitor Cell Heterogeneity and Specifies Their Regional Identity. *Stem Cell Reports*, *3*(6), 1015–1028. https://doi.org/10.1016/j.stemcr.2014.10.004

Moya, N., Shahryari, A., Burtscher, I., Beckenbauer, J., Bakhti, M., & Lickert, H. (2020). Generation of a homozygous ARX nuclear CFP (ARX) reporter human iPSC line (HMGUi001-A-4). *Stem Cell Research*, *46*. https://doi.org/10.1016/j.scr.2020.101874

Nadella, S., Burks, J., Huber, M., Wang, J., Cao, H., Kallakury, B., Tucker, R. D., Boca, S. M., Jermusyck, A., Collins, I., Vietsch, E. E., Pierobon, M., Hodge, K. A., Cui, W., Amundadottir, L. T., Petricoin, E., Shivapurkar, N., & Smith, J. P. (2019). Endogenous Gastrin Collaborates With Mutant KRAS in Pancreatic Carcinogenesis. *Pancreas*, *48*(7), 894–903. https://doi.org/10.1097/MPA.0000000000001360

Nair, G., & Hebrok, M. (2015). Islet formation in mice and men: lessons for the generation of functional insulin-producing β-cells from human pluripotent stem cells. *Current Opinion in Genetics & Development*, *32*, 171–180. https://doi.org/10.1016/j.gde.2015.03.004

Nair, G. G., Liu, J. S., Russ, H. A., Tran, S., Saxton, M. S., Chen, R., Juang, C., Li, M., Nguyen, V. Q., Giacometti, S., Puri, S., Xing, Y., Wang, Y., Szot, G. L., Oberholzer, J., Bhushan, A., & Hebrok, M. (2019). Recapitulating endocrine cell clustering in culture promotes maturation of human stem-cell-derived β cells. *Nature Cell Biology*, *21*(2), 263–274. https://doi.org/10.1038/s41556-018-0271-4

Nair, T., Precup, D., Arnold, D. L., & Arbel, T. (2020). Exploring uncertainty measures in deep networks for Multiple sclerosis lesion detection and segmentation. *Medical Image Analysis*, *59*, 101557. https://doi.org/10.1016/j.media.2019.101557

Nolan, C. J., & Prentki, M. (2019). Insulin resistance and insulin hypersecretion in the metabolic syndrome and type 2 diabetes: Time for a conceptual framework shift. *Diabetes and Vascular Disease Research*, *16*(2). https://doi.org/10.1177/1479164119827611

Nostro, M. C., Sarangi, F., Yang, C., Holland, A., Elefanty, A. G., Stanley, E. G., Greiner, D. L., & Keller, G. (2015). Efficient Generation of NKX6-1+ Pancreatic Progenitors from Multiple Human Pluripotent Stem Cell Lines. *Stem Cell Reports*, *4*(4), 591–604. https://doi.org/10.1016/j.stemcr.2015.02.017

Nowotschin, S., Hadjantonakis, A.-K., & Campbell, K. (2019). The endoderm: a divergent cell lineage with many commonalities. *Development*, *146*(11). https://doi.org/10.1242/dev.150920

Oleson, B. J., McGraw, J. A., Broniowska, K. A., Annamalai, M., Chen, J., Bushkofsky, J. R., Davis, D. B., Corbett, J. A., & Mathews, C. E. (2015). Distinct differences in the responses of the human pancreatic β-cell line EndoC-βH1 and human islets to proinflammatory cytokines. *American Journal of Physiology-Regulatory, Integrative and Comparative Physiology*, *309*(5). https://doi.org/10.1152/ajpregu.00544.2014

Pagliuca, F. W., Millman, J. R., Gürtler, M., Segel, M., Van Dervort, A., Ryu, J. H., Peterson, Q. P., Greiner, D., & Melton, D. A. (2014). Generation of Functional Human Pancreatic β Cells In Vitro. *Cell*, *159*(2). https://doi.org/10.1016/j.cell.2014.09.040

Pan, F. C., & Wright, C. (2011). Pancreas organogenesis: From bud to plexus to gland. *Developmental Dynamics*, *240*(3), 530–565. https://doi.org/10.1002/dvdy.22584

Patterson, C. C., Karuranga, S., Salpea, P., Saeedi, P., Dahlquist, G., Soltesz, G., & Ogle, G. D. (2019). Worldwide estimates of incidence, prevalence and mortality of type 1 diabetes in children and adolescents: Results from the International Diabetes Federation Diabetes Atlas, 9th edition. *Diabetes Research and Clinical Practice*, *157*. https://doi.org/10.1016/j.diabres.2019.107842

Petersen, M. B. K., Gonçalves, C. A. C., Kim, Y. H., & Grapin-Botton, A. (2018). *Recapitulating and Deciphering Human Pancreas Development From Human Pluripotent Stem Cells in a Dish* (pp. 143–190). https://doi.org/10.1016/bs.ctdb.2018.02.009

Peterson, Q. P., Veres, A., Chen, L., Slama, M. Q., Kenty, J. H. R., Hassoun, S., Brown, M. R., Dou, H., Duffy, C. D., Zhou, Q., Matveyenko, A. V., Tyrberg, B., Sörhede-Winzell, M., Rorsman, P., & Melton, D. A. (2020). A method for the generation of human stem cell-derived alpha cells. *Nature Communications*, *11*(1), 2241. https://doi.org/10.1038/s41467-020-16049-3

Phillips, P. A., Yang, L., Shulkes, A., Vonlaufen, A., Poljak, A., Bustamante, S., Warren, A., Xu, Z., Guilhaus, M., Pirola, R., Apte, M. V., & Wilson, J. S. (2010). Pancreatic stellate cells produce acetylcholine and may play a role in pancreatic exocrine secretion. *Proceedings of the National Academy of Sciences*, *107*(40), 17397–17402. https://doi.org/10.1073/pnas.1000359107

Pinto, L. C., Falcetta, M. R., Rados, D. V., Leitão, C. B., & Gross, J. L. (2019). Glucagon-like peptide-1 receptor agonists and pancreatic cancer: a meta-analysis with trial sequential analysis. *Scientific Reports*, *9*(1), 2375. https://doi.org/10.1038/s41598-019-38956-2

Plecitá-Hlavatá, L., Jabůrek, M., Holendová, B., Tauber, J., Pavluch, V., Berková, Z., Cahová, M., Schröder, K., Brandes, R. P., Siemen, D., & Ježek, P. (2020). Glucose-Stimulated Insulin Secretion Fundamentally Requires H2O2 Signaling by NADPH Oxidase 4. *Diabetes*, *69*(7), 1341–1354. https://doi.org/10.2337/db19-1130

Prasad, R., & Groop, L. (2015). Genetics of Type 2 Diabetes—Pitfalls and Possibilities. *Genes*, *6*(1), 87–123. https://doi.org/10.3390/genes6010087

Racz, G. Z. (2002). Extracellular calcium sensing receptor in human pancreatic cells. *Gut*, *51*(5), 705–711. https://doi.org/10.1136/gut.51.5.705

Raum, J. C., Gerrish, K., Artner, I., Henderson, E., Guo, M., Sussel, L., Schisler, J. C., Newgard, C. B., & Stein, R. (2006). FoxA2, NKX2-2, and PDX-1 Regulate Islet β-Cell-Specific *mafA* Expression through Conserved Sequences Located between Base Pairs −8118 and −7750 Upstream from the Transcription Start Site. *Molecular and Cellular Biology*, *26*(15). https://doi.org/10.1128/MCB.00249-06

Rehfeld, J. F. (2019). Premises for Cholecystokinin and Gastrin Peptides in Diabetes Therapy. *Clinical Medicine Insights: Endocrinology and Diabetes*, *12*. https://doi.org/10.1177/1179551419883608

Rezania, A., Bruin, J. E., Arora, P., Rubin, A., Batushansky, I., Asadi, A., O'Dwyer, S., Quiskamp, N., Mojibian, M., Albrecht, T., Yang, Y. H. C., Johnson, J. D., & Kieffer, T. J. (2014). Reversal of diabetes with insulin-producing cells derived in vitro from human pluripotent stem cells. *Nature Biotechnology*, *32*(11). https://doi.org/10.1038/nbt.3033

Rickels, M. R., & Robertson, R. P. (2019). Pancreatic Islet Transplantation in Humans: Recent Progress and Future Directions. *Endocrine Reviews*, *40*(2), 631–668. https://doi.org/10.1210/er.2018-00154

Rickels, M. R., Schutta, M. H., Markmann, J. F., Barker, C. F., Naji, A., & Teff, K. L. (2005). β-Cell Function Following Human Islet Transplantation for Type 1 Diabetes. *Diabetes*, *54*(1), 100–106. https://doi.org/10.2337/diabetes.54.1.100

Riedel, M. J., Asadi, A., Wang, R., Ao, Z., Warnock, G. L., & Kieffer, T. J. (2012). Immunohistochemical characterisation of cells co-producing insulin and glucagon in the developing human pancreas. *Diabetologia*, *55*(2), 372–381. https://doi.org/10.1007/s00125-011-2344-9

Rodriguez-Diaz, R., Dando, R., Jacques-Silva, M. C., Fachado, A., Molina, J., Abdulreda, M. H., Ricordi, C., Roper, S. D., Berggren, P.-O., & Caicedo, A. (2011). Alpha cells secrete acetylcholine as a non-neuronal paracrine signal priming beta cell function in humans. *Nature Medicine*, *17*(7), 888–892. https://doi.org/10.1038/nm.2371

Rodriguez-Diaz, R., Menegaz, D., & Caicedo, A. (2014). Neurotransmitters act as paracrine signals to regulate insulin secretion from the human pancreatic islet. *The Journal of Physiology*, *592*(16), 3413–3417. https://doi.org/10.1113/jphysiol.2013.269910

Rorsman, P., & Ashcroft, F. M. (2018). Pancreatic β-Cell Electrical Activity and Insulin Secretion: Of Mice and Men. *Physiological Reviews*, *98*(1), 117–214. https://doi.org/10.1152/physrev.00008.2017

Rosado-Olivieri, E. A., Anderson, K., Kenty, J. H., & Melton, D. A. (2019). YAP inhibition enhances the differentiation of functional stem cell-derived insulin-producing β cells. *Nature Communications*, *10*(1). https://doi.org/10.1038/s41467-019-09404-6

Roscioni, S. S., Migliorini, A., Gegg, M., & Lickert, H. (2016). Impact of islet architecture on β-cell heterogeneity, plasticity and function. *Nature Reviews Endocrinology*, *12*(12), 695–709. https://doi.org/10.1038/nrendo.2016.147

Rukstalis, J. M., & Habener, J. F. (2009). Neurogenin3: A master regulator of pancreatic islet differentiation and regeneration. *Islets*, *1*(3). https://doi.org/10.4161/isl.1.3.9877

Rukstalis, J. M., & Habener, J. F. (2009). Neurogenin3: A master regulator of pancreatic islet differentiation and regeneration. *Islets*, *1*(3), 177–184. https://doi.org/10.4161/isl.1.3.9877

Russ, H. A., Parent, A. V, Ringler, J. J., Hennings, T. G., Nair, G. G., Shveygert, M., Guo, T., Puri, S., Haataja, L., Cirulli, V., Blelloch, R., Szot, G. L., Arvan, P., & Hebrok, M. (2015). Controlled induction of human pancreatic progenitors produces functional beta-like cells *in vitro*. *The EMBO Journal*, *34*(13), 1759–1772. https://doi.org/10.15252/embj.201591058

Sachs, S., Bastidas-Ponce, A., Tritschler, S., Bakhti, M., Böttcher, A., Sánchez-Garrido, M. A., Tarquis-Medina, M., Kleinert, M., Fischer, K., Jall, S., Harger, A., Bader, E., Roscioni, S., Ussar, S., Feuchtinger, A., Yesildag, B., Neelakandhan, A., Jensen, C. B., Cornu, M., … Lickert, H. (2020). Targeted pharmacological therapy restores β-cell function for diabetes remission. *Nature Metabolism*, *2*(2). https://doi.org/10.1038/s42255-020-0171-3

Saillan-Barreau, C., Dufresne, M., Clerc, P., Sanchez, D., Corominola, H., Moriscot, C., Guy-Crotte, O., Escrieut, C., Vaysse, N., Gomis, R., Tarasova, N., & Fourmy, D. (1999). Evidence for a functional role of the cholecystokinin-B/gastrin receptor in the human fetal and adult pancreas. *Diabetes*, *48*(10). https://doi.org/10.2337/diabetes.48.10.2015

Saillan–Barreau, C., Clerc, P., Adato, M., Escrieut, C., Vaysse, N., Fourmy, D., & Dufresne, M. (1998). Transgenic CCK-B/gastrin receptor mediates murine exocrine pancreatic secretion. *Gastroenterology*, *115*(4), 988–996. https://doi.org/10.1016/S0016-5085(98)70271-9

Salinno, Cota, Bastidas-Ponce, Tarquis-Medina, Lickert, & Bakhti. (2019). β-Cell Maturation and Identity in Health and Disease. *International Journal of Molecular Sciences*, *20*(21). https://doi.org/10.3390/ijms20215417

Schlienger, J.-L. (2013). Complications du diabète de type 2. *La Presse Médicale*, *42*(5). https://doi.org/10.1016/j.lpm.2013.02.313

Schmidt, A. M. (2018). Highlighting Diabetes Mellitus. *Arteriosclerosis, Thrombosis, and Vascular Biology*, *38*(1). https://doi.org/10.1161/ATVBAHA.117.310221

Schonhoff, S. E., Giel-Moloney, M., & Leiter, A. B. (2004). Neurogenin 3-expressing progenitor cells in the gastrointestinal tract differentiate into both endocrine and non-endocrine cell types. *Developmental Biology*, *270*(2), 443–454. https://doi.org/10.1016/j.ydbio.2004.03.013

Schubert, M. L., & Rehfeld, J. F. (2019). Gastric Peptides—Gastrin and Somatostatin. In *Comprehensive Physiology*. Wiley. https://doi.org/10.1002/cphy.c180035

Schwitzgebel, V. M., Scheel, D. W., Conners, J. R., Kalamaras, J., Lee, J. E., Anderson, D. J., Sussel, L., Johnson, J. D., & German, M. S. (2000). Expression of neurogenin3 reveals an islet cell precursor population in the pancreas. *Development*, *127*(16), 3533–3542. https://doi.org/10.1242/dev.127.16.3533

Shahryari, A., Moya, N., Siehler, J., Wang, X., Burtscher, I., & Lickert, H. (2021). Increasing Gene Editing Efficiency for CRISPR-Cas9 by Small RNAs in Pluripotent Stem Cells. *The CRISPR Journal*, *4*(4). https://doi.org/10.1089/crispr.2021.0014

Shahryari, A., Moya, N., Siehler, J., Wang, X., Karolina Blöchinger, A., Burtscher, I., Bakhti, M., Mowla, S. J., & Lickert, H. (2020). Generation of a human iPSC line harboring a biallelic large deletion at the INK4 locus (HMGUi001-A-5). *Stem Cell Research*, *47*. https://doi.org/10.1016/j.scr.2020.101927

Shapiro, A. M. J., Lakey, J. R. T., Ryan, E. A., Korbutt, G. S., Toth, E., Warnock, G. L., Kneteman, N. M., & Rajotte, R. V. (2000). Islet Transplantation in Seven Patients with Type 1 Diabetes Mellitus Using a Glucocorticoid-Free Immunosuppressive Regimen. *New England Journal of Medicine*, *343*(4). https://doi.org/10.1056/NEJM200007273430401

Shulkes, A., & Baldwin, G. S. (1997). BRIEF REVIEW BIOLOGY OF GUT CHOLECYSTOKININ AND GASTRIN RECEPTORS. *Clinical and Experimental Pharmacology and Physiology*, *24*(3–4). https://doi.org/10.1111/j.1440-1681.1997.tb01809.x

Siehler, J., Blöchinger, A. K., Meier, M., & Lickert, H. (2021). Engineering islets from stem cells for advanced therapies of diabetes. *Nature Reviews Drug Discovery*, *20*(12), 920–940. https://doi.org/10.1038/s41573-021-00262-w

Skene, P. J., & Henikoff, S. (2017). An efficient targeted nuclease strategy for high-resolution mapping of DNA binding sites. *ELife*, *6*. https://doi.org/10.7554/eLife.21856

Smith, J. P., Fonkoua, L. K., & Moody, T. W. (2016). The Role of Gastrin and CCK Receptors in Pancreatic Cancer and other Malignancies. *International Journal of Biological Sciences*, *12*(3), 283–291. https://doi.org/10.7150/ijbs.14952

Speier, S., Nyqvist, D., Köhler, M., Caicedo, A., Leibiger, I. B., & Berggren, P.-O. (2008). Noninvasive high-resolution in vivo imaging of cell biology in the anterior chamber of the mouse eye. *Nature Protocols*, *3*(8). https://doi.org/10.1038/nprot.2008.118

Spijker, H. S., Song, H., Ellenbroek, J. H., Roefs, M. M., Engelse, M. A., Bos, E., Koster, A. J., Rabelink, T. J., Hansen, B. C., Clark, A., Carlotti, F., & de Koning, E. J. P. (2015). Loss of β-Cell Identity Occurs in Type 2 Diabetes and Is Associated With Islet Amyloid Deposits. *Diabetes*, *64*(8), 2928–2938. https://doi.org/10.2337/db14-1752

Staels, W., & Scharfmann, R. (2021). Pancreatic endocrinogenesis revisited: “I have all the answers, who has the questions?” *Cell Research*, *31*(8), 834–835. https://doi.org/10.1038/s41422-021-00489-7

Suissa, Y., Magenheim, J., Stolovich-Rain, M., Hija, A., Collombat, P., Mansouri, A., Sussel, L., Sosa-Pineda, B., McCracken, K., Wells, J. M., Heller, R. S., Dor, Y., & Glaser, B. (2013). Gastrin: A Distinct Fate of Neurogenin3 Positive Progenitor Cells in the Embryonic Pancreas. *PLoS ONE*, *8*(8). https://doi.org/10.1371/journal.pone.0070397

Szuszkiewicz-Garcia, M. M., & Davidson, J. A. (2014). Cardiovascular Disease in Diabetes Mellitus. *Endocrinology and Metabolism Clinics of North America*, *43*(1). https://doi.org/10.1016/j.ecl.2013.09.001

Takahashi, K., & Yamanaka, S. (2006). Induction of Pluripotent Stem Cells from Mouse Embryonic and Adult Fibroblast Cultures by Defined Factors. *Cell*, *126*(4), 663–676. https://doi.org/10.1016/j.cell.2006.07.024

Terashima, H., Debas, H. T., & Bunnett, N. W. (1992). Effects of Cholecystokinin and Gastrin Antagonists on Pancreatic Exocrine Secretion Stimulated by Gastrin-Releasing Peptide. *Pancreas*, *7*(2). https://doi.org/10.1097/00006676-199203000-00013

Thompson, P. J., Shah, A., Ntranos, V., Van Gool, F., Atkinson, M., & Bhushan, A. (2019). Targeted Elimination of Senescent Beta Cells Prevents Type 1 Diabetes. *Cell Metabolism*, *29*(5), 1045-1060.e10. https://doi.org/10.1016/j.cmet.2019.01.021

Thomson, J. A. (1998). Embryonic Stem Cell Lines Derived from Human Blastocysts. *Science*, *282*(5391). https://doi.org/10.1126/science.282.5391.1145

Tian, X., Gu, T., Patel, S., Bode, A. M., Lee, M.-H., & Dong, Z. (2019). CRISPR/Cas9 – An evolving biological tool kit for cancer biology and oncology. *Npj Precision Oncology*, *3*(1). https://doi.org/10.1038/s41698-019-0080-7

Triolo, T. M., & Bellin, M. D. (2021). Lessons from Human Islet Transplantation Inform Stem Cell-Based Approaches in the Treatment of Diabetes. *Frontiers in Endocrinology*, *12*. https://doi.org/10.3389/fendo.2021.636824

Velazco-Cruz, L., Song, J., Maxwell, K. G., Goedegebuure, M. M., Augsornworawat, P., Hogrebe, N. J., & Millman, J. R. (2019). Acquisition of Dynamic Function in Human Stem Cell-Derived β Cells. *Stem Cell Reports*, *12*(2), 351–365. https://doi.org/10.1016/j.stemcr.2018.12.012

Veres, A., Faust, A. L., Bushnell, H. L., Engquist, E. N., Kenty, J. H.-R., Harb, G., Poh, Y.-C., Sintov, E., Gürtler, M., Pagliuca, F. W., Peterson, Q. P., & Melton, D. A. (2019). Charting cellular identity during human in vitro β-cell differentiation. *Nature*, *569*(7756), 368–373. https://doi.org/10.1038/s41586-019-1168-5

Villasenor, A., Chong, D. C., & Cleaver, O. (2008). Biphasic Ngn3 expression in the developing pancreas. *Developmental Dynamics*, *237*(11). https://doi.org/10.1002/dvdy.21740

Wang, B., Moya, N., Niessen, S., Hoover, H., Mihaylova, M. M., Shaw, R. J., Yates, J. R., Fischer, W. H., Thomas, J. B., & Montminy, M. (2011). A Hormone-Dependent Module Regulating Energy Balance. *Cell*, *145*(4), 596–606. https://doi.org/10.1016/j.cell.2011.04.013

Wang, Z., Ramanadham, S., Ma, Z. A., Bao, S., Mancuso, D. J., Gross, R. W., & Turk, J. (2005). Group VIA Phospholipase A2 Forms a Signaling Complex with the Calcium/Calmodulin-dependent Protein Kinase IIβ Expressed in Pancreatic Islet β-Cells. *Journal of Biological Chemistry*, *280*(8), 6840–6849. https://doi.org/10.1074/jbc.M405287200

Wild, S., Roglic, G., Green, A., Sicree, R., & King, H. (2004). Global Prevalence of Diabetes. *Diabetes Care*, *27*(5), 1047–1053. https://doi.org/10.2337/diacare.27.5.1047

Wu, T., Xu, J., Xu, S., Wu, L., Zhu, Y., Li, G., & Ren, Z. (2017). 17β-Estradiol Promotes Islet Cell Proliferation in a Partial Pancreatectomy Mouse Model. *Journal of the Endocrine Society*, *1*(7), 965–979. https://doi.org/10.1210/js.2016-1073

Yamanaka, S. (2020). Pluripotent Stem Cell-Based Cell Therapy—Promise and Challenges. *Cell Stem Cell*, *27*(4), 523–531. https://doi.org/10.1016/j.stem.2020.09.014

Ye, D. Z., & Kaestner, K. H. (2009). Foxa1 and Foxa2 Control the Differentiation of Goblet and Enteroendocrine L- and D-Cells in Mice. *Gastroenterology*, *137*(6), 2052–2062. https://doi.org/10.1053/j.gastro.2009.08.059

Yorifuji, T. (2014). Congenital hyperinsulinism: current status and future perspectives. *Annals of Pediatric Endocrinology & Metabolism*, *19*(2), 57. https://doi.org/10.6065/apem.2014.19.2.57

Zaehres, H., & Schöler, H. R. (2007). Induction of Pluripotency: From Mouse to Human. *Cell*, *131*(5). https://doi.org/10.1016/j.cell.2007.11.020

Zanner, R., Hapfelmeier, G., Gratzl, M., & Prinz, C. (2002). Intracellular signal transduction during gastrin-induced histamine secretion in rat gastric ECL cells. *American Journal of Physiology-Cell Physiology*, *282*(2), C374–C382. https://doi.org/10.1152/ajpcell.00366.2001

Zeng, Q., Ou, L., Wang, W., & Guo, D.-Y. (2020). Gastrin, Cholecystokinin, Signaling, and Biological Activities in Cellular Processes. *Frontiers in Endocrinology*, *11*. https://doi.org/10.3389/fendo.2020.00112

Zhou, Q., & Melton, D. A. (2018). Pancreas regeneration. *Nature*, *557*(7705). https://doi.org/10.1038/s41586-018-0088-0

Zhu, Y., Liu, Q., Zhou, Z., & Ikeda, Y. (2017). PDX1, Neurogenin-3, and MAFA: critical transcription regulators for beta cell development and regeneration. *Stem Cell Research & Therapy*, *8*(1). https://doi.org/10.1186/s13287-017-0694-z

8. Acknowledgement

First and foremost, I would like to express my deepest gratitude to my supervisor, Prof. Dr. Heiko Lickert, for granting me the opportunity to conduct this research and prepare the thesis work in his laboratory. I am appreciative of the exceptional scientific environment he provided, as well as his unwavering support, innovative ideas, and enthusiasm. Over the past years, his scientific approach, organizational skills, work ethic, and knowledge have been invaluable to my learning experience.

I extend my thanks to Prof. Dr. Heinrich Leonhardt for facilitating my enrollment in the program. I am also grateful to Dr. Ingo Burtscher for his supervision and guidance throughout my project. His assistance and support, both academically and personally, have been integral to my progress, and it has been a pleasure working alongside him.

I wish to acknowledge my thesis committee members, Prof. Dr. Heiko Lickert, Prof. Dr. Heinrich Leonhardt, and Dr. Sabrina Desbordes, for their insightful comments and suggestions on my projects during the thesis meetings. Lastly, I would like to express my gratitude to Dr. Mostafa Bakhti, Dr. Alireza Shahryari, Dr. Aimee Bastidas-Ponce, and Dr. Ingo Burtscher for their invaluable contributions to the publications associated with this research.

I would like to extend a special acknowledgement to Dr. Mostafa Bakhti for his unwavering belief in my potential as both an individual and a scientist, as well as his assistance with thesis corrections. My appreciation also goes to Dr. Aimee Bastidas-Ponce and Dr. Alireza Shahryari for their scientific contribution to the project, professional advice, and cherished friendship. I am grateful for Mara's exceptional work, which has greatly influence the trajectory of this research.

A pivotal individual in my work has been Donna Thomson, whose kindness, care, and unwavering support have made a substantial and positive impact on my research endeavors.

I express my gratitude to the entire stem cell group, including Julia Beckenbauer, Dr. Johanna Siehler, and Dr. Xianming Wang, for their countless scientific discussions and numerous challenges that have enriched my research experience.

Furthermore, I would like to thank Prof. Dr. Heinrich Leonhardt, Prof. Dr. Heiko Lickert, Prof. Dr. Laura Buses, Prof. Dr. Maria Elena Torres-Padilla, Prof. Dr. Wolfgang Enard, and, Prof. Dr. Korbinian Schneeberger for evaluating my Ph.D. examination and providing valuable feedback.

Finally, I would like to express my heartfelt gratitude to my incredible family for their unwavering emotional and financial support throughout this journey. I am deeply appreciative of my mother, Dr. Carmen Betancourt, and my late father Dr. Noel Moya for serving as strong moral and professional inspirations in my life. I extend a special acknowledgment to my sister Carmen Moya, for her unconditional love and support.

I am profoundly grateful to my extraordinary wife, Danae Moya, for her kindness, assertiveness, and the trust she has placed in me during this process. To my entire family, completing a six-year Ph.D. program so far from home would have been impossible without your support and love.

9. Publications

Shahryari, A., **Moya, N.**, Siehler, J., Wang, X., Burtscher, I., & Lickert, H. (2021). Increasing Gene Editing Efficiency for CRISPR-Cas9 by Small RNAs in Pluripotent Stem Cells. *The CRISPR Journal*, *4*(4), 491–501. https://doi.org/10.1089/crispr.2021.0014

Shahryari, A., **Moya, N.,** Siehler, J., Wang, X., Karolina Blöchinger, A., Burtscher, I., Bakhti, M., Mowla, S. J., & Lickert, H. (2020). Generation of a human iPSC line harboring a biallelic large deletion at the INK4 locus (HMGUi001-A-5). *Stem Cell Research*, *47*, 101927. https://doi.org/10.1016/j.scr.2020.101927

Moya, N., Shahryari, A., Burtscher, I., Beckenbauer, J., Bakhti, M., & Lickert, H. (2020). Generation of a homozygous ARX nuclear CFP (ARX) reporter human iPSC line (HMGUi001-A-4). *Stem Cell Research*, *46*, 101874. https://doi.org/10.1016/j.scr.2020.101874

Moya, N., Cutts, J., Gaasterland, T., Willert, K., & Brafman, D. A. (2014). Endogenous WNT Signaling Regulates hPSC-Derived Neural Progenitor Cell Heterogeneity and Specifies Their Regional Identity. *Stem Cell Reports*, *3*(6), 1015–1028. https://doi.org/10.1016/j.stemcr.2014.10.004

Brafman, D. A., **Moya, N.**, Allen-Soltero, S., Fellner, T., Robinson, M., McMillen, Z. L., Gaasterland, T., & Willert, K. (2013). Analysis of SOX2-Expressing Cell Populations Derived from Human Pluripotent Stem Cells. *Stem Cell Reports*, *1*(5), 464–478. https://doi.org/10.1016/j.stemcr.2013.09.005

Wang, B., **Moya, N.**, Niessen, S., Hoover, H., Mihaylova, M. M., Shaw, R. J., Yates, J. R., Fischer, W. H., Thomas, J. B., & Montminy, M. (2011). A Hormone-Dependent Module Regulating Energy Balance. *Cell*, *145*(4), 596–606. https://doi.org/10.1016/j.cell.2011.04.013

Eidesstattliche Erklärung

Satutory declaration

Ich versichere hiermit an Eides statt, dass die vorgelegte Dissertation von mir selbständig und ohne unerlaubte Hilfe angefertigt ist.
I hereby declare on oath that the thesis submitted is my own work and that I have not sought or used inadmissible help of third parties to produce this work.

München, den December 21, 2023 Noel Moya
Munich, (Unterschrift/signature)

Erklärung

Declaration

Hiermit erkläre ich, *
Hereby I declare

[X] dass die Dissertation nicht ganz oder in wesentlichen Teilen einer anderen Prüfungskommission vorgelegt worden ist.
that this work, complete or in parts, has not yet been submitted to another examination institution

[X] dass ich mich anderweitig einer Doktorprüfung ohne Erfolg **nicht** unterzogen habe.
that I did **not** undergo another doctoral examination without success

[ ] dass ich mich mit Erfolg der Doktorprüfung im Hauptfach .....
that I successfully completed a doctoral examination in the main subject

und in den Nebenfächern .....
and in the minor subjects

bei der Fakultät für ..... der .....
at the faculty of at
(Hochschule/University)

unterzogen habe.

[ ] dass ich ohne Erfolg versucht habe, eine Dissertation einzureichen oder mich der Doktorprüfung zu unterziehen.
that I submitted a thesis or did undergo a doctoral examination without success

München, den. December 21, 2023 Noel Moya
Munich, (Unterschrift/signature)

*) Nichtzutreffendes streichen/delete where not applicable

END